DETERMINATION OF LATERAL RESISTANCE OF RAILROAD DECK TIE FASTENERS IN SMOOTH TOP BRIDGE GIRDERS

Vishali Mylapore Vasudevan

Thesis submitted to the faculty of the Virginia Polytechnic Institute and State University in partial fulfillment of the requirements for the degree of

MASTER OF SCIENCE

In

CIVIL ENGINEERING

Matthew H. Hebdon, Chair

Ioannis Koutromanos

Matthew R. Eatherton

4 May 2018

Blacksburg, Virginia

Keywords: Railroad, Bridges, Fasteners, Lateral Resistance

DETERMINATION OF LATERAL RESISTANCE OF RAILROAD DECK TIE FASTENERS IN SMOOTH TOP BRIDGE GIRDERS

ABSTRACT

Vishali M. Vasudevan

The purpose of this research was to investigate and create preliminary design aids for the determination of lateral resistance capacity and spacing requirements of deck tie fasteners in curved railroad bridges with smooth top girders. In railroad bridge design, required lateral resistance dictates the spacing of deck tie fasteners. Currently, no provisions exist to aid in the calculation of lateral resistance for systems that include bridge ties, fasteners, and girders which experience centrifugal or lateral forces. Thus, design practices specific to each railroad vary, producing inconsistent fastener spacing in existing railroad bridges.

This project identified and quantified three factors contributing to lateral resistance through experimental testing: resistance due to friction at the tie-girder interface; resistance from the fastener; and resistance from dapped ties bearing against the girder flange. Three fastener types were studied in this research: Square body hook bolts, Lewis Forged hook bolts, and Quikset Anchors. Results indicated that frictional resistance is a product of the train wheel load and the friction coefficient. Fastener resistance was determined to be a function of fastener type and lateral track displacement. Finally, dap resistance was found to be a function of the area of the shear plane in a dapped tie. A preliminary equation for calculating the total lateral resistance capacity was developed utilizing superposition of all three resistance contributions. Lateral demand loads were compared with reported lateral capacity to create a preliminary design aid to determine fastener spacing.

DETERMINATION OF LATERAL RESISTANCE OF RAILROAD DECK TIE FASTENERS IN SMOOTH TOP BRIDGE GIRDERS

GENERAL AUDIENCE ABSTRACT

Vishali M. Vasudevan

Railroad bridges are constructed by securing wooden ties to I-shaped steel beams (girders) using deck tie fasteners. Curved railroad bridges should provide lateral resistance to resist lateral loads from trains negotiating the curve. Currently, there is no official practice for determining lateral strength, which is a function of fastener spacing. Thus, each railroad company uses a proprietary fastener spacing, producing inconsistencies in existing railroad bridges.

The purpose of this research was to create a preliminary table or equation for determining the lateral strength and spacing requirements of deck tie fasteners through experimental testing. This project identified and quantified three factors contributing to lateral resistance: resistance due to friction at the tie-girder interface; resistance from the fastener; and resistance from dapped ties (ties that are notched to sit on the girder flanges). Three fastener types were studied. Results showed that frictional resistance was directly proportionate to the magnitude of the vertical wheel load. Fastener resistance was found to be a function of the type of fastener used. Finally, the dap was determined to be a function of the area of the shear plane in a dapped tie. A preliminary equation for calculating the total lateral resistance capacity was developed by summing the resistance contributions from all three resistance factors. Lateral loads were compared with lateral capacity to create a preliminary design aid to determine fastener spacing.

ACKNOWLEDGEMENTS

I would like to thank Dr. Matthew Hebdon for his patience and guidance throughout this research project. These past two years have been a wonderful learning experience and I am very grateful for the opportunity that has been given to me.

I would also like to thank Dr. Mehdi Ahmadian, Dr. Matthew Eatherton, Dr. Daniel P. Hindman and members from TTCI for their valuable insight and assistance with this research project.

I would like to thank CSX, Norfolk Southern and Lewis Nut & Bolt and for their generous donation of all the materials that were required for testing.

I would also like to specially thank Brett Farmer, David Mokarem, Dennis Huffman and Jalen Hill for their assistance during testing. I could not have completed this project without them.

I would also like to thank Ryan Stevens and all my fellow graduate students for their help during this project.

Finally, I would like to thank my family for their unfailing support and encouragement during the entire research project.

Table of Contents

List of Figures

List of Tables

CHAPTER 1: INTRODUCTION AND BACKGROUND

1.1 Project Objective and Scope

The railroad industry has two different kinds of deck tie fasteners that are used to connect a bridge tie to the top flange of a steel plate girder. Hook bolts and spring clips constitute the most common fastener system currently in practice in the railroad industry as seen in Figure 1. However, the spacing of these fasteners varies from railroad to railroad depending on historical design practices specific to each railroad. Fastener spacing ranges from fasteners at every other tie to every fourth tie. Little research has been performed to determine their spacing and capacity.

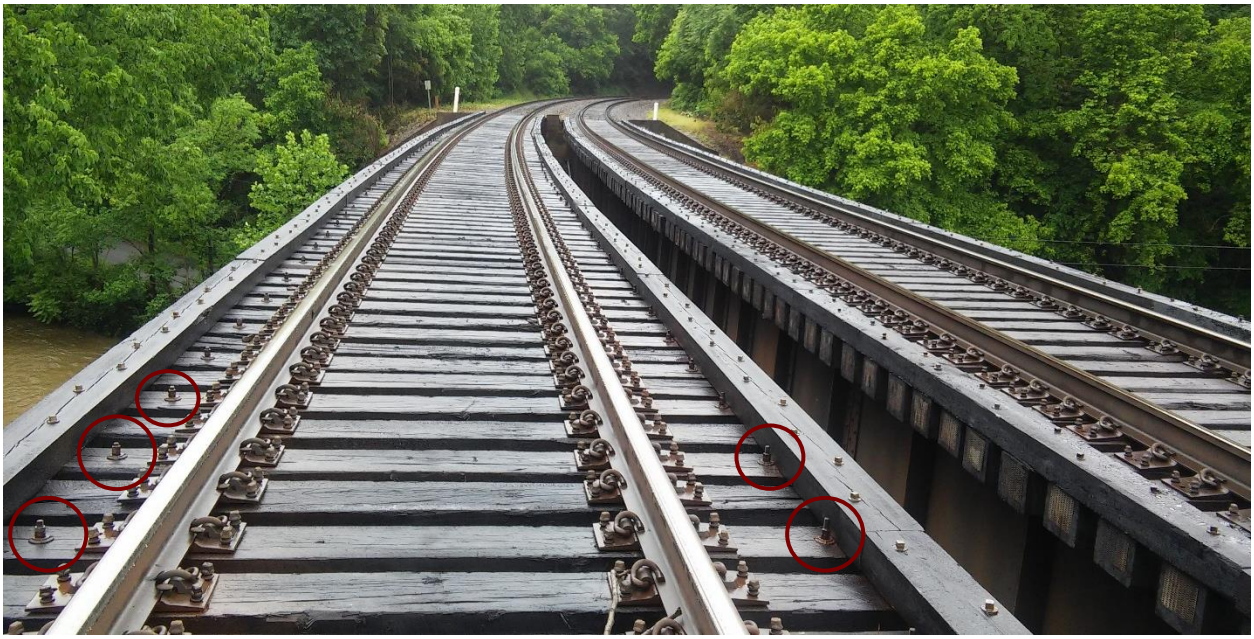

Figure 1: Deck tie fasteners on a curved railroad bridge

Currently there are no design provisions in the AREMA (American Railways and Maintenance of Way Association) manual regarding tie-girder fastener capacity or spacing in railroad bridges. Chapter 15 of the AREMA design manual states that for open deck railroad bridges with riveted girders, deck tie fasteners should be spaced at every fourth tie with the center to center distance between fasteners not to exceed 4’8” (AREMA, 2017a). However, for smooth

top bridge girders the AREMA manual specifies that depending on the lateral and longitudinal forces generated and the transfer of these loads to the smooth top girders, spacing of fasteners should be reduced from the spacing provided for riveted open deck bridges. Lack of design aids has raised a concern about the lateral resistance needed in instances where bridge tie and girder systems experience centrifugal or lateral forces.

The recent commercial introduction of a new type of fastener called the Quikset Anchor by Lewis Nut and Bolt company in industry has raised questions regarding the required spacing and lateral capacity since there is no historical performance data available within each railroad company that can aid in the use of this fastener in practice. Since each railroad company has different standards for attaching bridge ties to girders, a 2016 Steel Bridge Technical Advisory Group meeting consensus determined that further research was required to determine the lateral capacity and spacing of tie-girder fasteners.

This purpose of this research project is to experimentally determine the lateral capacity and spacing of tie-girder fasteners in steel bridges to ensure that adequate lateral resistance is provided upon their installation. Lateral forces are experienced in curved railway bridges. These forces are functions of several factors such as the degree of the curve, speed of the train negotiating the curve, material and physical properties of the tie and axle loads from the train. This project will identify and quantify each of these contributing factors and present data in the form of a preliminary design aid for each of the fastener types studied. It will focus on both dapped ties (ties that are notched to sit on top of the girder and adjust for superelevation) and undapped timber ties as well as three kinds of fasteners: square body hook bolts, forged hook bolts, and Quikset anchors.

1.1.1 Track Components

A typical railroad track structure has components shown in Figure 2 and explained in detail in sections 1.1.2 and 1.1.3

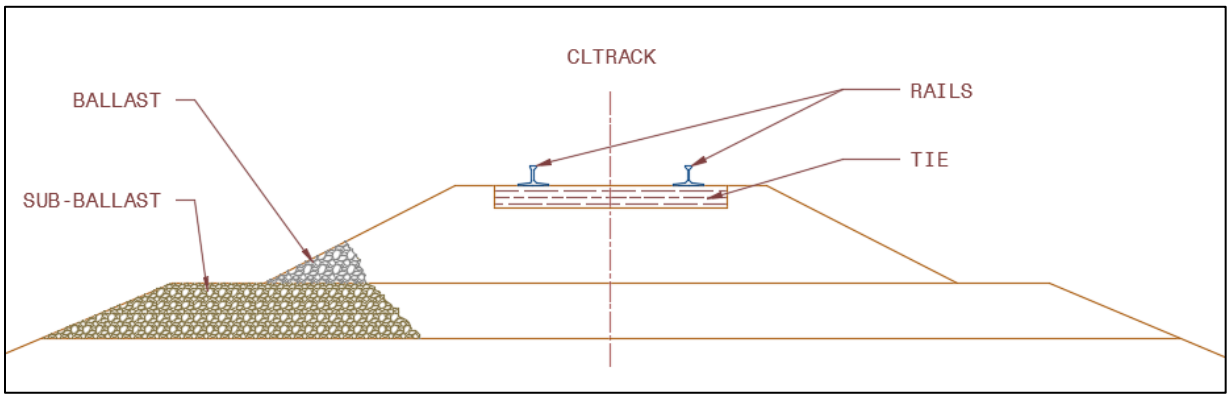

Figure 2: Typical railroad track structure

1.1.2 Track Superstructure

Track superstructure consists of an assembly of rails, crossties and the rail fastening system. The rail fastening system helps to anchor the rail to the ties and helps in the efficient transfer of forces from the train to the track substructure. Rail clips, railroad spikes, tie plates and tie pads constitute the rail fastening system

1.1.3 Track Substructure

Track substructure is made up of granular material and crushed rock which supports the track superstructure. It serves multiple functions like aiding in the drainage of the track superstructure, transfer of loads from the superstructure to the roadbed, reducing vibrations from the train and minimizing erosion of the roadbed. The roadbed is the groundwork on which the rails, ties, and ballast of a railroad are laid and it serves as the foundation for a railroad track. The ballast is the upper portion of the track substructure which supports the track superstructure and the sub-ballast is the bottom portion which rests on the roadbed. The depth of the ballast and the sub-ballast varies and is specified by the individual railroad company.

1.2 Railroad Bridges

Railroad bridges can be classified into two types based on the type of deck. They are explained in sections 1.2.1 and 1.2.2.

1.2.1 Ballasted Bridges

A ballasted deck is constructed by placing a concrete slab across the top of two bridge girders as shown in Figure 3. Curbs are added to the concrete deck along the bridge length and this structure is then filled with ballast which supports the track superstructure. Loads from the train are transferred from the wheels to the rails, rails to the ties, ties to the ballast and concrete slab, slab to the girders and then from the girders to the columns and finally from the columns to the foundation.

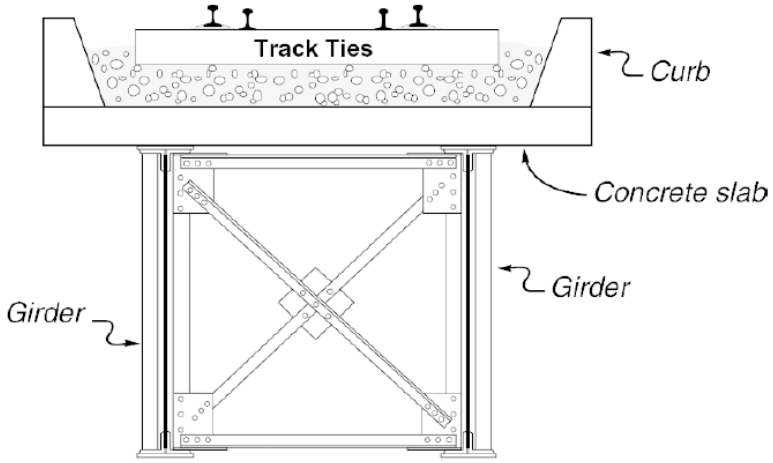

Figure 3: Ballasted deck (AREMA, 2003a)

1.2.2 Open Deck Bridges

This style of bridge deck does not contain any ballast. The crossties are directly connected to the bridge girders with the help of steel deck tie fasteners as shown in Figure 4. Loads from the train are transferred from the wheels to the rails, from the rails to the ties, from the ties to the bridge girders, from the girders to the columns and then finally from the columns to the foundation. Deck

fasteners typically connect bridge ties to the bridge girder by hooking onto the bottom of the top flange of the girder. They prevent any lateral, rotational or longitudinal displacements. This research project only included the study of deck tie fasteners on open deck bridges.

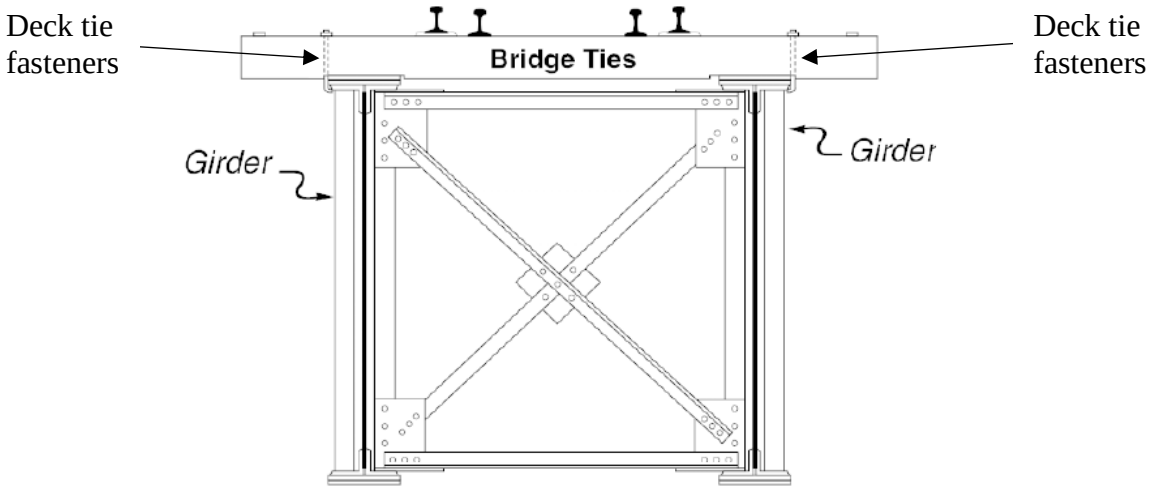

Figure 4: Open deck (AREMA, 2003a)

1.3 Crosstie properties

According to the Railroad Tie Association (RTA) more than 90% of the crossties used in the railroad industry are wood ties. Concrete, plastic and steel ties make up the remaining 10% (Railway Tie Association, 2018a). Hardwood species such as oak, maple and hickory or a blend of these woods mostly from eastern and mid-western forests are used to make wood ties. The scope of this research project only included wood crossties. A list of hardwood species approved by AREMA for railroad track purposes can be seen in Table 1. Railroad crossties are pressure treated with preservatives to prevent the wood from termite attacks, fungi and decay and thereby increase the service life of the tie. Based on information from the "Tie Guide" published by the Railway Tie Association, over 90% of preservatives used to treat wood crossties consist of an EPA registered pesticide containing creosote and its solutions (Webb, Webb, Zarembski, Smith, & Gauntt, 2016).

Table 1: Hardwood species used in railroad crossties (AREMA, 2017b)

Ashes	Elms	Larches	Poplars
Beech	Firs	Locusts	Redwoods
Birches	Gums	Maples	Sassafras
Catalpas	Hackberries	Mulberries	Spruces
Cherries	Hemlocks	Oaks	Sycamores
Douglas Fir	Hickories	Pines	Walnuts

1.3.1 Bridge Ties

Bridges are crucial for the smooth operation of a railway line, therefore, AREMA has strict conditional requirements for crossties that are used in bridges. Bridge ties are longer and larger than standard railroad ties as shown in Figure 5. Standard railroad tie dimensions are 7”x 9”x 8.5’ (Railway Tie Association, 2018a). Bridge ties are required by AREMA standard to have a minimum width of 8”. The length is governed by the greater of 10’ or the center to center distance between outer supports of the bridge plus three feet (AREMA, 2017b). Bridge ties are also spaced more closely together at a center to center distance of 12” - 16” whereas standard railroad ties have a larger spacing of 19.5”. All bridge ties are required to be free of any defects such as shakes, splits, knots or decay in order to maintain increased strength and durability throughout their service life.

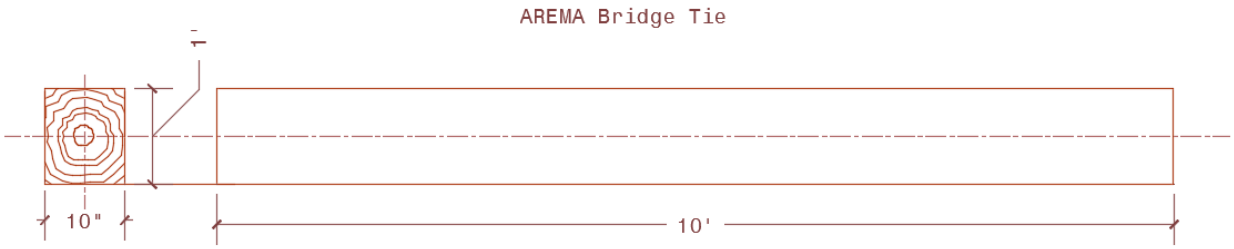

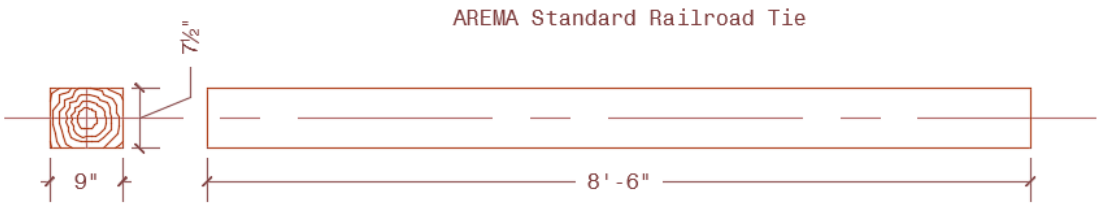

Figure 5: AREMA Tie Dimensions

1.4 Fastener Types

Three types of deck tie fasteners were tested within the scope of this project which are described in sections 1.4.1, 1.4.2 and 1.4.3.

1.4.1 Square Body Hook bolt

The bolt goes through the railroad tie and hooks onto the top flange of the bridge girder as seen in Figure 6(a). As per their name, this type of fastener has a bolt with a square shaft as shown in Figure 6(b). Bridge ties are pre-drilled at a diameter of 1” before the hook bolts are installed, typically from below the deck. Based on the height of the bridge girder flange being used, hook bolts are manufactured in various lengths and specified by the designer. Square body hook bolts are attached to the ties using a washer and two nuts on top of the tie. The nuts are snug tightened and do not have any specified pretension in them. For this research project, hook bolts with a ¾” diameter, a thread length of 5 inches, total length of 16 inches and a hook length of 3 inches were used.

(a)

(b)

Figure 6: Square body hook bolts

1.4.2 Lewis Forged Hook bolt

The forged hook bolt is similar to the square hook bolt except that it has a circular shaft instead of a square one as seen in Figure 7. The shape of the hook is different from the shape of the hook found in a square body hook bolt. This project aims to investigate how lateral capacity and spacing are affected by the shape of the cross sectional area of a hook bolt shaft. The cross section of the bolt changes near the hook where four splines can be found in the bolt before the cross section of the bolt becomes round near the threaded portion of the bolt.

Figure 7: Lewis forged hook bolt

1.4.3 Quik Set Anchor

The Quikset Anchor is a fastener that was introduced to the railroad industry in 2014(Austin, Personal Communication, 25 April 2018). It consists of a hook bolt similar to the Lewis Forged hook bolt which grips the top flange of a bridge girder with the help of a lock plate as seen in right most picture in Figure 8. The hook bolt in the Quikset Anchor also has four splines near the hook like the Lewis Forged hook bolt before the cross section of the bolt becomes round. Unlike the Lewis Forged hook bolt, the Quikset Anchor bolt is angled when it clamps to the girder flange as seen in the left most picture in Figure 8. The hook bolt passes through the gap between two adjacent bridge ties and through a bracket which is secured to both ties with lag screws. The bolt is then secured to the bracket using two nuts. The Quik set anchor is relatively easier to install compared to the Square body hook bolt and the Forged hook bolt, because it can be installed from above the bridge deck and does not require the user to be below the bridge deck. Also, no holes need to be predrilled through the entire height of the tie, thus increasing tie strength and aiding in the overall life of the tie by preventing ingress of rainwater and other contaminants.

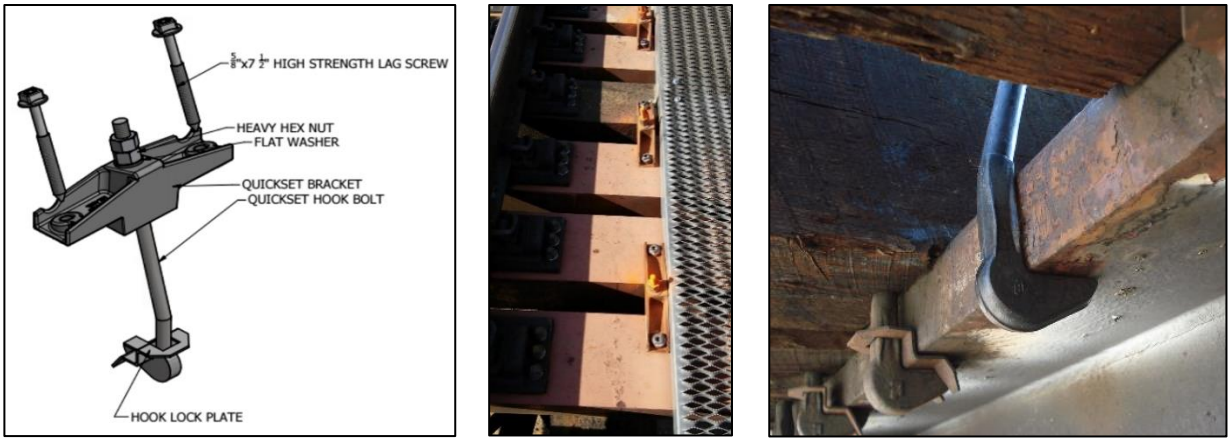

Figure 8: Quikset Anchor installation

1.5 Bridge surveys at Virginia Tech

Eight railroad bridges were surveyed in order to obtain data regarding existing deck tie fastener spacing and performance. All of the bridges used open-decked construction. Five of the bridges were located in Virginia and three were in West Virginia as indicated in the map shown in Figure 9.

Figure 9: Locations of railroad bridges that were surveyed

1.5.1 Bridges Surveyed

1. Berkley Road, VA

This railroad bridge spanned a creek that ran adjacent to Berkley Road in Roanoke, VA. It was a two span bridge with riveted bridge girders and undapped ties. It had a single railroad track with one girder running parallel to each rail. Square body hook bolts were found on this bridge at every fourth tie. The fasteners were loose since the hook was not in contact with the flange of the bridge girder as shown in Figure 10. This railroad bridge was not curved.

Figure 10: Berkley Road Bridge - Riveted girders with hook bolts

2. Glade Creek, VA

This was a straight railroad bridge that crossed Glade Creek in Roanoke, VA. It was a six span bridge supporting two railroad tracks. Each of the four rails had a riveted bridge girder supporting it throughout the entire length of the bridge. It had square body hook bolts spaced at every third tie as shown in Figure 11. This bridge had riveted girders with undapped ties. The fasteners on this bridge were loose because the nuts on top of the track were not snug tight and they could be moved by hand.

Figure 11: Glade Creek Bridge - Hook bolts at every 3rd tie

3. Ellet Road, VA

The railroad bridge was located in Christiansburg, VA and it crossed over Ellet Road. It was a single span bridge with smooth topped steel girders. This bridge had four bridge girders with two steel girders supporting each rail along the entire span of this bridge. It was not a curved bridge. Square body hook bolts were found at every fourth tie on this bridge. It was not possible to gain close range access to the bridge from below, therefore it was not possible to determine whether the bridge ties were dapped or undapped. The top nuts were missing on the hook bolts in this bridge as shown in Figure 12. As a result of missing top nuts, the hook bolts were not held in a state of tension.

Figure 12: Ellet road bridge - Hook Bolts at every 4th tie

4. Highway 10, WV

The Highway 10 railroad bridge was a curved bridge with riveted girders and it crossed Highway 10 in West Virginia, close to the town of Covel. This was a multiple span bridge supported two railroad tracks with only one track in service. Each rail had a bridge girder underneath it throughout the length of the bridge. The track which was not in service had clip anchors connecting dapped ties to the top flange of the bridge girder as shown in Figure 13. Clip anchors are not within the scope of this research project. However, it was noted that the clip

anchors were loose because they had rotated. These were spaced at every third tie on the de-commissioned track. It was not possible to gain access to the underside of the track that was in service because the bridge was tall and had steep embankments. Therefore, the type of fastener and the type of tie (dapped/ undapped) could not be determined.

Figure 13: Bridge across Highway 10, WV - Clip anchors at every 4th tie

5. Covel, WV

This railroad bridge was located in the town of Covel, West Virginia. This bridge had seventeen spans with each rail supported by a girder throughout the entire length of the bridge. It had two railway tracks that were in service. This bridge had riveted girders with dapped ties and hook bolts spaced at every second tie as shown in Figure 14. The top nuts on the hook bolts were loose and they could be turned by hand.

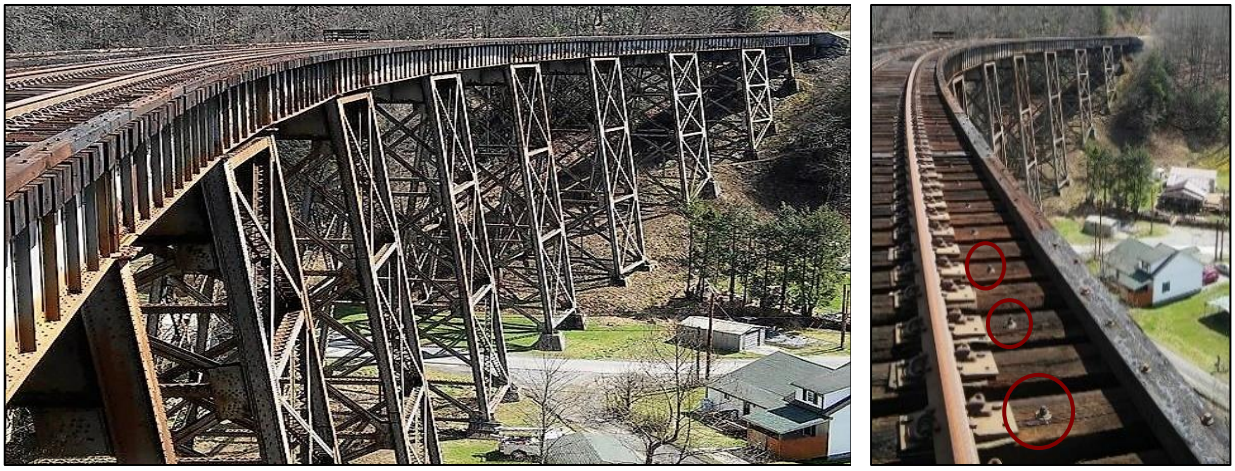

Figure 14: Bridge at Covel, WV - Hook bolts at every 2nd tie

6. Smokeless Road, WV

This was a curved, multiple span railroad bridge crossing over Smokeless Road in West Virginia as seen in Figure 15. It had hook bolts spaced at every second tie as shown in Figure 16. It was not possible to gain access to the top of the bridge because it had steep embankments. As a result, the type of ties could not be determined. Observations from below the bridge revealed that it had four riveted girders per span. Assuming that each rail was supported by a girder, it can be estimated that this bridge supported two railroad tracks, thus having a total of four rails.

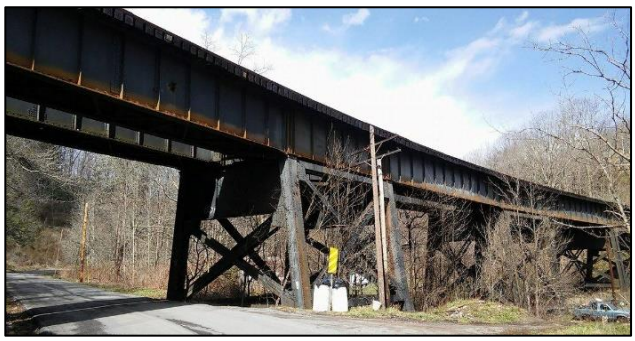

Figure 15: Bridge over Smokeless Road, WV

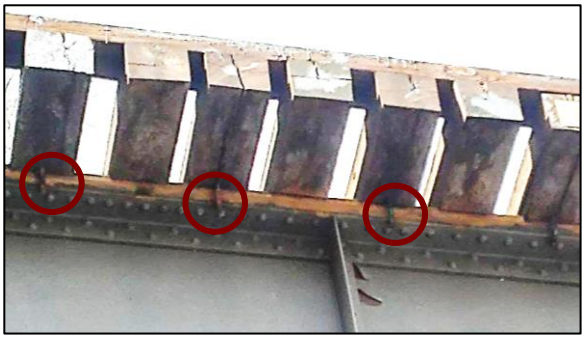

Figure 16: Hook bolts spaced at every 2nd tie

7. 4784 West River Road, VA

This curved railroad bridge was located in Salem, VA where it spanned across the Roanoke river as shown in Figure 17. This bridge had three spans supporting two railroad tracks with a

bridge girder below each of the four rails. This bridge had riveted bridge girders with square body hook bolts spaced on every second tie. The nuts on the hook bolts were loose and they could be moved by hand. It was not possible to observe the type of ties that were used because the river was swollen and there was no access to the underside of the bridge.

Figure 17: 4784 West River Road - Hook bolts spaced at every 2nd tie

8. 4829 South West River Road, VA

This curved railroad bridge also crossed the Roanoke River and it had a single railroad track. A riveted bridge girder supported each rail throughout the entire length of the bridge. Square body hook bolts spaced at every second tie were found on this bridge. Some of the square body hook bolts were missing where the ties had been pre-drilled as shown in Figure 18.

Figure 18: 4829 SW River Rd - Hook bolts spaced at every 2nd tie

The relevant observations results of the bridge survey are summarized in Table 2. The blank spaces in the table below indicate cases where it was not possible to determine if the ties were dapped (notched to sit on top of the bridge girder) or undapped because the bridge was inaccessible.

Table 2: Summary of bridge surveys

Bridge Location	Fastener Type	Fastener Spacing	Bridge girder type	Dapped/Undapped Tie
Berkley Road, VA	Square body hook bolt	4th Tie	Riveted Girder	Undapped
Glade Creek, VA	Square body hook bolt	3rd Tie	Riveted Girder	Undapped
Ellet Road, VA	Square body hook bolt	4th Tie	Smooth Top	-
WV Highway 10	Clip Anchor	2nd Tie	Riveted Girder	Dapped
Covel, WV	Square body hook bolt	2nd Tie	Riveted Girder	Dapped
Smokeless Road, WV	Square body hook bolt	2nd Tie	Riveted Girder	-
4784 West River Road, VA	Square body hook bolt	2nd Tie	Riveted Girder	-
4829 SW River Road, VA	Square body hook bolt	2nd Tie	Riveted Girder	-

1.5.2 Survey Observations

Important observations from the field survey of all the eight bridges are summarized below:

1. Out of the eight bridges that were surveyed, seven bridges had square body hook bolts. One bridge had clip anchors, which is a type of deck tie fastener that is not included in the scope of this project.
2. Fasteners were loosely connected; where the fastener hook was not in contact with the top flange of the bridge girder. In most of the bridges which were surveyed, it was possible to shake the top ends of the fasteners that were on top of the bridge deck by hand. Loosely connected hook bolts can be seen in the figures
3. Nuts are missing on the hook bolt fasteners as shown in Figure 21. It is possible that these nuts came loose because of repeated vibrations from train passing over the bridge.

Figure 19: Loose hook bolt from Glade Creek bridge

Figure 20: Loose hook bolt from Berkley Road bridge

4. Fastener spacing was not consistent since spacing ranged from fasteners at every second tie to every fourth tie. Spacing differences can be observed in Figure 21 and Figure 22. Figure 21 has hook bolts present at every fourth tie whereas Figure 22 has hook bolts at every third tie.

Figure 21: Missing nuts on hook bolts

Figure 22: Fasteners spaced every 3rd tie

CHAPTER 2: LITERATURE REVIEW

This chapter explains the forces that the fastener system on a railroad bridge has to resist. Loads are primarily resisted in three principal directions: longitudinal, lateral and vertical, as described in "Tie Report 6" (Railway Tie Association, 2018b). Loading scenarios on a curved railroad bridge in each of the three directions are described in detail in sections 2.1, 2.2 and 2.3.

2.1 Longitudinal Direction

Longitudinal loads are generated in the direction of the railroad track due to the motion of the train as a whole. The magnitude of longitudinal forces depends on the connections between rail cars and the overall length of the train. In the book, "Handbook of Railway Vehicle Dynamics" (Iwnicki, Wickens, Orlova, & Boronenko, 2006) relative motion between rail cars is referred to as 'slack action' which is created due to slack in the coupling connections between rail cars. During the braking action of a train, rail cars run into one another and there is progressive impact between rail cars as the train reduces in length. During train acceleration, the coupling connections are in a state of tension as the train stretches. The fastener system on a railroad bridge needs to provide strength in the longitudinal direction by preventing movement due to mechanical loading from the train, such as braking and acceleration.

2.2 Lateral Direction

As a train passes over a curved track, centrifugal or lateral loads are generated in the radial direction, perpendicular to the railroad track. Lateral loads are a function of the train freight type, the curve radius, superelevation (or banking) of the curve and the speed of the train. Factors affecting the loading scenario in the lateral (radial) direction of the track are explained in sections 2.2.1, 2.2.2, 2.2.3 and 2.2.4.

2.2.1 Train Wheel Dynamics

Train wheels have a fixed axle, therefore both wheels rotate at the same speed. Fixed axles are ideal for a straight track because they help center the wheels on the rails. However, on a curved track, they do not solve the problem of the outer wheel having to cover a larger distance than the inner wheel. Therefore, train wheels are conical as shown in Figure 23, so that the wheels are self-centering based on the degree of the curve and the speed of the train. Self-centering is achieved by increasing the diameter of the outer wheel and reducing the diameter of the inner wheel to compensate for the difference in the distance that needs to be travelled, with both wheels rotating at the same speed.

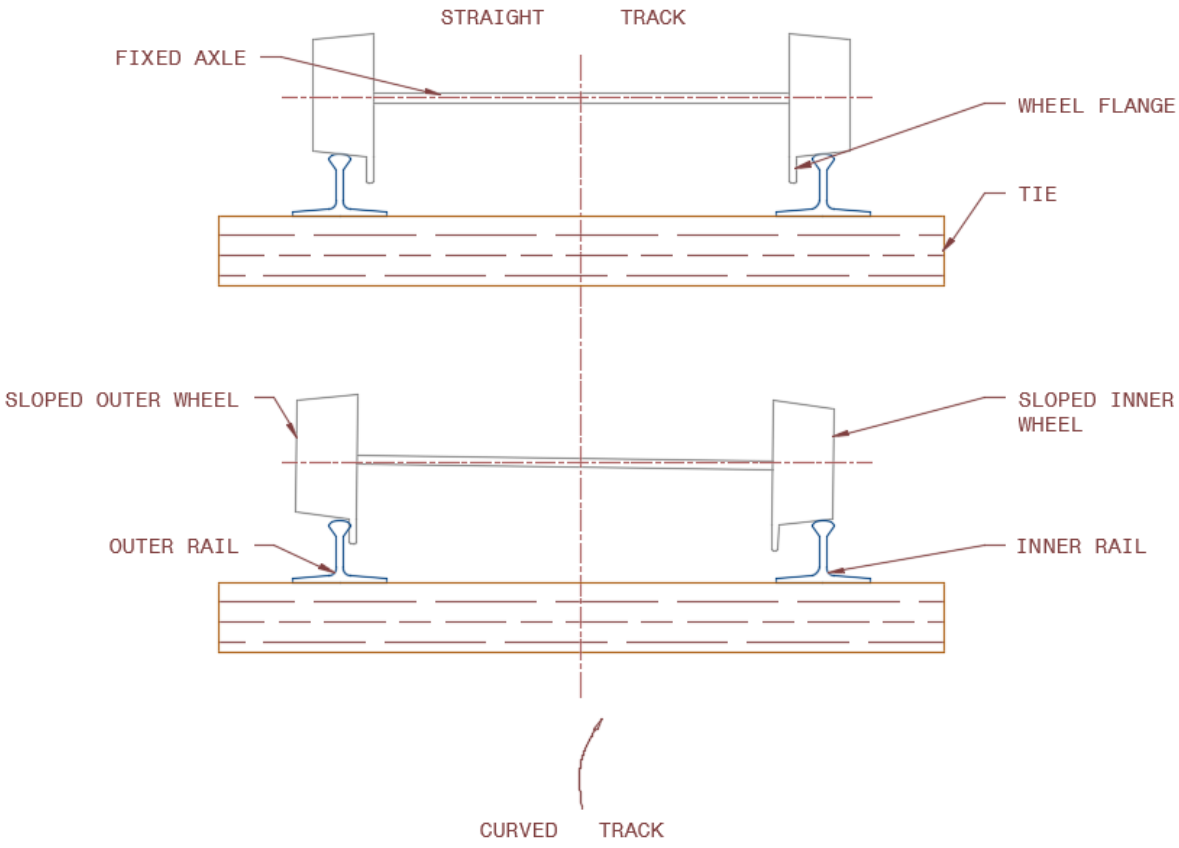

Figure 23: Train wheel dynamics at a curve

The flanges on the outer wheels come into contact with the rail as the train passes through a curve and high friction forces can be generated to counteract the centrifugal forces and prevent the wheel from sliding off the rail (Nilmani, 2011). Lateral creep forces are generated on the inner rail due to contact forces with the inner wheel. The outer wheel and outer rail experience lateral frictional forces due to the flange of the wheel bearing against the rail as seen in Figure 24.

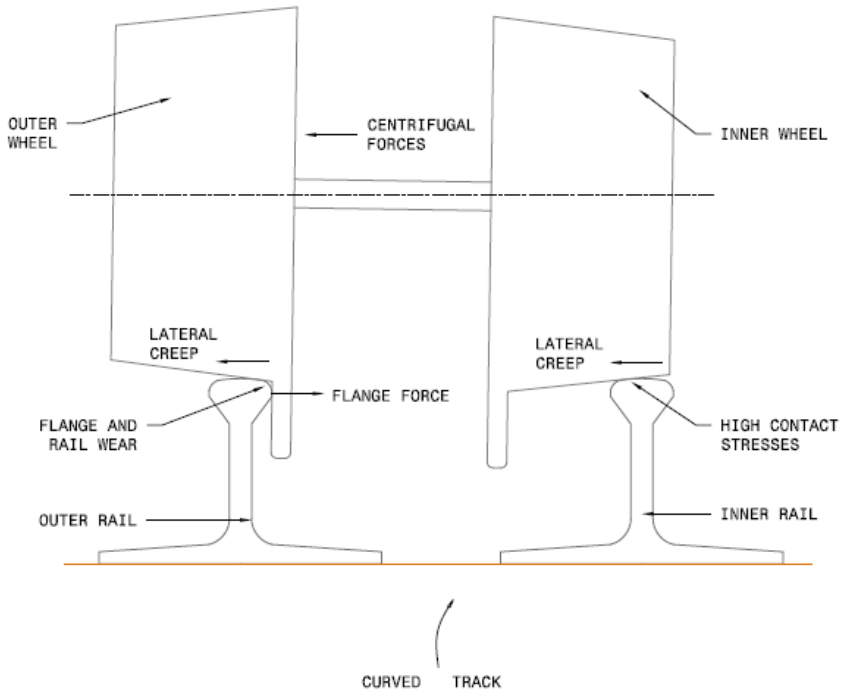

Figure 24: Rail to wheel contact forces at a curve

Research done by the American Association of Railways (AAR) measured the lateral forces on the rails from the motion of a 100-ton car negotiating a 5-degree curve. This research showed that at higher speeds, maximum lateral forces were generated in the outer rail whereas at low speeds lateral loads on the inner rail were greater. Results from this study revealed that at low curve speeds (below 20 mph), a maximum lateral load of 14 kip was measured in the inner rail and at higher speeds (above 20 mph) a maximum lateral load of 13 kip was measured in the outer rail (A. Zarembski, n.d.).

2.2.2 Superelevation

The outer rail of the track is superelevated to counteract centrifugal forces that act on a train as it passes through a curve. When the weight of the train is equally distributed to the inner and outer rails on a superelevated track, the train is said to be in a condition of equilibrium. When more weight is transferred to the inner rail, the train is said to be in a condition of overbalance and when a higher percentage of the train weight is transferred to the outer rail, the train is said to be in a state of underbalance (Oldknow, 2017). During overbalance, higher lateral forces are generated at the inner rail because of the shift in the center of gravity of the train towards the inner rail. Similarly, when the center of gravity of a train shifts to the outer track, underbalance causes higher lateral creep forces on the outer rail. Therefore, lateral forces on the rails are a function of the axle weight of the train, since the superelevation is fixed, and how the center of gravity of the train shifts as it negotiates the curve.

2.2.3 Wheel Hunting

Lateral forces are also generated due to lateral track irregularities such as defects in the rail and the response of the wheel set to lateral instabilities such as hunting (A. Zarembski, n.d.). Hunting is a phenomenon where the wheel set over corrects due to lateral irregularities and oscillates in a self-centering action from one rail to the other (Nilmani, 2011). Hunting occurs on both tangent tracks and on curved tracks. Loaded cars as well as empty cars exhibit hunting once they exceed a critical speed. Research done by AAR has shown that lateral forces as high as 15 kip were measured for a 100-ton car negotiating a 5-degree curve after the onset of hunting compared to the 13 kip of lateral load without hunting (A. Zarembski, n.d.).

2.2.4 Train Speeds

The speed of the train as it negotiates a curve affects the frictional flange forces and lateral creep forces on the rails. Research done by the Transportation Technology Center Inc. (TTCI), measured lateral forces using wayside detectors for bridge design and bridge load rating purposes. The study included concrete bridges, steel bridges and tangent track. Results showed that lateral forces increased with increase in train speeds and the increase was the same for open track as well as bridges (Otter, Doe, & Belport, 2005). Research done by AAR has also shown that lateral forces on the outer rail increase with increase in speed, for tangent track as well as a curved track (A. Zarembski, n.d.). The Federal Railway Association (FRA) restricts the superelevation of the outer rail to 5 - 6 inches, relative to the elevation of the inner rail, in order to regulate train speeds at curves. The maximum speed of operation on a curve is calculated using Equation 1 (AREMA, 2003b).

$$V_{max} = \sqrt{\frac{3 + E_a}{0.0007D}} \qquad \text{Equation 1}$$

Where:

V_{max} = Maximum allowable operating speed (mph.)

E_a = Average elevation of the outer rail relative to the inner rail (in.)

D = Degree of curvature (degrees)

The limit on train speed is to prevent overturning or derailment of the train. When the maximum train speed on a curve is exceeded, centrifugal forces cause the resultant force from the center of gravity of the train to fall outside of either of the rails, thus causing the train to overturn. According to the book, "Practical Guide To Railway Engineering", the shift in the center of gravity of the train usually causes it to derail first before overturning (AREMA, 2003b).

2.3 Vertical Direction

This section explains the vertical loads on a steel railroad bridge such as dead loads, live loads and impact train loads.

2.3.1 Dead Loads

Forces in the vertical direction include dead loads and live loads from the train which are a function of the train axle loads and track loads. Loads on bridges include the weight from track superstructure such as track rails, guard rails, and their rail fastenings. The AREMA manual for railway engineering specifies a track dead load of 200 lbs. per linear foot for each track for bridge design (AREMA, 2017a). The axle loads based on train freight type, ranging from 12 kip for empty cars to 72 kip for general freight, are shown in Table 3. These loads were partially obtained from the "Car and Locomotive Cyclopedia of American Practices" (Kratville, 1997) and supplemented by Dr. Steve Dick from TTCI (Dick, personal communication, April 2, 2018).

Table 3: Axle loads and wheel loads based on train freight type

FREIGHT TYPE	*Axle Load (kip)*	*Wheel Load (kip)*
General Freight	72	36
Standard Interchangeable Freight	72	36
Double Stack cars	79	39
Empty cars	17	8
Empty Aluminum coal cars	12	6

2.3.2 Live Loads

For live loads on bridges, AREMA recommends the application of a Cooper E-80 live load in lbs. per axle or the Alternative live load on 4 axles for steel bridges only, whichever produces higher stresses (AREMA, 2017a). The Cooper E-80 load is a series of point loads representing the axle loads from two locomotives followed by 8 kip per linear foot of distributed load as shown in

Figure 25. Axle spacing and the load per axle are different for both E-80 and Alternative live load on 4 axle load scenarios. as seen by comparing Figure 25 with Figure 26.

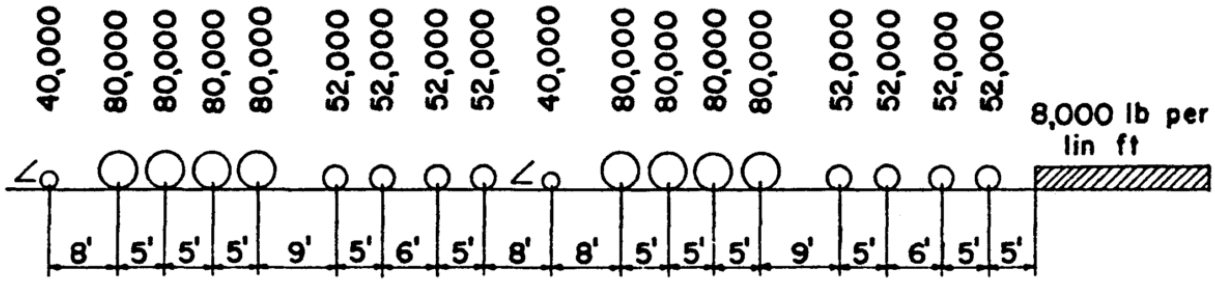

Figure 25: Cooper E-80 live load with permission from AREMA (AREMA, 2017a)

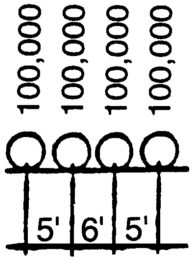

Figure 26: Alternative live load on 4 axles with permission from AREMA (AREMA, 2017a)

2.3.3 Impact Loads

Impact loads are generated on a railroad bridge because of the train passing over a bridge. They are a factor of the bridge span length and the train speed. Impact forces are calculated as a percentage of the live loads on a train as per AREMA code provisions. The percentage of live load to be considered is obtained using Equation 2 and Equation 3 based on span length L:

For L less than 80 feet: $40 - \frac{3L^2}{1600}$ Equation 2

For L greater than 80 feet: $16 + \frac{600}{L-30}$ Equation 3

From research done by (Igwemezie, 1987) it is known that impact forces only depend on the approach speed of the train and that they are not a multiplicative factor of the static axle load from a train. For open deck bridge design, AREMA recommends using a percentage of the impact load in order to account for the rocking effect of a train. The transfer of train weight from one rail to the other because of the lateral motion of the train is called rocking effect. Additional vertical loads on the rails are generated due to rocking. These loads are calculated as a vertical force couple with 20% of the impact load acting upward on one rail and the same load acting downward on the other rail (AREMA, 2017a).

2.4 Wheel to Rail Loads

The loads experienced on the rail from loading scenarios described in sections 2.2 and 2.3 are explained in detail in sections 2.4.1 and 2.4.2.

2.4.1 Previous Research

Wheel to rail loads can be calculated using equations developed by Igwemezie (1987) in a study involving the field test of a railroad bridge with concrete ties. In Equation 4 and Equation 5 shown below, the first term indicates the static contribution to the overall wheel to rail load. The second term in the equations is a factor of the train speed and the Impact Load Distribution Factor (IDF). IDF can be calculated from calibration charts shown in Figure 27 that were developed by Igwemezie (1987) through experimental testing in the field and in the lab by varying tie spacing and the type of rail.

$$P_{rail} = 31 + (2.37v)IDF \qquad \text{For } 0 \leq v \leq 30\ mph. \qquad \text{Equation 4}$$

$$P_{rail} = 31 + (61.74 + 0.30v)IDF \qquad \text{For } v > 30\ mph. \qquad \text{Equation 5}$$

Where:

P_{rail} = Force on the rail in kips

v = Speed of the train in mph.

IDF = Impact Load Distribution Factor obtained from Figure 27 based on rail size.

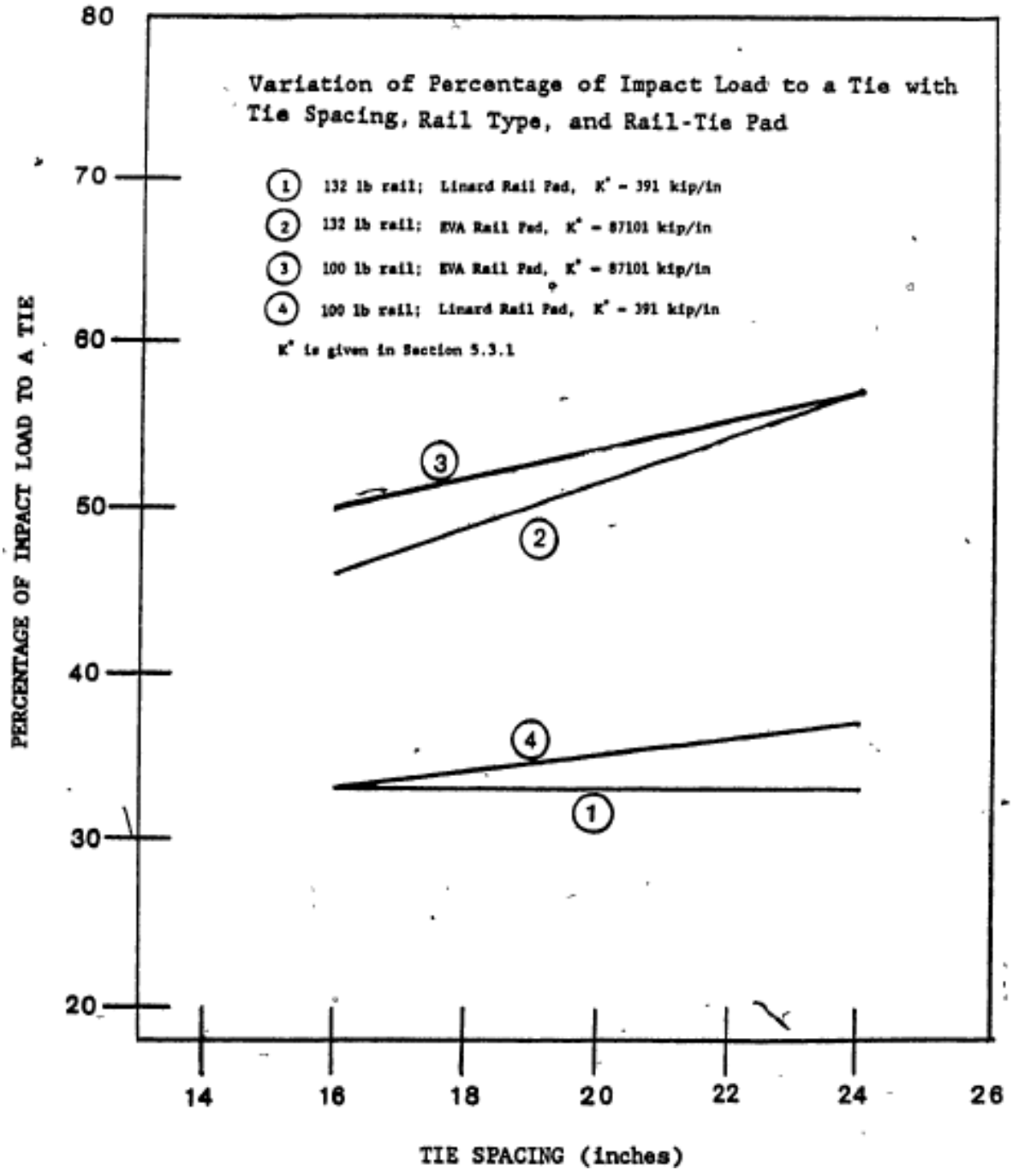

Figure 27: Calibration charts for determining the impact load distribution factor with permission Igwemezie (1987)

2.4.2 AREMA Provisions

AREMA summarizes the loading scenarios explained in sections 2.1, 2.2 and 2.3 in Figure 28 for a conventional railroad track. Vertical, Lateral and longitudinal loads are represented as point loads acting on the rails from the wheels. These loads take into account dead loads, live loads and impact loads. The longitudinal, lateral and vertical loads in Figure 28 are categorized based on the loading environment such as the degree of the curve, freight type of the train and the speed of the train. The longitudinal loads range between 25 kip and 50 kip, lateral loads range between 10 kip and 30 kip and the vertical loads range between 80 kip to 120 kip.

CURVE	<2 DEG			2-5 DEG			>5 DEG		
SPEED	VERT	LAT	LONG	VERT	LAT	LONG	VERT	LAT	LONG
MAINLINE FREIGHT									
<40	80	20*	50	80	30*	50	80	30	50
40 to 60	120	30*	50	120	30*	50	120	30	50
>60	120	30	50	120	30	50	**	**	**
LIGHT DENSITY FREIGHT (no A/C Traction)									
<40	80	20	30	80	30*	30	80	30	30
40 to 60	120	30	30	120	30	30	120	30	30
>60	120	30	30	120	30	30	**	**	**
HIGH SPEED PASSENGER									
<90	100	10	25	100	18	25	100	20*	25
>90	100	18	25	100	18	25	**	**	**
TRANSIT									
No data available									

* This data estimated or interpolated

** Generally accepted superelevation practice excludes these values

Figure 28: Wheel to rail load in kipsb with permission from AREMA (AREMA, 2010)

2.5 Load Distribution from Rails to Ties

For determining the lateral capacity of deck tie fasteners, it is important to estimate the loads experienced by a single tie due to rail loads. In order to simplify the loading environment, this research project ignored all loads in the longitudinal direction and only focused on vertical

and lateral loads. After wheel loads are transferred to the rails they are never carried by a single tie but by several ties. The distribution of vertical loads from the rails to a single tie is explained in sections 2.5.1 and 2.5.2.

2.5.1 Previous Research

Research conducted on the vertical wheel load distribution to the track components, analyzed the rails and ties on a railroad track as a beam on an elastic foundation, where the rail is the beam that is supported by multiple ties or springs. Results have shown that a single wheel load is carried by the tie directly underneath the wheel and by multiple adjacent ties on either side of the central tie (A. M. Zarembski, n.d.). The load distribution for a conventional railroad track where wheel load was carried by seven ties was studied. It was found that the center tie typically carried 15% to 40% of the wheel load on a conventional track (A. M. Zarembski, n.d.). Research also showed that wheel load distribution was a function of the stiffness of the "beam" or the size and shape of the rail, and the spacing of the ties. Therefore, the percentage of wheel load carried by a tie was found to be directly proportional to the stiffness modulus of the rail. Increasing the tie spacing caused the percentage of wheel loads carried per tie to also increase.

According to the paper, "Understanding Stresses in Rails" vertical and lateral loads are distributed over several ties (Igwemezie, 2014). Igwemezie points out that static rail load distribution depends on several factors such as tie spacing, ballast, rail size and axle spacing. Previous research done on pre-stressed concrete bridge ties have verified that static axle load distribution is a function of tie spacing, tie-girder pad stiffness and rail size (Igwemezie, 1987). Through field and lab tests, Igwemezie proved that the static load distribution to a single pre-stressed concrete tie is 33.5% of the wheel axle load and that static load was not a function of the train speed. Later studies done on impact load distribution show that the impact load transferred

to a single tie varies from 48% to 57% on increasing the tie spacing from 16 in. to 24 in. (Igwemezie, Mirza. 1989). Results also showed that impact load distribution depends on the stiffness and shape factor of the rail tie pad. Therefore, these studies proved that the percentage of static load experienced by a tie are influenced by and the axle load of the train whereas the percentage of dynamic loads experienced by a tie are a function of train speed and tie-girder pad properties.

Through the research involving the field test of an open deck railway bridge with concrete ties, Equation 6 and Equation 7 were developed by Igwemezie (1987) to calculate the load carried per tie:

$$P_{tie} = (SDF * P_w) + (2.37v)IDF \qquad \text{For } 0 \leq v \leq 30\ mph \qquad \text{Equation 6}$$

$$P_{tie} = (SDF * P_w) + (61.74 + 0.30v)IDF \qquad \text{For } v > 30\ mph \qquad \text{Equation 7}$$

Where:

SDF = Static Load Distribution Factor

IDF = Impact Load Distribution Factor from Figure 27.

P_w = Wheel load applied to the rail or Cooper E80 load

v = Speed of the train in mph.

Igwemezie & Mirza, (1989) also showed that individual bridge ties at the ends of the bridge experience 2-3 times the load that an intermediate tie in the center portion of the bridge experiences. It was concluded that this was due to the increase in impact load caused by the change in stiffness of the track. Bridges have a higher stiffness than the wood tie-ballast and subgrade approach, therefore the end ties are subjected to higher impact forces as the train moves from the approach to the bridge.

2.5.2 AREMA Provisions

The AREMA manual for railway engineering specifies the percentage of wheel to rail loads that is transferred to a single tie based on the spacing and material of the tie as seen in Figure 29. This plot indicates that loads from the rails which are distributed to a single tie are a function of the effect of ballast, sub grade reactions, rail fastening system and rail stiffness (AREMA, 2010). It is clear from the plot that wood ties spaced 20 inches apart carry 40% of the wheel to rail load. However, these results do not apply to ties on an open deck bridge that does not have ballast and a subgrade reaction. Consequently, open deck bridges experience greater impact loads and less load is dissipated to the track substructure. Therefore, it is safe to assume that the percentage of the wheel to rail load carried by a wood bridge tie spaced 20 inches apart is greater than 40%.

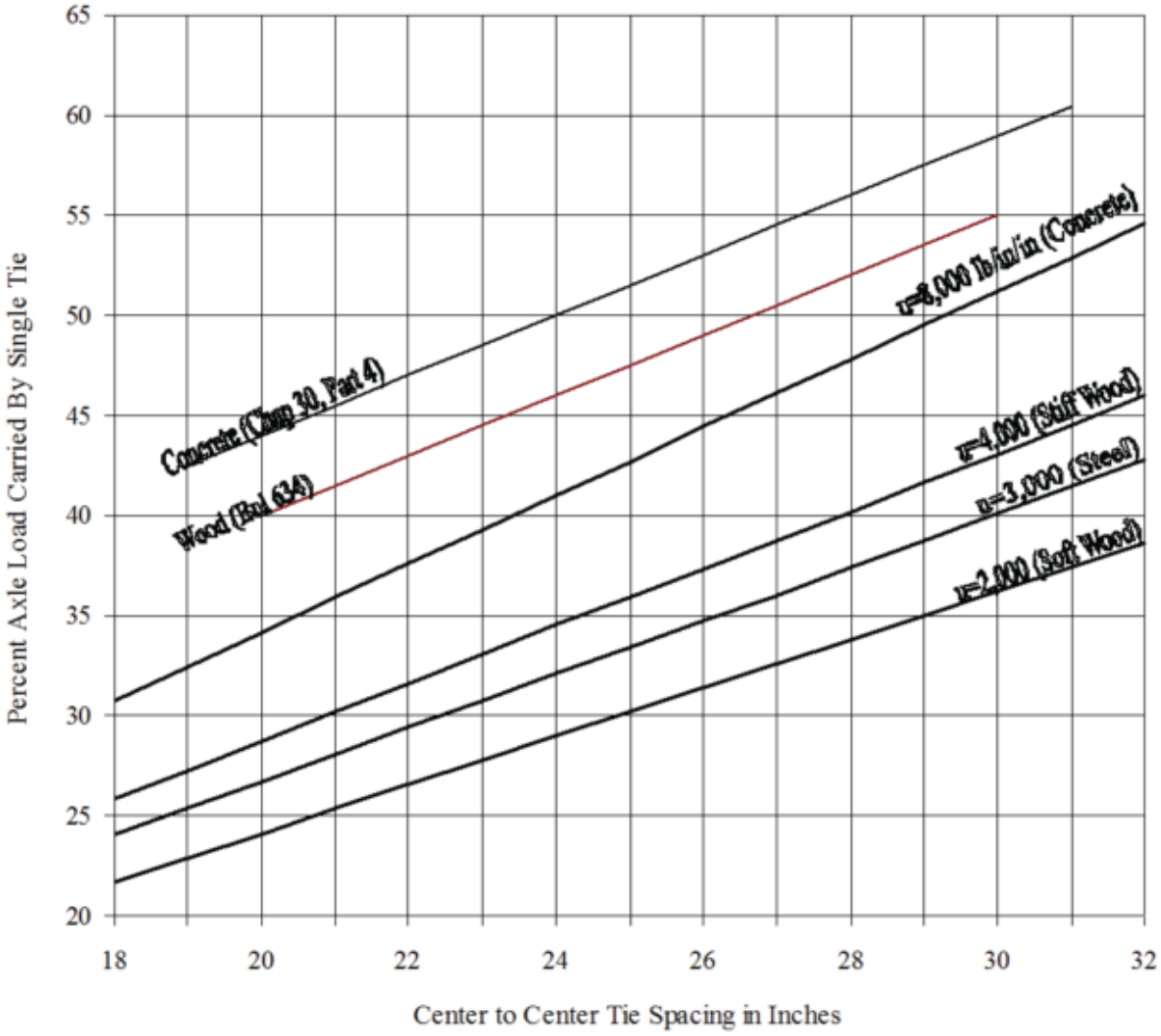

Figure 29: Axle load distribution based on tie spacing and tie material with permission from AREMA (AREMA, 2017b)

For the purposes of this research project, it was assumed that the maximum percentage of load carried by a single bridge tie is 60%. It can be seen in Figure 29 that the percentage of load distributed to a single tie increases by approximately 3% on increasing the tie spacing by 2 in. Since nominal spacing of ties on a bridge is in the range of 14 in. – 16 in., the percentage of load carried per tie should decrease to less than 20% as per Figure 29. But since bridge ties experience greater impact loads, a conservative distribution of 60% was assumed for both lateral and vertical loads experienced by a single bridge tie. The vertical demand loads used for this project range

from 5 kip to 45 kip of wheel load acting on a single rail based on the loads given in Table 3. The lateral demand loads used in this research are within the range of 10 kip – 30 kip based on the range of lateral wheel loads given by AREMA in Figure 28.

2.6 Study of Lateral Track Strength (Choros, Zarembski, & Gitlin, 1980)

A study to determine lateral track strength was conducted by the American Association of Railroads where a section of railroad track was loaded laterally. The railroad track was specially constructed at AAR's track testing laboratory as per guidelines presented in the AREMA manual of railway engineering. Loads simulating the capacity of a 100-ton freight car were applied to the track. Vertical loads were applied from four vertical hydraulic jacks with a capacity of 100 kip. The vertical loads were held constant after which the track was pushed laterally using two hydraulic jacks with a capacity of 50 kip. The lateral load was increased until a target displacement of 1 inch was reached after which the track was realigned before re-loading. The track was loaded three times at various vertical loads of 10 kip, 20 kip and 30 kip until a track displacement of 1 inch was achieved through lateral loading for each test. Load versus displacement plots from this study revealed that the track stiffness increased on increasing the vertical loads. Lateral testing was also conducted for a single tie until a displacement of 2 inches was achieved. The lateral stiffness of the tie was calculated by dividing the lateral strength values by their corresponding lateral displacement values.

Structural testing done in this research project followed a similar method of testing where a vertical load was applied on the system. The vertical load was held constant following which the system was loaded laterally in increments until a target displacement of 2 in. was achieved. The lateral load and lateral displacements were recorded throughout the test. The lateral stiffness of the system was calculated by dividing the lateral load by the corresponding lateral displacement.

CHAPTER 3: METHODS

This chapter outlines the methods and procedures used to generate test results and data.

3.1 Material Testing

The wood species and associated material properties of the bridge ties were initially unknown. Material testing was conducted to classify the wood species and the compressive strength of the wood parallel to grain and perpendicular to grain. The actual compressive strength properties of the wood after the ties had been in service since 2003 were assumed to be different from the NDS specified compressive strength values for a particular species of wood. Therefore, material testing was performed in order to determine the compressive strength values. Samples from five different bridge ties were collected for compression strength testing and wood species classification. The samples were cut and prepared to meet the size specification of ASTM D143 (ASTM Standard, 2014).

3.1.1 Wood species classification

Twenty samples from five different ties, with four samples from each tie, were used in classifying the species of wood. The samples were 4in. x 1in. x 1in. They were first classified as hardwoods or softwoods by checking the end grain of the samples under a microscope to see if there were any vessels present. Vessels are tubes in the stem of a plant that help in transporting sap, water and nutrients along the height of the tree. They appear as black spots while observing the cross section in a wood sample as seen in Figure 30 and Figure 31. All the samples had vessels, therefore they were classified as hardwoods. The samples were then checked for specific distinctions such as a ray pattern to determine the species of wood.

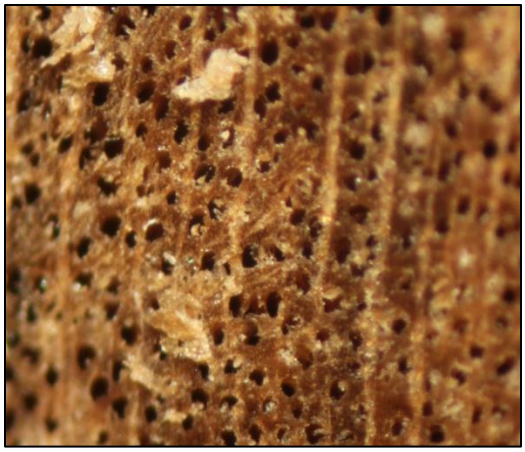

Figure 30: American Beech end grain

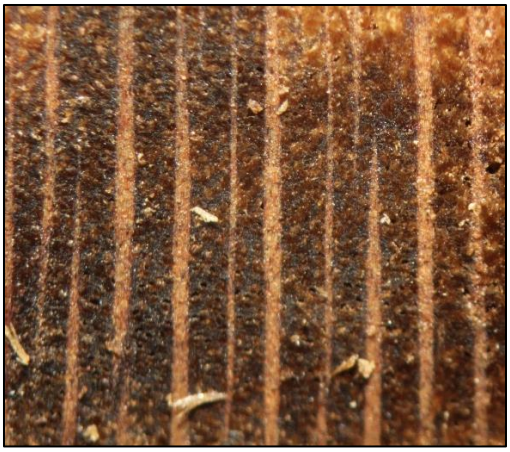

Figure 31: Sycamore end grain

The bridge ties were made up of a mixed species of wood. The wood species were identified as American Beech and Sycamore. The pattern of rays in a wood sample which appear as light colored lines running in the vertical direction, led to the final classification of both these wood species. Sycamore had a very distinctive ray pattern as shown in Figure 31 whereas the ray pattern in American Beech was not quite as uniform, shown in Figure 30.

3.1.2 Compression Testing

A total of twenty specimens were tested as per ASTM D143 (2014) to determine the compressive strength perpendicular to grain as shown in Figure 32. A steel plate having a length of 4 in., width of 2 in. and a thickness of 1 in. was used to load the sample perpendicular to grain. The samples were loaded at a rate of 0.002in/second until a maximum deflection of 0.1 in. was reached. The force versus displacement plot for samples tested in compression, perpendicular to grain is shown in Figure 33. Load versus deflection graphs were plotted for all twenty samples. The ultimate compressive load for each sample tested perpendicular to grain was divided by the cross sectional area under bearing, which was the width of the steel plate multiplied by the width of the sample, to obtain the ultimate compressive strength value.

Figure 32: Compressive testing perpendicular to grain

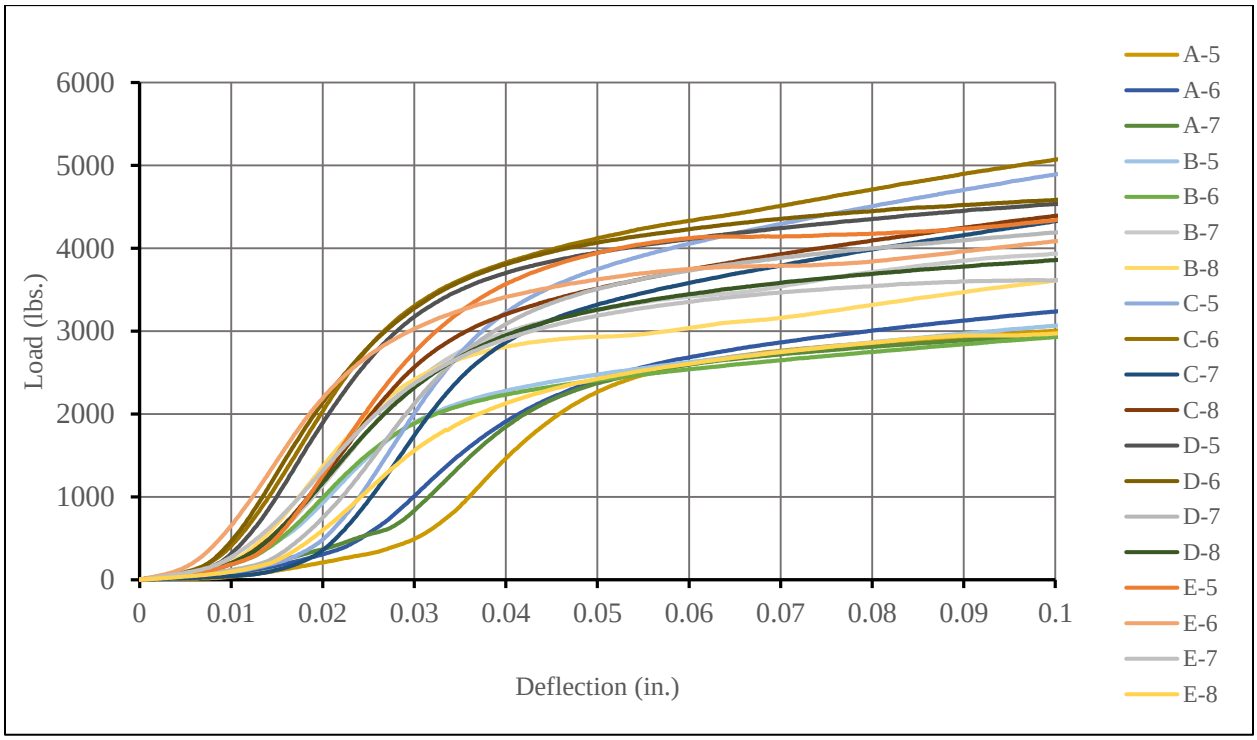

Figure 33: Force - displacement graph for compression perpendicular to grain

Twenty samples were tested as per ASTM D143 (2014) to determine the compression strength parallel to grain as seen in Figure 34. The samples were loaded at a load rate of 0.002in/second. The test was stopped when the load dropped by 100 pounds from the ultimate load

for that specimen or when a maximum displacement of 0.1 inches was obtained. Load versus deflection graphs were plotted for each sample as can be seen in Figure 35. The ultimate load for each sample was recorded and divided by the cross sectional area of the sample to obtain the maximum compressive strength value for loading parallel to grain. The ultimate compressive strengths for each sample tested in compression perpendicular to grain and in compression parallel to grain is shown in Table 4.

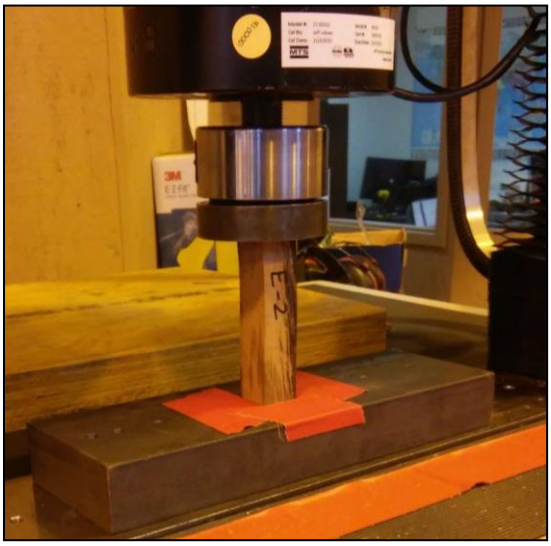

Figure 34: Compression testing parallel to grain

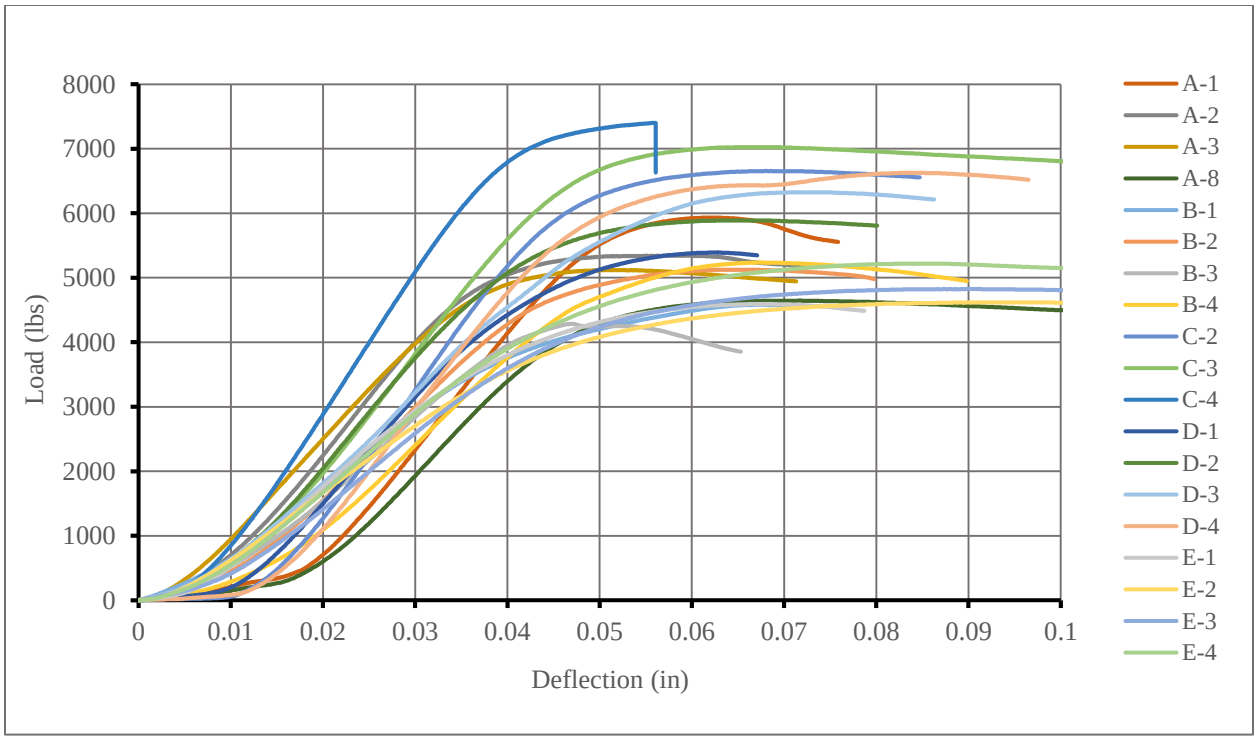

Figure 35: Force – displacement graph parallel to grain

Table 4: Ultimate compressive stress values

Compression Testing of Tie Specimens					
Parallel to grain			*Perpendicular to grain*		
Sample	Max load (lbs)	Fc (psi)	Sample	Max load (lbs)	Fc perp (psi)
A-1	5956	**5897**	A-4	3009	**1506**
A-2	5358	**5277**	A-5	3084	**1530**
A-3	5136	**5052**	A-6	3462	**1722**
A-8	4661	**4640**	A-7	2995	**1490**
B-1	4605	**4555**	B-5	3111	**1550**
B-2	5142.5	**5086**	B-6	2946	**1474**
B-3	4304	**4263**	B-7	4078	**2042**
B-4	5251	**5214**	B-8	3730	**1858**
C-1	5627.12	**5508**	C-5	4961	**2448**
C-2	6672.5	**6595**	C-6	5105	**2545**
C-3	7035	**6983**	C-7	4398.5	**2194**
C-4	7418	**7266**	C-8	4521	**2246**
D-1	5405	**5382**	D-5	4665	**2312**

D-2	5909	**5865**	D-6	4591	**2287**
D-3	6349	**6299**	D-7	4256	**2099**
D-4	6640	**6587**	D-8	3884	**1935**
E-1	4606	**4544**	E-5	4388	**2171**
E-2	4631	**4598**	E-6	4268	**2119**
E-3	4842	**4807**	E-7	3637.5	**1799**
E-4	5231.5	**5107**	E-8	3030.7	**1512**

The ultimate compressive strength values obtained from test data for samples tested in compression perpendicular to grain and parallel to grain respectively, were scaled as per ASTM D2915 and ASTM D245 to obtain NDS design values. Equation 8 was applied separately for each loading direction:

$$Test\ Statistic = R - Ks \qquad \text{Equation 8}$$

Where:

R = Mean compressive strength

K = Table 3 value (75% CI, 1-p = 0.95) from ASTM D 2915

n = Total number of samples

s = Standard deviation of the compressive strength values

Test Statistic = Material property being calculated (Compression perpendicular to grain or Compression parallel to grain)

Table 5: Table 3 in ASTM D2915

Table 3 in ASTM D2915					
n	**K-Factor**	**n**	**K-Factor**	**n**	**K-Factor**
10	2.104	23	1.908	120	1.747
11	2.074	24	1.901	140	1.739
12	2.048	25	1.895	160	1.733
13	2.026	30	1.869	180	1.727
14	2.008	35	1.849	200	1.723
15	1.991	40	1.834	250	1.714
16	1.977	45	1.822	300	1.708

17	1.964	50	1.811	350	1.703
18	1.952	60	1.795	400	1.699
19	1.942	70	1.783	500	1.693
20	1.932	80	1.773	1000	1.679
21	1.924	90	1.765	1500	1.672
22	1.916	100	1.758	Inf.	1.645

The test statistic was divided by a safety factor as shown in Equation 9 to obtain the scaled compressive NDS strength value. The safety factor was obtained from Table 8 in ASTM D 245 based on whether the sample was loaded in compression parallel or perpendicular to grain. For compression parallel to grain, the safety factor was 1.9 or 2.1 based on the results of wood species classification as can be seen in Table 6. For compression perpendicular to grain, the safety factor was chosen as 1.67.

$$Compressive\ strength = \frac{Test\ Statistic}{Safety\ Factor} \qquad \text{Equation 9}$$

Table 6: Safety factor from Table 8 ASTM D 245

Safety Factor - Table 8 ASTM D 245		
Loading	**Softwoods**	**Hardwoods**
Bending Strength	2.1	2.3
MOE in Bending	0.94	0.94
Tension Parallel	2.1	2.3
Compression Parallel to grain	1.9	2.1
Horizontal Shear	2.1	2.3
Proportional Limit and Stress at Deformation (Compression Perpendicular to grain and Connections)	1.67	1.67

The final scaled compressive strength of the wood in the direction perpendicular to grain was 1820 psi as shown in Table 7.

Table 7: Scaled compressive strength parallel to grain

Compressive strength parallel to grain		
Mean	5476.31	psi
Safety factor	2.10	(From Table 8, ASTM D 245)
K-factor	1.93	(From Table 3 ASTM D 2915 for n = 20)
Standard deviation	856.05	
Test Statistic	3822.42	
Scaled compressive strength		**1820 psi**

The final scaled compressive strength of the wood in the direction parallel to grain was 766 psi as shown in Table 8.

Table 8: Scaled compressive strength perpendicular to grain

Compressive strength perpendicular to grain		
Mean	1941.90	psi
Safety factor	1.67	(From Table 8, ASTM D 245)
K-factor	1.93	(From Table 3 ASTM D 2915 for n = 20)
Standard dev.	342.60	
Test Statistic	1280.00	
Scaled compressive strength		**766 psi**

After the compressive strength values they can be used in engineering design after they have been scaled as per NDS provisions. It was estimated that knowing the material properties and species of wood would be beneficial for performing finite element modeling that might be required as future work in this research project. NDS scaling procedures were also assumed to be beneficial should any further material testing (shear strength, tension perpendicular and parallel to grain) be required in the future.

3.2 Ties

The bridge ties used for this project were donated by Norfolk Southern railroad company and are shown in Figure 36. These bridge ties were removed from a bridge in North Carolina in

June 2017 after having been in service since 2003. The bridge ties had variable dimensions. The length of individual ties varied between 11 ft. to 12 ft. The cross-sectional dimensions also varied between 7.5 in. x 8 in. for the horizontal dimension and 12 in. x 10 in. for the vertical dimension. The ties had two daps (rectangular notches in the tie so that ties can rest on the bridge girder) one on either ends where they were placed on the bridge girder. The dap length varied from 13 in. to 23 in. and the dap height also varied from 0.25 in. to 2.5 in. It was also observed that some ties had a coating of grease on their surface as shown in Figure 37. The amount of grease that was varied from tie to tie with some ties not having any grease to some having a thick coating. All of the bridge ties which were used for testing purposes were selected as per AREMA standards for bridge ties, which specifies that ties having physical defects such as shakes or splits cannot be used in service (AREMA, 2017b).

Figure 36: Bridge ties donated by Norfolk Southern

Figure 37: Grease on bridge tie

The bridge ties were cut and prepared before they were used for structural testing. All the bridge ties had tie plates and bearing pads held in place by railroad spikes as shown in Figure 38. All the components of the rail fastening system such as bearing pads, tie plates, hook bolts and railroad spikes were removed from the ties prior to testing. Railroad spikes were pried out of the wood using a railroad spike puller. For testing purposes, each of these ties was cut into test samples, approximately 3.5 ft. in length using a chainsaw as shown in Figure 39. The chainsaw cuts on the

tie samples were uneven, therefore, the ends were squared up using a band saw to make them exactly perpendicular.

Figure 38: Bridge ties having tie plates, bearing pads, railroad spikes and hook bolts

Figure 39: Tie samples were cut with a chainsaw

3.3 Test Set up

For this research project, one half of the railroad track was simulated and the bridge girder, fastener and tie assembly were observed as a system. A schematic view of the experimental test set up of the simulated bridge assembly is shown in Figure 40. For further details regarding the structural test set up refer to Appendix C. This set up was used for structural testing to quantify the overall lateral resistance of the tie, girder and fastener assembly both independently and jointly.

The test frame consisted of W21x62 columns which were 15 feet tall and spaced 8 feet apart. W21x62 crosshead beams were connected to the columns with six A325 bolts having a diameter of 3/4” per connection, at an elevation of 13 ft. from the ground. Each column was fastened to the strong floor by four A490 bolts having a diameter of 1in. A 220 kip MTS actuator was attached to the crosshead of the load frame through a W21x101 stub section which was 21 inches long.

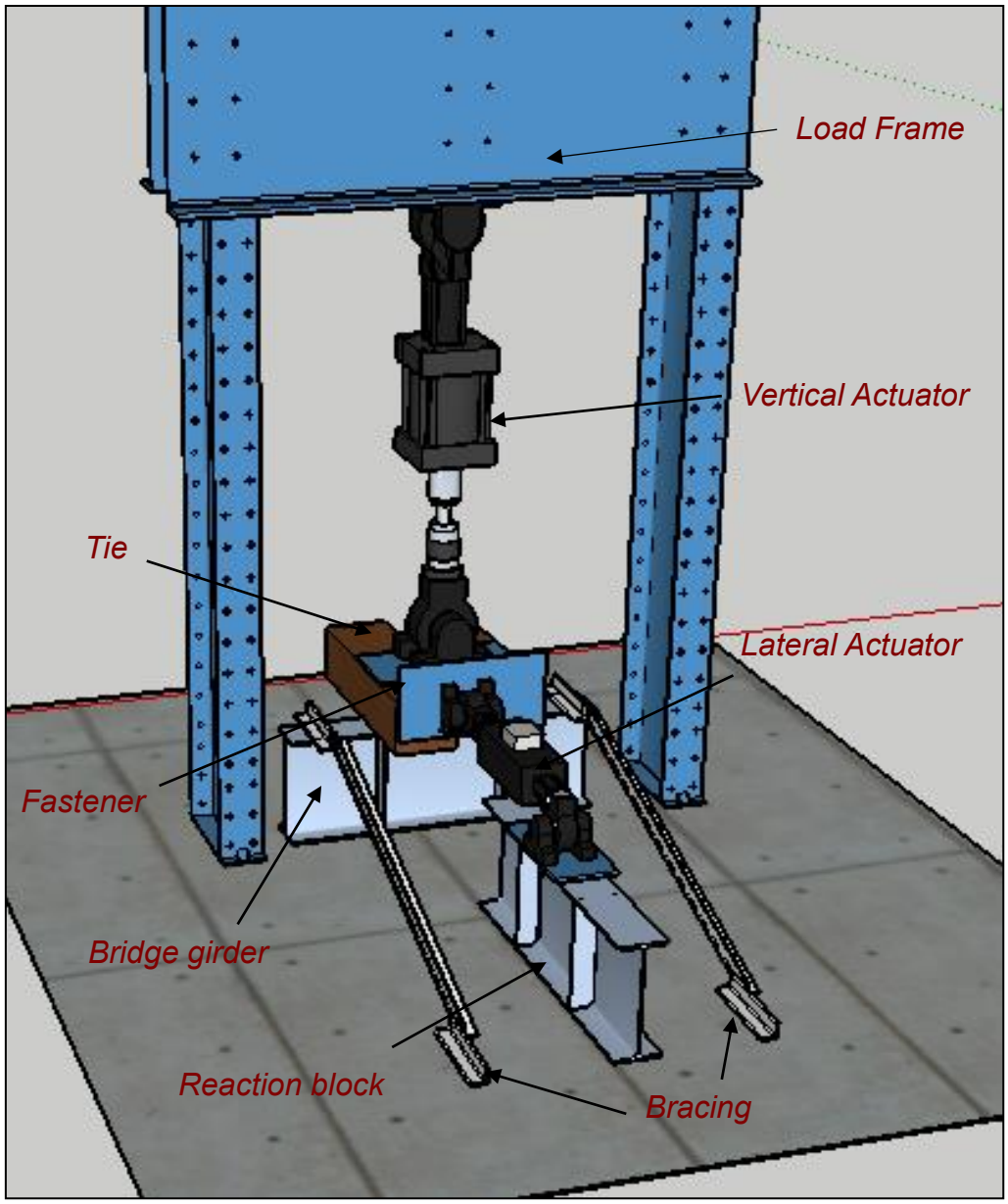

Figure 40: Schematic view of experimental bridge assembly

Two identical W27x235 sections were used as a part of the tie and fastener assembly as the reaction block and the bridge girder section. Both W27x235 sections had four vertical stiffeners which were 0.5 in. thick. One W27x235 section was used as the bridge girder and the second W27x235 section which was used as a reaction block was placed perpendicular to the W27x235 bridge girder section and connected to the strong floor using four A490 bolts having a diameter of 1in. A 55 kip MTS actuator was attached to the reaction block using four bolts. Four 3.5in. spacers and a 1in. thick 14" x 30" plate was used to connect the actuator to the reaction block. Two L3x3x1/2 angle sections were used as bracing members in order to prevent weak axis bending of the W27x235 bridge girder section. The 55 kip actuator was chained to the reaction block in order to prevent the actuator from lifting up or kicking back during testing. The chain used as a bracing mechanism for the actuator had a capacity of 10 kip and was wrapped around the reaction block as shown in Figure 41.

Figure 41: Structural Test set up

The W27x235 section which was used as the bridge girder was connected to the strong floor by fourteen A490 bolts having a diameter of 1 in. Four 3.5 in. spacers and a 30” x 14” plate having a thickness of 1 in. was attached to the top of the W27x235 bridge girder section as shown in Figure 42 using four A490 bolts of diameter 1”. Since the 55-kip lateral actuator was raised by 3.5 in. because of spacers that connected it to the W27x235 reaction block, lateral force was applied above the center of the tie. It was necessary for the center of the tie to be on the same level as the 55 kip actuator in order to prevent a potential moment in the tie that would cause the tie to

push upwards. The 14” x 30” steel plate was used to raise the vertical elevation of the tie so that the line of application of the lateral force was on the same level as the tie.

Figure 42: 14” x 30” steel plate attached to the W27x235 bridge girder section

The bridge girder, tie and fastener system for one half of the railway track is shown in Figure 43. Three major factors were identified in this system that contribute towards the overall lateral resistance of a curved railroad bridge:

1. Friction resistance between the surface of the bridge tie and the flange of the steel girder due to axle loads
2. Resistance of the fastener (bearing against the wood of the tie, tension in the fastener, fastener bearing against the top flange of the steel girder)
3. Resistance from the dap in the bridge tie when it bears against the flange of the bridge girder.

Each of these contributing factors were decoupled and quantified individually to determine how each one contributes to overall lateral resistance. Experimental testing was completed in phases to quantify the contribution of each of the three lateral resistance factors.

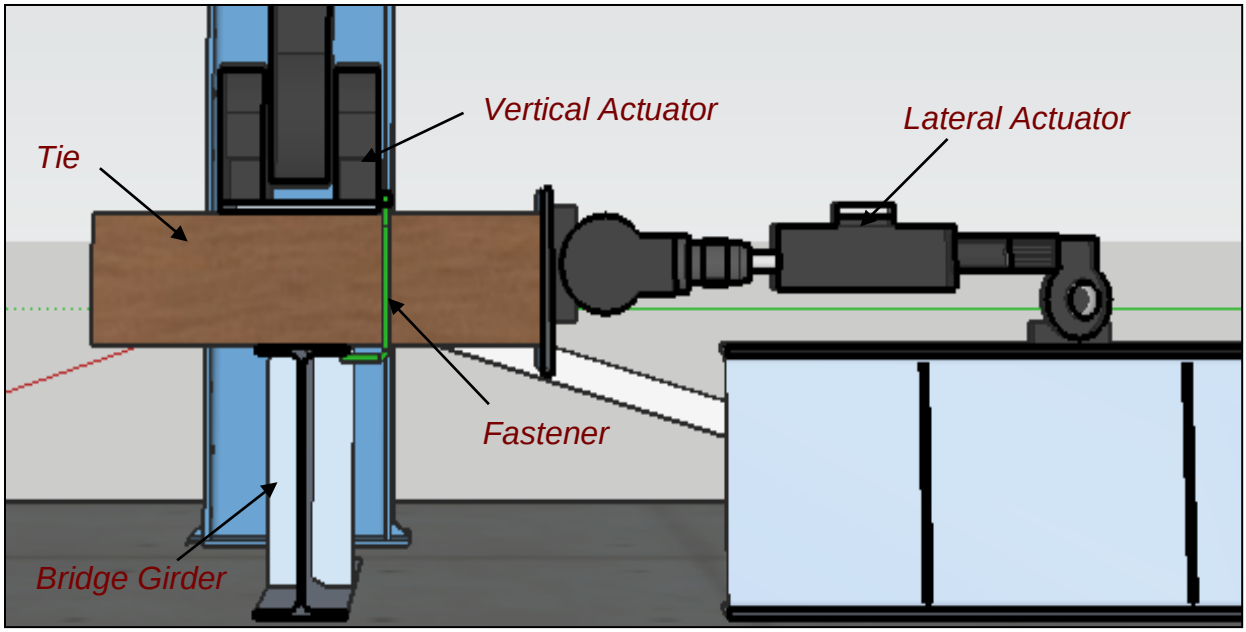

Figure 43: Resistance Contributions

3.4 Friction Contribution

The methods used for the isolation of lateral resistance due to the friction between the bridge tie and the surface of the girder flange is explained in sections 3.4.1 and 3.4.2.

3.4.1 Friction Coefficient

The friction between the surface of the flange of the bridge girder and the surface of the bridge tie resting on the flange, is a function of the normal force multiplied by the coefficient of friction between steel and wood. The equation relating the normal force, friction force and the friction coefficient is:

$$F = \mu N$$

Where:

F = Friction force

N = Normal force

μ = Coefficient of friction

The normal force in the tie, girder and fastener assembly is the gravity load from the train passing over the railroad bridge that is transferred to the tie from the rails. Since only one half of the bridge track structure is being considered, only half of the gravity load from the train is transferred to the girder, tie and fastener assembly. As the normal load increases, the friction force between the surface of the bridge tie and the flange of the bridge girder also increases, thus increasing the lateral resistance of the system against centrifugal forces generated by the train. The friction force is directly proportionate to the magnitude of the gravity load from the train. Loads from the train are a function of multiple factors such as the speed of the train, freight type of the train and the curve geometry of the railroad bridge. Frictional resistance is maximum when the loads from the train are high and it is less when the loads from the train are smaller.

3.4.2 Friction Testing

To determine the contribution of friction to overall lateral strength, undapped ties were tested without a fastener, thus eliminating strength contributions from the fastener and the dap. A 220 kip vertical actuator was used to simulate gravity loads from the train by applying a vertical load on the tie. A 55 kip lateral actuator was used to load the tie in the horizontal direction. Observations from the railroad bridge surveys showed that the edge of the bridge tie was approximately 27 in. to 28 in. away from the rail, or the point of application of the normal force from the train. Since the flange of the W27x235 section used as the bridge girder for testing was 14 inches wide, the undapped tie was placed on the plate attached to the girder section such that the end facing the 55 kip actuator was 20 inches away from the edge of the girder flange, as shown in Figure 44.

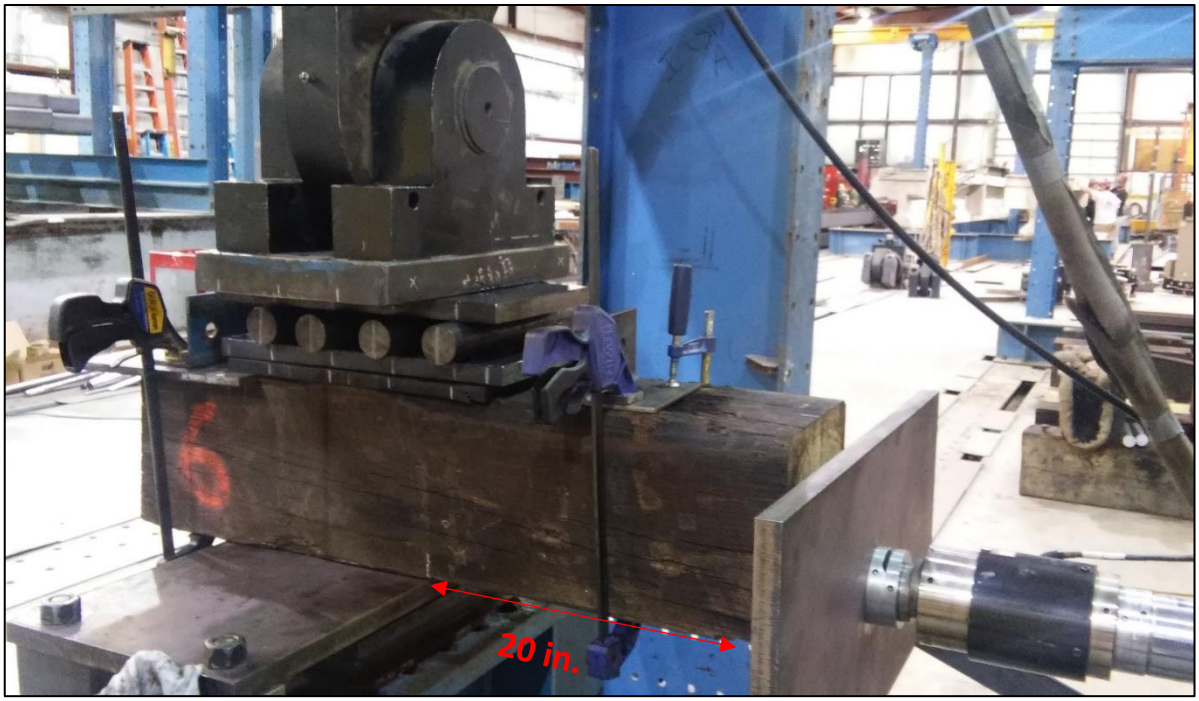

Figure 44: Undapped tie without a fastener

Based on the magnitude of the vertical wheel loads given in Table 3, vertical wheel loads ranging between 5 kip and 45 kip at 10 kip intervals were used for testing. The 220 kip vertical actuator was used to apply a constant vertical load on the tie and the 55 kip horizontal actuator was used to apply a ramp load at the rate of 1 inch/minute on the tie till a final displacement of 2 inches was reached. Jim Carter from Norfolk Southern provided information regarding lateral failure in the railroad industry where 2 inches of displacement in the tie represents track failure since it signifies a lateral displacement of 2 inches in the track which is a cause for train derailment (Carter, personal communication, November 9, 2017).

In order to load the tie vertically, bearing pads were placed on top of the tie and a greased 10” x 18” steel plate was placed on it. The vertical load from the actuator was kept constant during tie displacement by placing four rollers having a diameter of 2 in. on top of the steel plate. Another greased steel plate having similar dimensions of 10” x 18” was placed on top of the rollers, which was in contact with the 18” x 12” x 2” plate attached to the actuator. Bearing pads, rollers and

greased steel plates that were used to load the tie vertically are shown in Figure 45. Teflon grease was used to further reduce the friction between the plates and the rollers. The rollers and plates were placed at exactly the same position underneath the vertical actuator for every test. White lines marking the position of bearing pads, steel plates, rollers and the actuator plate are shown in Figure 45. Two 8 inches long angle sections were clamped to the top of the tie on either side of the vertical actuator. These were installed as a safety measure in order to restrict the movement of rollers during testing in case they suddenly rolled out from between the load bearing steel plates.

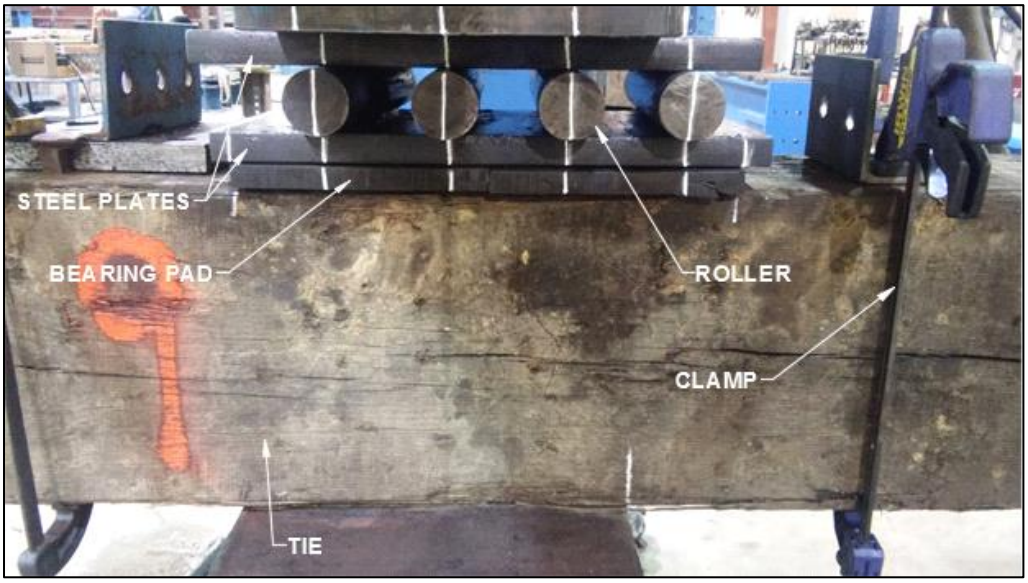

Figure 45: Bearing pads, rollers and greased steel plates

Five tests were conducted per tie for five tie samples at vertical loads of 5 kip, 15 kip, 25 kip, 35 kip and 45 kip where the vertical load was held constant and the tie was pushed laterally at a load rate of 1inch per minute till a displacement of 2 inches was obtained. The sequence in which each of these five tests were conducted per tie, varied for each tie, so that changes in test results due to loading and reloading of a tie sample could be observed. The order in which tests were conducted for each tie is shown in Table 9. Tie samples were photographed before and after testing. The steel plate on which the tie samples were placed for testing, was cleaned before every test to

prevent variations in the friction surface due to the presence of creosote, wood particles and rail lubricant that were present on the surface from the tie sample from the previous test.

Table 9: Test order of tie samples

Tie sample	Applied Vertical Load				
	5 kip	15 kip	25 kip	35 kip	45 kip
Tie 2	1st	2nd	3rd	4th	5th
Tie 3	5th	1st	2nd	3rd	4th
Tie 4	1st	2nd	3rd	4th	5th
Tie 5	3rd	4th	5th	1st	2nd
Tie 8	4th	5th	1st	2nd	3rd

Prior to using the combination of bearing pads, rollers and steel plates to load the tie vertically, tests were attempted by only using rollers, without any Teflon grease or steel plates. These preliminary tests did not perform well because the surface of the tie was uneven and vertically loading the tie with only the rollers as points of contact made the system unstable when the tie was pushed laterally. The test was stopped when the rollers disengaged from under the vertical actuator and force from the lateral actuator was then resisted by the shaft of the vertical actuator in flexure. The tie could not displace 2 inches successfully when only rollers were used for vertical loading. The next attempt at loading the tie vertically involved using a steel plate and Teflon grease in order to increase the contact area between the vertical actuator and the tie as shown in Figure 46. The surface between the plate and actuator was greased to enable lateral movement of the plate with the tie during the application of lateral load.

Figure 46: Steel plate with Teflon grease

The method of vertically loading the tie was successful for vertical loads of 5 kip and 15 kip where the tie displaced by 2 inches as shown in Figure 47. Using only the steel plate with Teflon grease did not work for the higher range of vertical loads at 25 kip, 35 kip and 45 kip because the grease between the steel plate and the actuator plate was not sufficient to overcome the increased friction due to application of higher vertical loads. Therefore, the tie did not displace 2 inches laterally. A combination of rollers and greased steel plates was then attempted to laterally displace the tie by 2 inches which proved to be successful. In order to isolate the friction component, all the tests were conducted with a combination of rollers and greased steel plates.

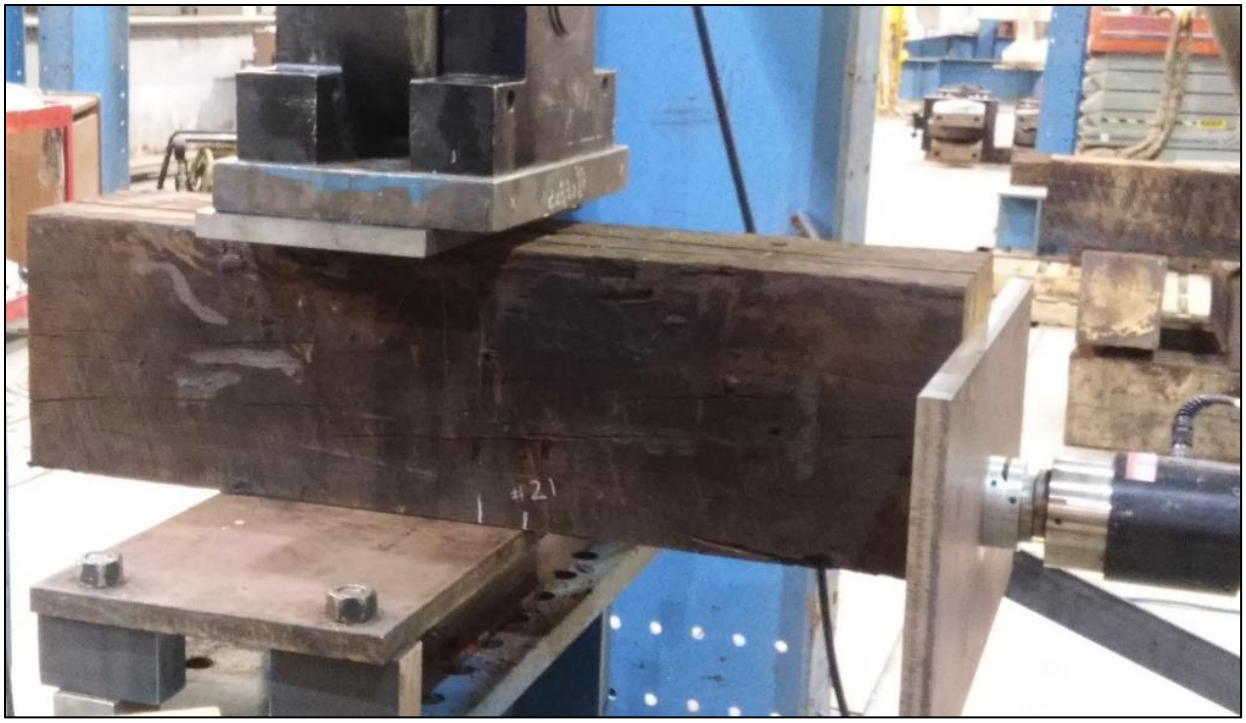

Figure 47: Displaced tie and greased steel plate after friction testing

3.5 Fastener Contribution

The centrifugal forces generated due to the passing of a train on a curved bridge are resisted by the fastener loaded in shear when it bears against the top flange of the bridge girder. Hook bolts also provide bearing resistance when the body of the hook bolt, passing through the tie, bears against the wood of the tie. The test set up was altered for testing the contribution from fasteners. The 55 kip lateral actuator was replaced by a 110 kip lateral actuator. A higher lateral load was needed for testing all the fasteners, ties with daps and full assembly tests. The 110 kip actuator was bolted and also chained to the W27x235 reaction block using four A490 bolts of diameter $1^{1/4}$" as shown in Figure 48. The 30" x 14" plate which was originally attached to the 55 kip actuator was then attached to the clevis of the 110 kip actuator.

Figure 48: 110 kip horizontal actuator

The axis of the 110 kip actuator was not parallel to the ground because the actuator support resting on the flange of the reaction block made the actuator angle slightly upwards. To correct the direction of application of lateral force and make the actuator exactly parallel to the ground, three washers were used to raise each bolt that connected the actuator to the W27x235 reaction block as shown in Figure 49.

Figure 49: 110 kip actuator raised by washers

3.5.1 Square Body Hook Bolt Testing

The tie samples used for testing square body hook bolts were prepared similarly to the tie samples that were used for testing the Lewis forged hook bolts. The test set up also remained unchanged from what was used for the forged hook bolts. Square body hook bolts were installed and tightened similar to the square body hook bolt and the tie was held in place by two angle sections clamped using bridge clamps as shown in Figure 50. Once the square body hook bolt was installed, a lateral force was applied to the tie at a load rate of 1 inch/minute until a final displacement of 2 inches was recorded. Five square body hook bolts were tested for this research project. In order to determine the ultimate capacity of a square body hook bolt, one fastener was tested using the same load rate of 1 inch/minute beyond 2 inches of displacement till the fastener failed.

Figure 50: Installed square body hook bolt

3.5.2 Lewis Forged Hook Bolt Testing

Tie samples which were used for testing the Lewis forged hook bolt were pre-drilled before installing the fastener. Each hole was adjacent to the edge of the steel plate at approximately 20 inches away from the end of the tie sample which was pushed laterally. The 1-inch diameter hole was drilled using a Hole Hawg drill which had a drill bit that was 12 inches long, so that the hole could go through the entire height of the tie. Lewis forged hook bolts were installed from below the 30”x 14” steel plate such that the hook was securely clamped to the edge of the plate as shown in Figure 51.

Figure 51: Round body hook bolt attached to 30" x 14" steel plate

The hook bolt was secured to the top of the tie using a bridge washer and snug tightened using two ¾ inch hexagonal nuts as seen in Figure 52. The first nut was snug tightened uing a cresent wrench and the second nut was then threaded on top of the first nut and snug tighened. In order to prevent the tie sample from moving out of the line of application of lateral force during testing, a L3x3x1/2 angle section was placed on the steel plate, along both sides of the tie. Each angle was held in place by two bridge clamps which were snug tightened as shown in Figure 53.

Figure 52: Bridge washer and round body hook bolt secured with two nuts

After the forged hook bolt was installed and tightened, a lateral force was applied to the tie at a load rate of 1 inch/minute until a final displacement of 2 inches was recorded. Five forged

hook bolts were tested until each tie sample was displaced by 2 inches. In order to determine the ultimate capacity of a forged hook bolt, one fastener was tested using an identical load rate of 1 inch/minute beyond 2 inches of displacement until the fastener failed.

Figure 53: L3x3x1/2 angles clamped using bridge clamps to prevent tie movement

3.5.3 Quikset Anchor Testing

Quikset Anchors were pre-assembled on the ground where the Quikset bracket was installed on two tie specimens. The ties were aligned against the flange of a W-section at the lab and were spaced 5.5 in. apart from edge to edge since nominal edge to edge spacing for bridge tie varies between 4in. – 6 in. The bracket was then placed on top of the ties at a length of 21.5 inches from the edge of the ties that would be loaded laterally, and its position was marked. The ties were pre-drilled where the bracket holes were on the ties, using a spade bit of diameter 3/8 in. The bracket was then secured to the ties by drilling lag screws using an air wrench. Two 2x4 members were screwed into both ties at either ends to hold the ties in position while lifting and mounting

the assembly on top the 14” x 30” steel plate. The assembled ties were aligned after they were mounted so that the bracket was centered with the point of lateral load application. The tie and bracket assembly along with the dimensions used during pre-installation are shown in Figure 54.

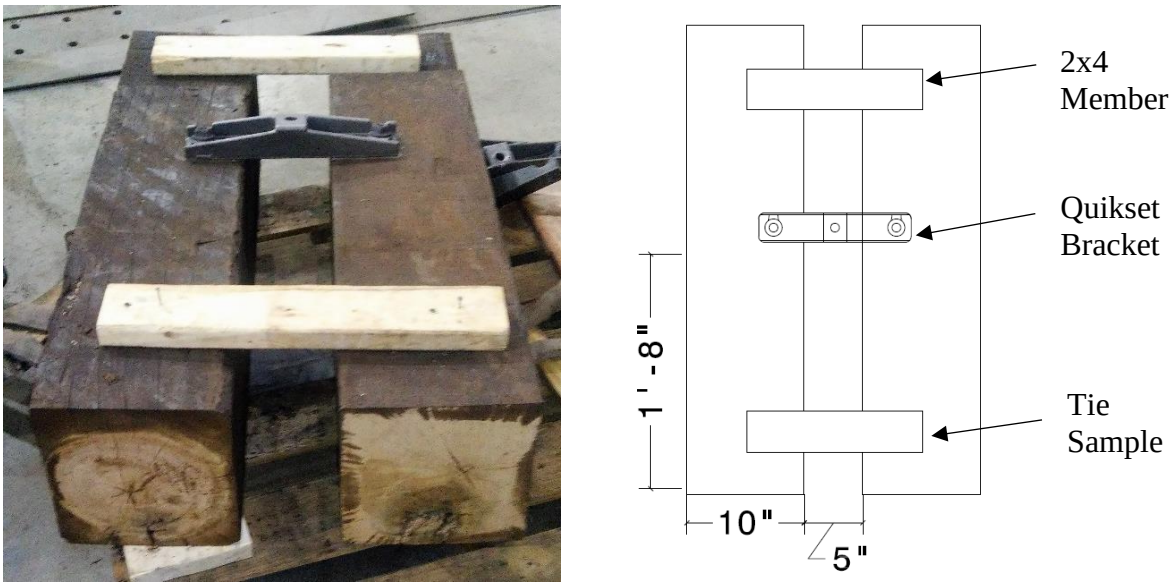

Figure 54: Quikset Anchor assembly

After the assembly was mounted and aligned, a hook bolt with a lock plate was inserted through the bracket. The hook bolt was given a few taps using a hammer from below to ensure that the hook bolt and lock plate were properly engaged to the steel plate. The hook bolt was then bolted to the steel plate using a ¾ inch diameter washer and two ¾ inch diameter hexagonal nuts. The first nut was installed first and snug tightened using a wrench. The nut, bolt and washer were marked after being snug tightened and a cheater bar of length 40 in. was used to tighten the nut by one full turn before installing the second nut. The second nut was also tightened using a cheater bar. The ties were held in place using L3x3x1/2 angle sections clamped to the simulated top flange in place using bridge clamps as shown in Figure 55. Both the 2x4 members were removed prior to testing. A total of five samples were tested at a load rate of 1 inch per minute till a final

displacement of 4.5 inches was achieved. One Quikset anchor was tested without a lock plate to investigate the effect of the lock plate on fastener resistance.

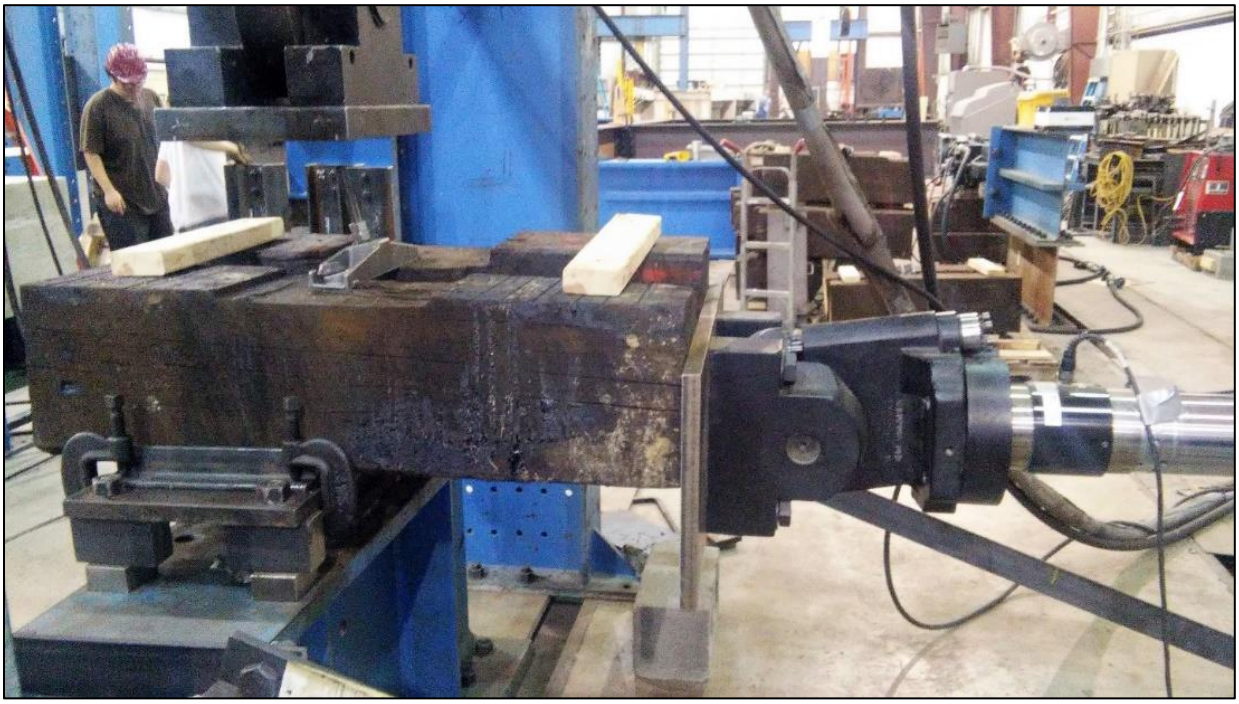

Figure 55: Installation of Quik-set anchors

3.6 Dap Contribution

Dapped tie samples were used for testing the contribution to lateral resistance from the dap. Tie sample used for dap testing did not have any pre-drilled holes since no hook bolts were required. The dapped portion of the tie was placed on the steel plate such that the end facing the horizontal actuator was approximately 18-20 inches from the edge of the steel plate as shown in Figure 56. When the tie was loaded with the actuator plate pushing against the entire cross section of the tie, the dapped portion of the tie failed in parallel shear at a lateral load of 53.6 kips. The failed tie is shown in Figure 58 and Figure 58. The ultimate failure strength was not representative of the actual strength of the dap since the full cross section of the tie was loaded, which prevented the dap from failing in shear at the ultimate shear strength of the wood.

Figure 56: Dapped tie sample prior to testing

Figure 57: Parallel shear failure of the dap

Figure 58: Shear failure of the dap (other side)

The test set up was modified to load only the top portion (undapped portion) of the tie so that the dapped portion could shear by bearing against the flange of the bridge girder. A 10 inch x 30 inch steel plate was attached to the actuator plate using steel hangars as shown in Figure 59 so that only the top portion of the tie could be loaded. The tie began to lift up over the bridge flange once the lateral load was applied as shown in Figure 60. This was because the lateral load was

eccentric to the center of rotation, which was where the dap was in contact with the bridge flange, creating a moment in the tie and causing it to lift up over the bridge flange.

Figure 59: Loading the undapped portion of the tie

Figure 60: Tie lifting up during loading

Since the test set up could not be modified successfully to load only the undapped portion of the tie, each of the individual tie samples were modified to induce a shear failure in the dap. The ties were notched at a distance of 12 inches away from the edge of the bridge flange. The notch was 1-inch thick and its depth was the same as the dap depth of the tie as shown in Figure 61. Therefore, the notch depth varied with the depth of the dap for each tie sample. Creating a notch in the tie caused a shear failure to occur without creating a moment in the tie. It also kept the length of the shear plane constant by restricting the occurrence of the dap failure between the notch and the edge of the bridge flange. For this research project five dapped ties were notched and tested. They were laterally loaded at a rate of 1 inch/minute till dap failure occurred. The tie width and dap depth for each tie were recorded before testing.

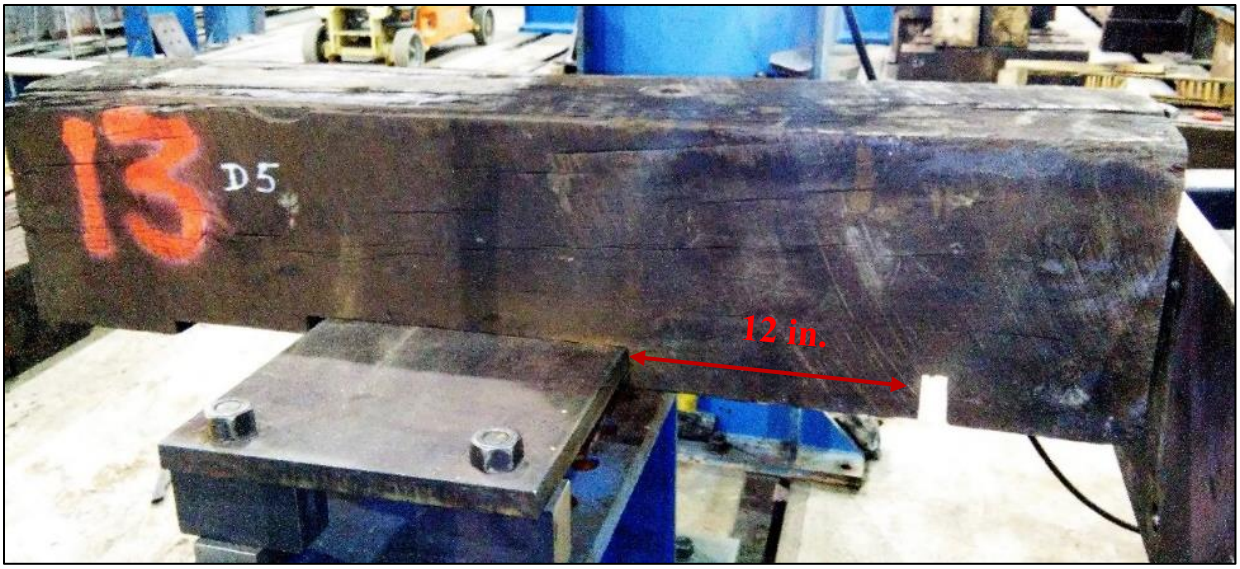

Figure 61: Dapped tie with a 1 inch thick notch

CHAPTER 4: RESULTS AND DISCUSSION

This chapter presents the results from the data obtained using the structural testing methods and procedures described in Chapter 4.

4.1 Friction Contribution

Two kinds of friction coefficients were calculated from the data obtained by varying the normal force on the tie. Horizontal load versus horizontal displacement graphs were plotted for all the ties that were tested. As per ASTM G115 – 10 Measuring and Reporting Friction Coefficients, a system with a higher static friction than its kinetic friction, henceforth referred to as Case 1, exhibits a large breakaway force before it begins sliding as shown in Figure 62 (ASTM Standard, 2013).

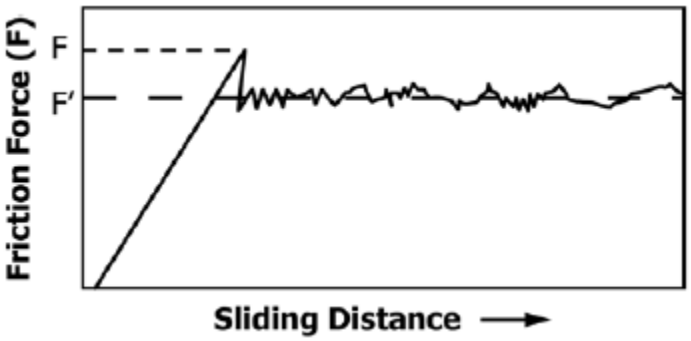

Figure 62: Case 1 - Force vs. displacement plot for a system with a high breakaway force

Case 1:

The kinetic friction coefficient is calculated using F' as per Equation 10.

$$\mu_{kinetic} = \frac{F'_1}{N} \quad \text{Equation 10}$$

.

The static friction coefficient is calculated using F as per Equation 11.

$$\mu_{static} = \frac{F_1}{N} \quad \text{Equation 11}$$

Where:

F'_1 = Average force required to overcome kinetic friction after initial slip

F_1 = Peak breakaway force required to overcome static friction and cause slip

N = Normal force

However, all the tie specimens that were tested for determining the lateral resistance due to friction, exhibited a very small breakaway force with the kinetic friction coefficient being greater than the static friction coefficient henceforth referred to as Case 2 and shown in Figure 63. The second friction model represents the lack of interlocking between the two friction surfaces, wood and steel, thus exhibiting no breakaway force.

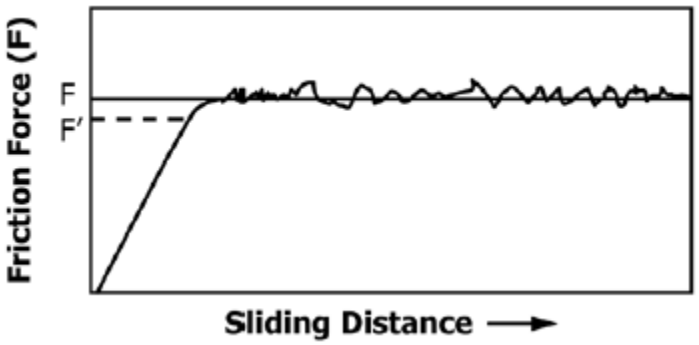

Figure 63: Case 2 - Force vs. Displacement plot for a system with no breakaway force.

Case 2:

The kinetic friction coefficient is calculated using F_2 as per Equation 12.

$$\mu_{kinetic} = \frac{F_2}{N} \qquad \text{Equation 12}$$

.

The static friction coefficient is calculated using F_2'

$$\mu_{static} = \frac{F'_2}{N} \qquad \text{Equation 13}$$

Where:

F_2 = Average force required to overcome kinetic friction after initial slip

F'_2 = Peak force required to overcome static friction and cause slip

For analyzing where F' lay on a graph the slope at each point on the lateral force versus lateral displacement graph was calculated. F' was located at the point on the plot where there was a sudden decrease in the slope between two points. F was calculated by averaging all the lateral force values on the graph following F' as specified in ASTM G115.

4.2 Friction Test Results

For all tests that were conducted to determine the lateral resistance due to friction, the lateral displacement was recorded in the tie up to a maximum of 2 in. The railroad industry considers 2 in. of lateral displacement in a bridge tie as track failure because of the potential for train derailment. Therefore, the data for all the tests was analyzed for lateral displacements ranging between 0 – 2 in. Figure 64 shows the position of the tie, the steel plates, bearing pad and rollers prior to testing. Figure 65 shows the roller position at the completion of testing. The steel plate above the rollers moved to the right, relative to the tie whereas the bearing pad and the steel plate on top of the bearing pad did not move relative to the tie. Depending on the surface condition of the ties that were tested, grease or lubrication on the sliding surface of the tie was transferred after each test to the steel plate which supported the tie. It was observed that all the results of tests conducted to determine frictional resistance conformed to Case 2 described in ASTM G115 for materials without a breakaway force before initial slip.

Figure 64: Tie, steel plates, rollers and bearing pads before testing

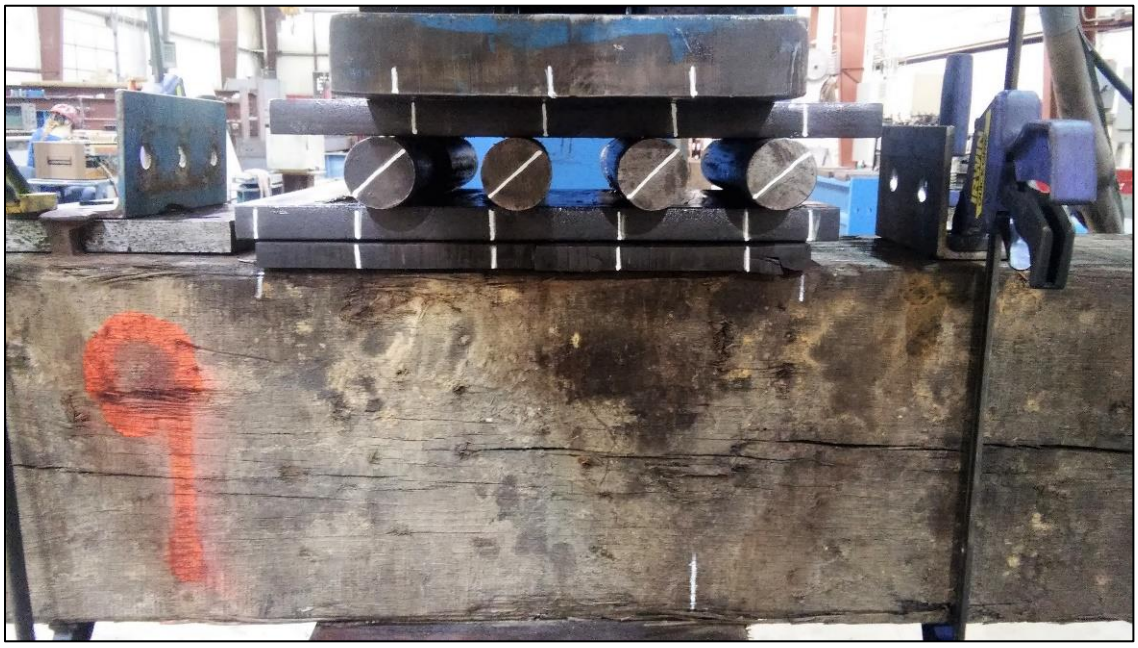

Figure 65: Tie, steel plates, rollers and bearing pads after testing

Results from all tie samples which were tested to study lateral resistance from friction are presented in sections 4.2.1 to 4.2.7. All the tie specimens are described in the order in which they

were tested. Tie 1 and Tie 7 were not included as a part of the results for this research project since they were used for preliminary tests which were conducted to ensure that there were no issues in the structural test set up.

4.2.1 Tie 2

The lateral force versus displacement graph for Tie 2 can be seen in Figure 66. Five lateral push tests were done, starting at a vertical load of 5 kip and increasing the vertical load in 10 kip increments. The lateral load increased at the same rate for each test as shown in the plots for all five tests, which have a similar slope before initial slip of the tie occurred. After initial lateral movement of the tie, the lateral load remained relatively constant for each test. It was observed that lateral resistance was directly proportionate to the magnitude of the applied vertical load. Fluctuations in the lateral load were attributed to the stick slip behavior of the tie which is a function of surface interaction of the tie and the steel plate supporting the tie under the application of lateral load. The tie surface was clean of any grease. The steel plate supporting the tie was free of grease after each test was completed, as seen in Figure 67.

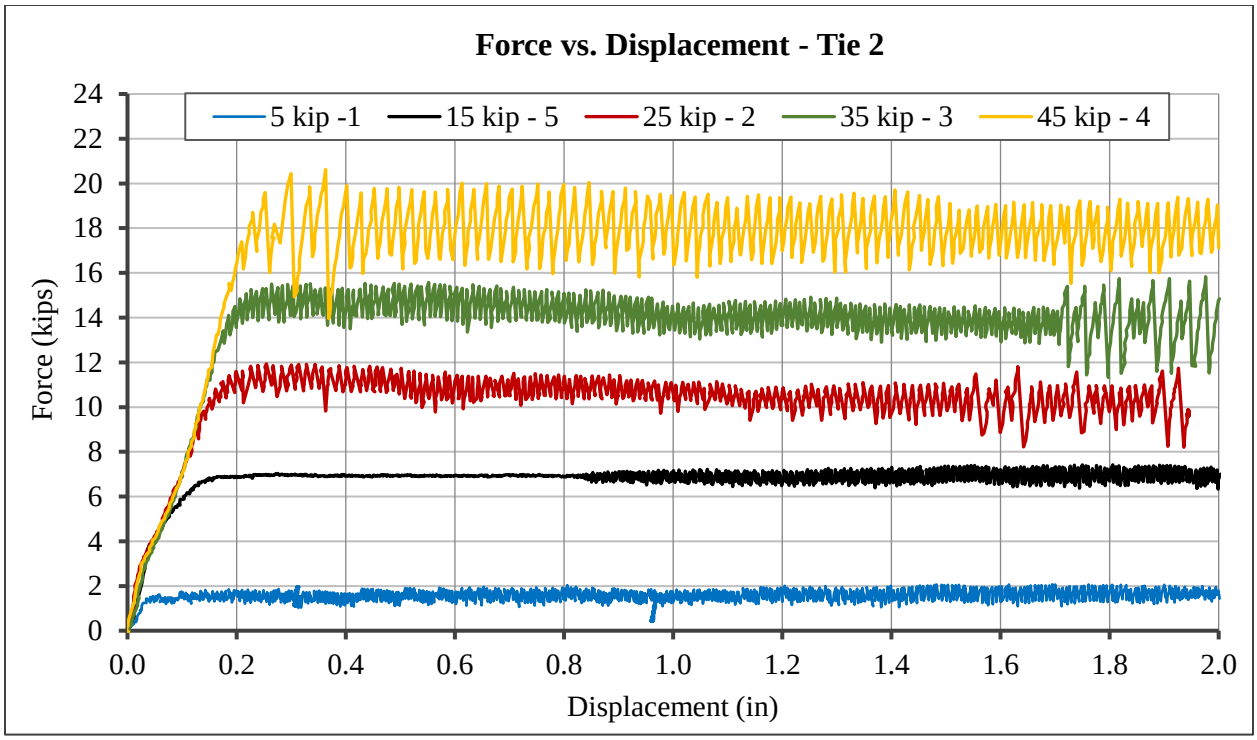

Figure 66: Lateral Force vs. Lateral Displacement for Tie 2

Figure 67: Steel plate after lateral push tests on Tie 2

4.2.2 Tie 3

The lateral force versus displacement graph for Tie 3 can be seen in Figure 68. The first test was conducted at a vertical load of 15 kip. Tie 3 did not exhibit stick slip behavior. The tie surface sliding over the steel plate had grease on it which remained on the plate after each test was completed as can be seen in Figure 69. It is estimated that the slight increase in lateral load after initial slip for each test is due to the resistance provided by the dried grease on the tie surface. The lateral load increased at a similar rate for each lateral test before initial slip of the tie occurred. Lateral resistance was proportionate to the vertical force applied on the tie.

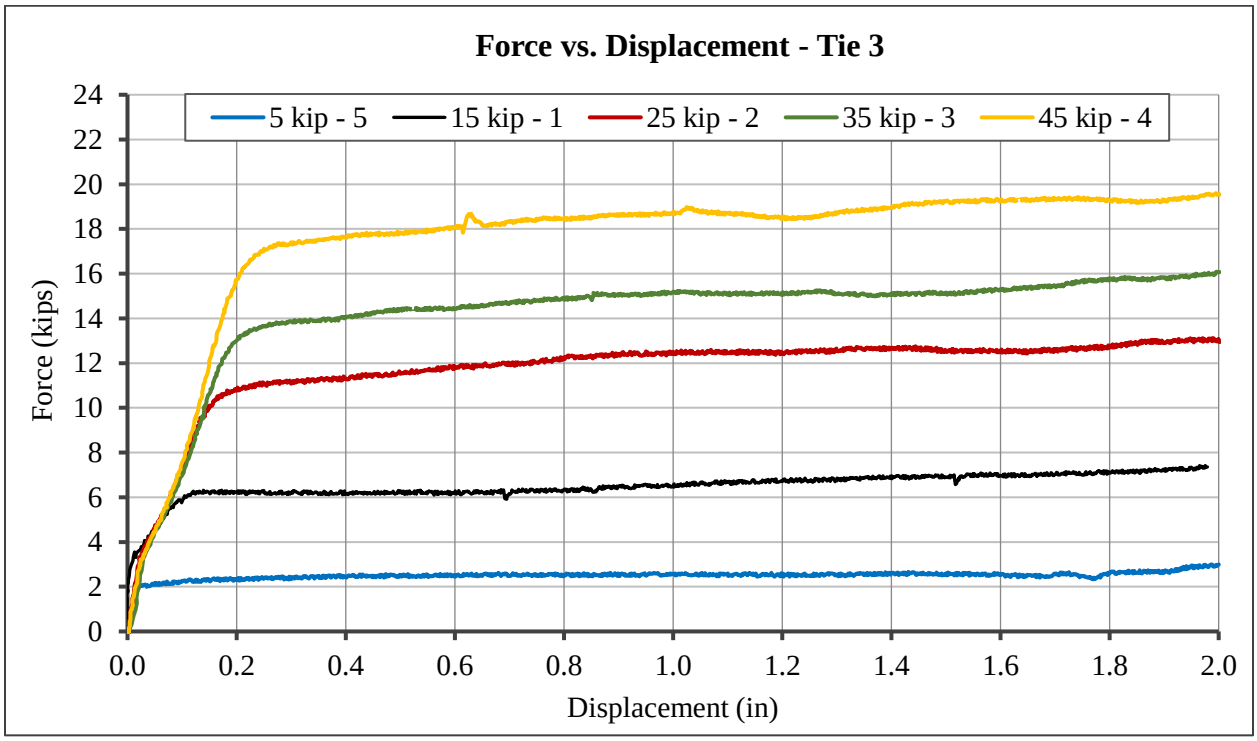

Figure 68: Lateral Force vs. Lateral Displacement for Tie 3

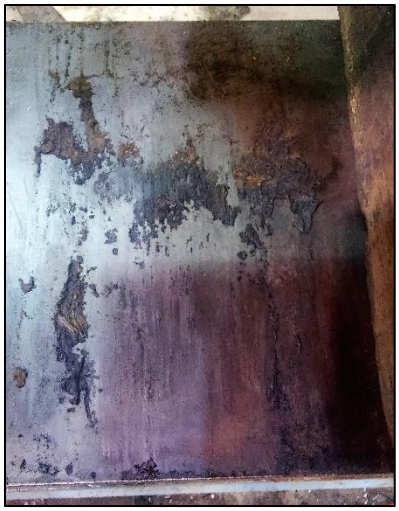

Figure 69: Steel plate after lateral push tests on Tie 3

4.2.3 Tie 4

The lateral force versus displacement graph for Tie 4 can be seen in Figure 70. The first test was conducted at a vertical load of 5 kip. The lateral load increased at a similar rate for lateral push tests conducted at all vertical loads except for the test where a vertical load of 45 kip was applied. It is possible that a variation in original tie alignment caused the lateral load to increase at a different rate. The sliding surface of Tie 4 was clean of any rail lubricant or grease. There was relatively less grease remaining on the steel plate after testing as can be seen in Figure 71. Similar to Tie 2 and Tie 3, it was observed that lateral resistance was proportionate to the magnitude of the vertical load.

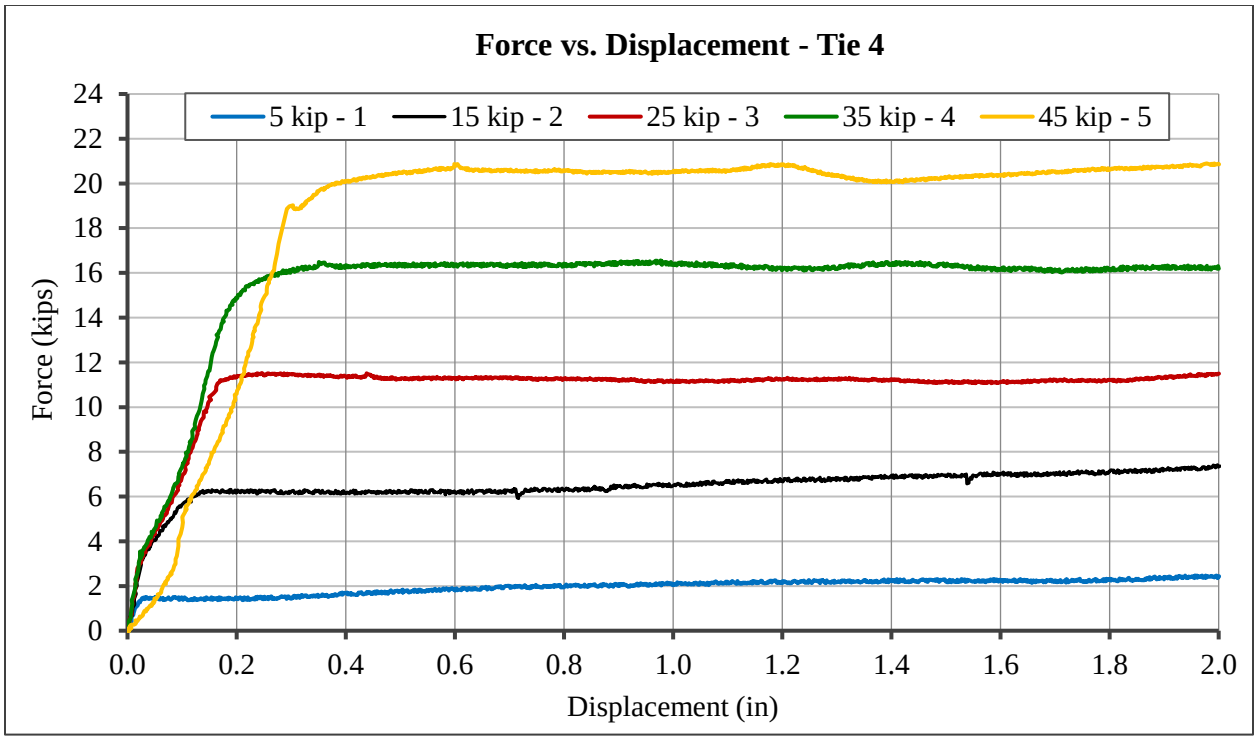

Figure 70: Lateral Force vs. Lateral Displacement for Tie 4

Figure 71: Steel plate after lateral push tests on Tie 4

4.2.4 Tie 5

The lateral force versus displacement graph for Tie 5 can be seen in Figure 72. The first test was conducted at a vertical load of 35 kip. The lateral load increased at the same rate for all

five lateral push tests. The sliding surface of Tie 5 was free of any lubricants and very little grease remained on the steel plate after lateral testing as can be seen in Figure 73. From Figure 72 it can be observed that the lateral load for all five tests peaked after a displacement of 1.8 in. was recorded in the tie. It is estimated that this increase in lateral load was caused due to imperfections or irregularity in the tie.

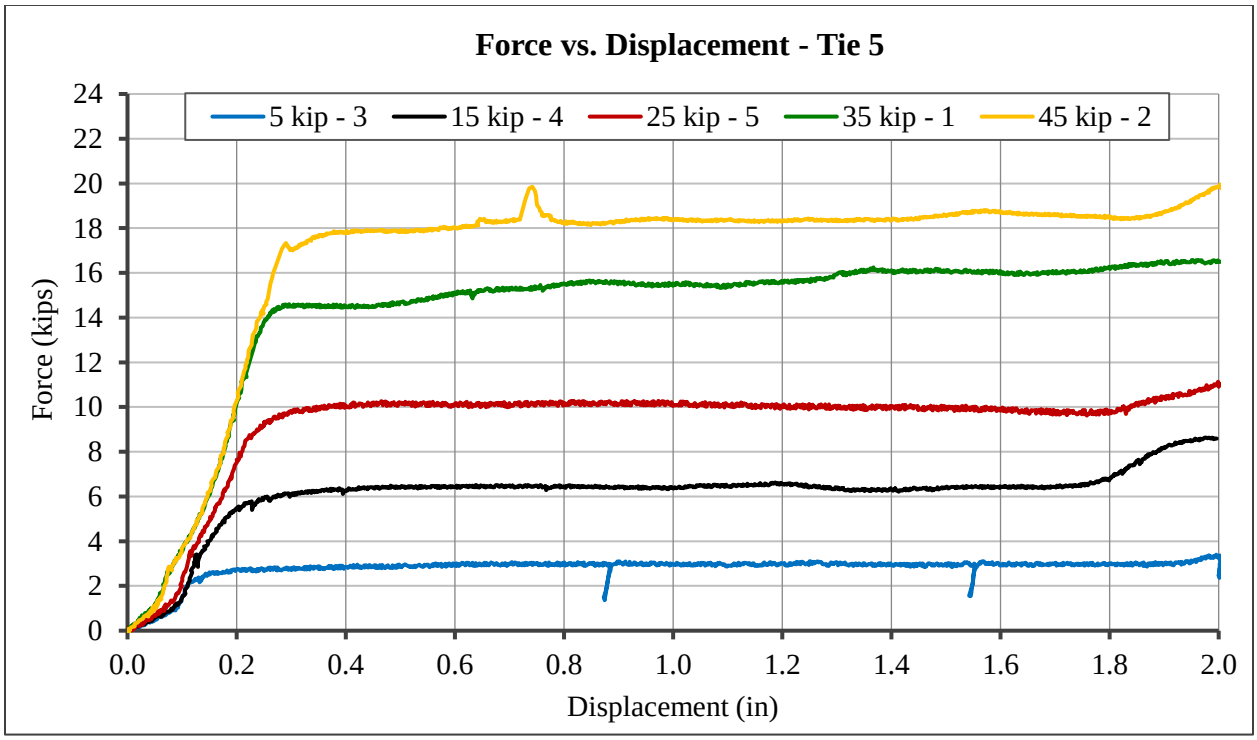

Figure 72: Lateral Force vs. Lateral Displacement for Tie 5

Figure 73: Steel plate after lateral push tests on Tie 5

4.2.5 Tie 8

The lateral force versus displacement graph for Tie 8 can be seen in Figure 74. The first test was conducted at a vertical load of 25 kip. The load rate increased at a similar rate for all the tests. It is estimated that this was caused by an uneven sliding surface. A thin layer of wood was scraped off from the sliding surface of the tie while testing. The tie surface had a significant amount of grease or lubricant. Grease and wood chips remaining on the steel plate can be seen in Figure 75.

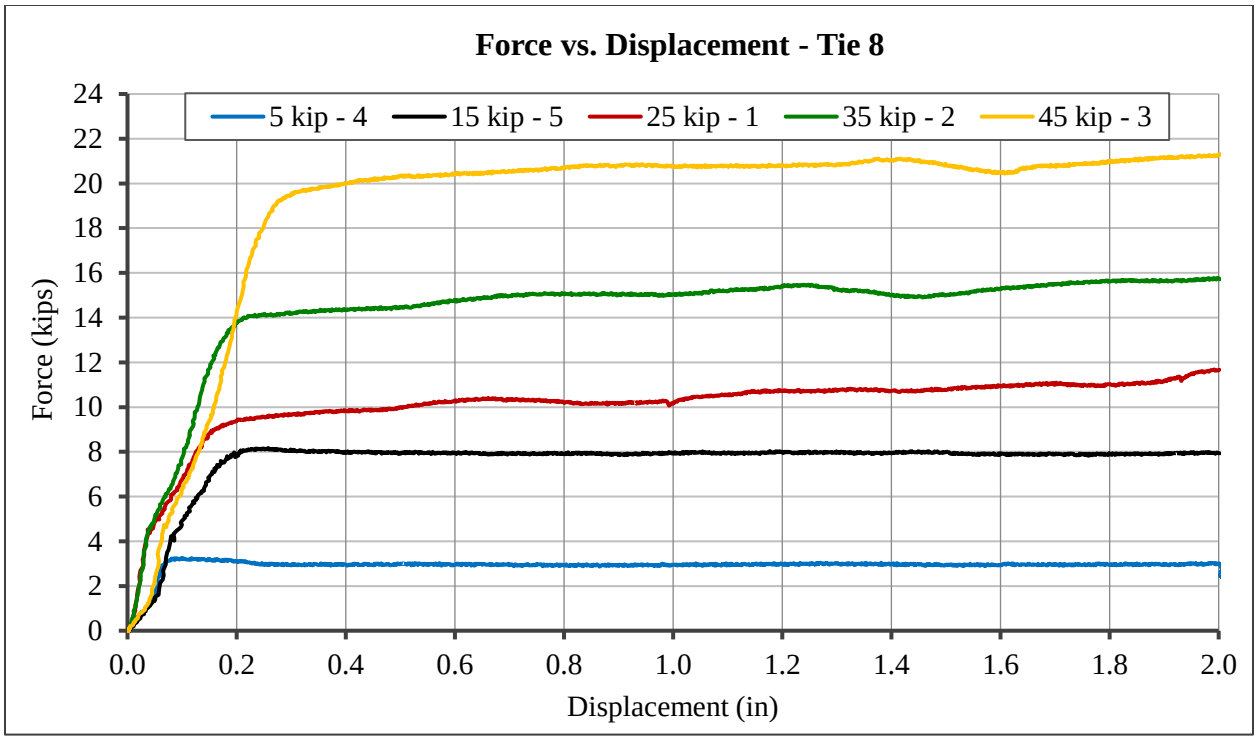

Figure 74: Lateral Force vs. Lateral Displacement for Tie 8

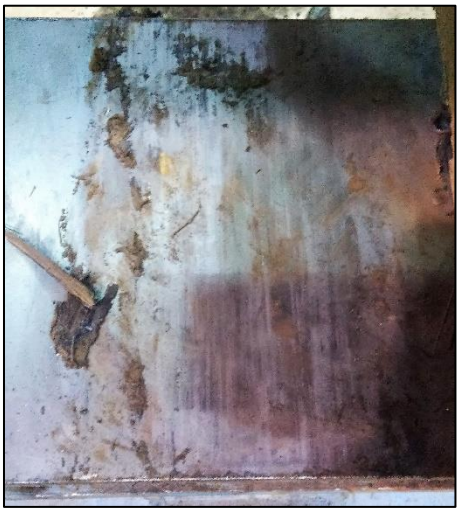

Figure 75: Steel plate after lateral push tests on Tie 8

4.2.6 Tie 6

The lateral force versus displacement graph for Tie 6 can be seen in Figure 76. The rate of increase in lateral load was the same for all the tests. The sliding surface of Tie 6 was relatively clean and the steel plate did not contain a significant amount of grease remaining from lateral testing as can be seen in Figure 77. All five tests were conducted at a vertical load of 45 kip on Tie 6 in order to study the effect of relaxation of the tie on lateral strength. Wood fibers in the tie compress under loading. The fibers gradually revert to their original configuration or 'relax' on unloading the tie over a period of time. A vertical load of 45 kip was chosen in order to consider the worst case scenario for a bridge tie in the field when it experiences the highest possible vertical loads. Tests 1, 2 and 3 were conducted on the first day and tests 4 and 5 were performed 2 days later so that the wood fibers in the tie could relax and revert to their original configuration. From Figure 76 it can be observed that test 1 showed an ultimate lateral resistance of 22 kip and tests 2, 3, 4 and 5 recorded a lateral resistance of approximately 20 kip. Through these tests it can be concluded that tie relaxation does not affect lateral resistance because test 4 and 5 did not show an increase in lateral load after 2 days.

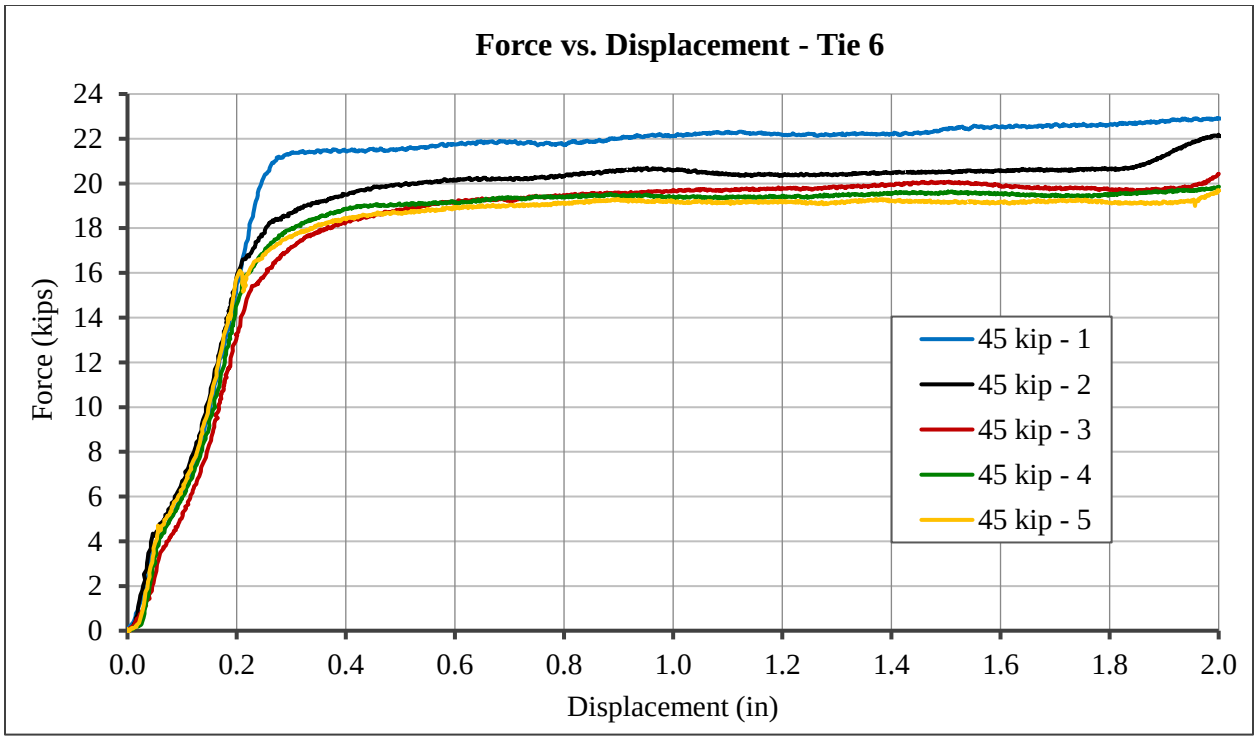

Figure 76: Lateral Force vs. Lateral Displacement for Tie 6

Figure 77: Steel plate after lateral push tests on Tie 6

4.2.7 Tie 9

The lateral force versus displacement graph for Tie 9 can be seen in Figure 78. In order to confirm the conclusion that relaxation of the wood does not affect lateral resistance from testing of Tie 6, five lateral push tests were conducted on Tie 9 at a vertical load of 45 kip. Similar to tests performed on Tie 6, tests 1, 2 and 3 were conducted on the first day and tests 4 and 5 were performed 2 days later. Since test 4 and 5 did not record lateral loads greater than the loads from tests 1, 2 and 3, it appears that relaxation of the tie does not affect lateral resistance.

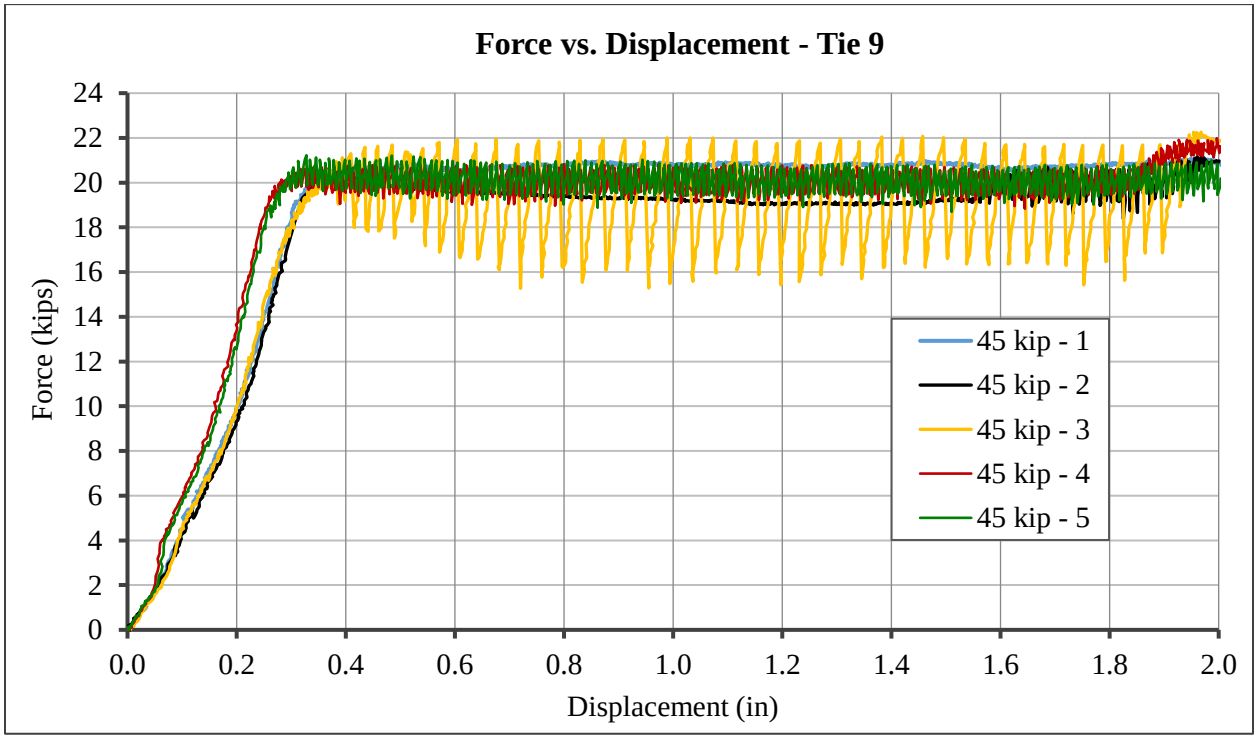

Figure 78: Lateral Force vs. Lateral Displacement for Tie 9

From Figure 78 it can be observed that the lateral load increased similarly for test 4 and 5. It was observed that Tie 9 exhibited stick slip behavior with increased fluctuations in the lateral load when loaded successively for the second or the third time at 45 kip. Stick slip behavior can be attributed to the sliding surface of Tie 9 being free of any grease. However, the reason for

increase in stick slip during successive testing is not clear. There was no grease residue remaining on the steel plate after testing as can be seen in Figure 79.

Figure 79: Steel plate after lateral push tests on Tie 9

From all the tests conducted on Tie 2, Tie 3, Tie 4, Tie 5 and Tie 8, it was observed that lateral resistance remained similar for all ties during the application of a given magnitude of vertical load (5 kip – 45 kip). Results were similar at a particular vertical load regardless of the order in which each of the five lateral tests per tie were conducted. Since order of testing per tie does not affect results, it can be assumed that a tie specimen can be reused for multiple tests for determining frictional resistance.

4.3 Load Graphs

Test results from friction testing were compiled as per the provisions of ASTM G115. Since all the ties exhibited a low breakaway force, the friction coefficients were calculated using Equation 12 and Equation 13 from Case 2. All the test results were categorized based on the magnitude of the applied vertical load. The lateral loads corresponding to each of the five vertical load magnitudes were averaged and a bilinear curve was used to calculate the static and kinetic coefficients of friction. The average lateral force at a vertical load of 45 kip can be seen in Figure

80. In Figure 81 a bilinear curve is used to capture the average lateral. The slope of the line before slip of the tie is henceforth referred to as S1 and the slope of the line after initial slip is henceforth referred to as S2. S1 and S2 values for all the five vertical load cases are summarized in Table 10. The slope of the first equation matching the plot shown in Figure 81 before initial slip of the tie, is the coefficient of static friction. The slope of the second equation matching the plot in Figure 81 after initial slip of the tie, is the coefficient of kinetic friction. The lateral forces versus lateral displacement graphs for the average lateral load at each of the five vertical loads can be found in Appendix B.

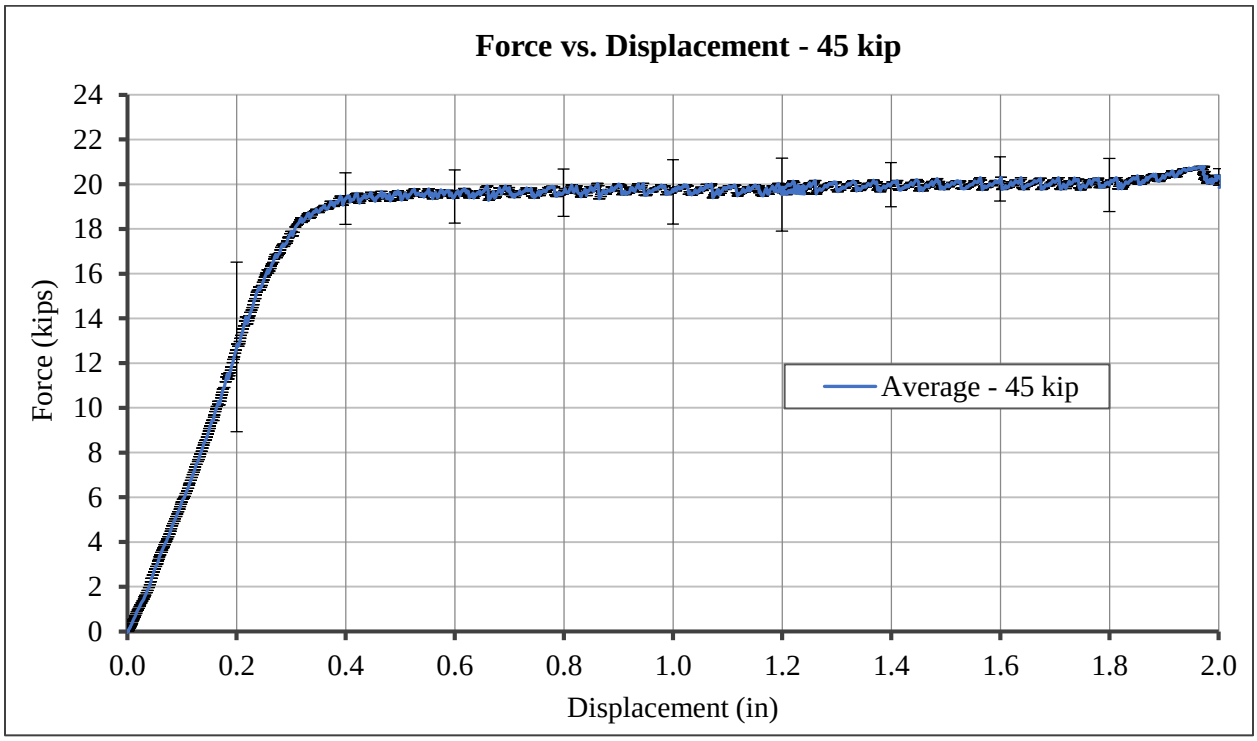

Figure 80: Average lateral load at a vertical load of 45 kip

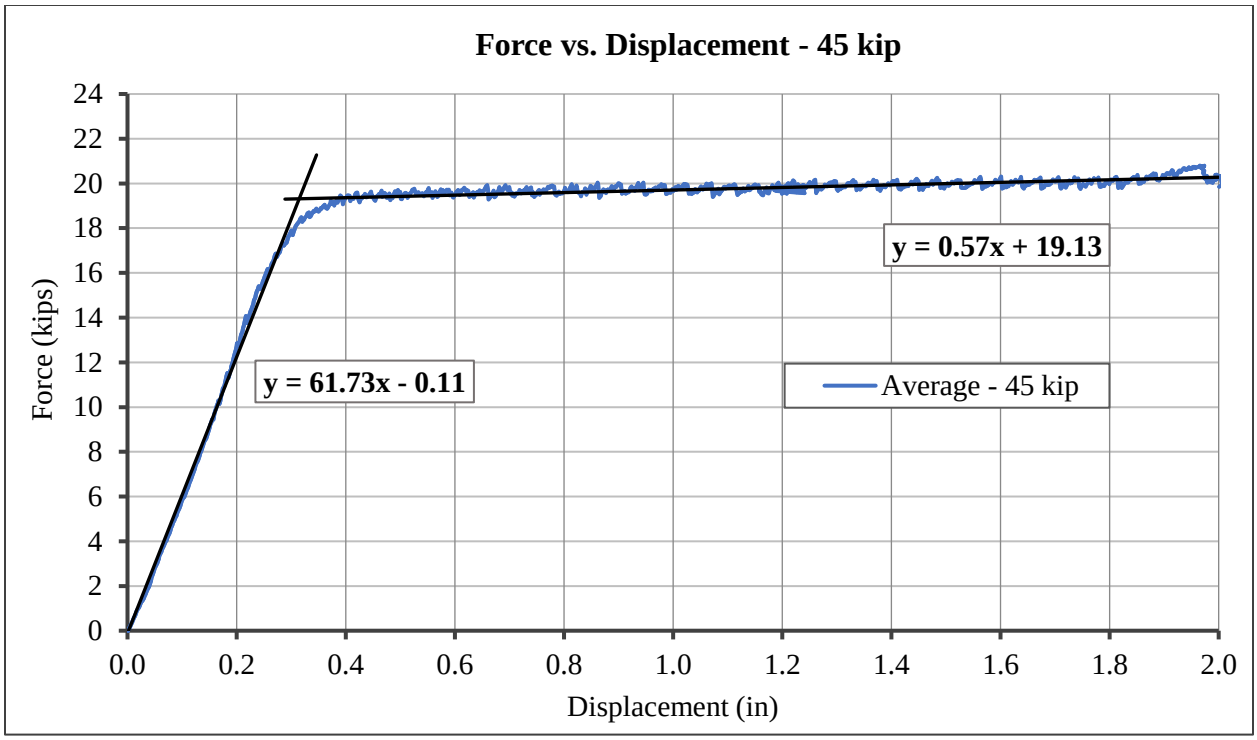

Figure 81: Bilinear plot of the average lateral load at a vertical load of 45 kip

Table 10: S1 and S2 values for lateral loads averaged for vertical loads ranging from 5 kip to 45 kip

Sample (kip)	Slope (kip/in)	
	S1	S2
5	19.7	0.26
15	42.7	0.48
25	55.6	0.29
35	65.4	0.39
45	61.7	0.57
Average Slope	**49.0**	**0.40**

The railroad industry measures the magnitude of lateral forces on a curved track based on the magnitude of the axle loads from the train and not as a function of the lateral track displacement. Therefore, the average lateral resistance was graphed as a function of the normal force as seen in Figure 82. The average lateral load values which were used to create the graph in Figure 82 represent the F' values from Case 2 in ASTM G115 at the time of initial slip. These

average lateral loads can be seen in Table 11. F' values corresponding to the coefficient of static friction were chosen instead of F values that correspond to kinetic friction because F' values are always smaller than F values. Therefore, it was more conservative to determine lateral resistance using the static friction coefficient because it is smaller.

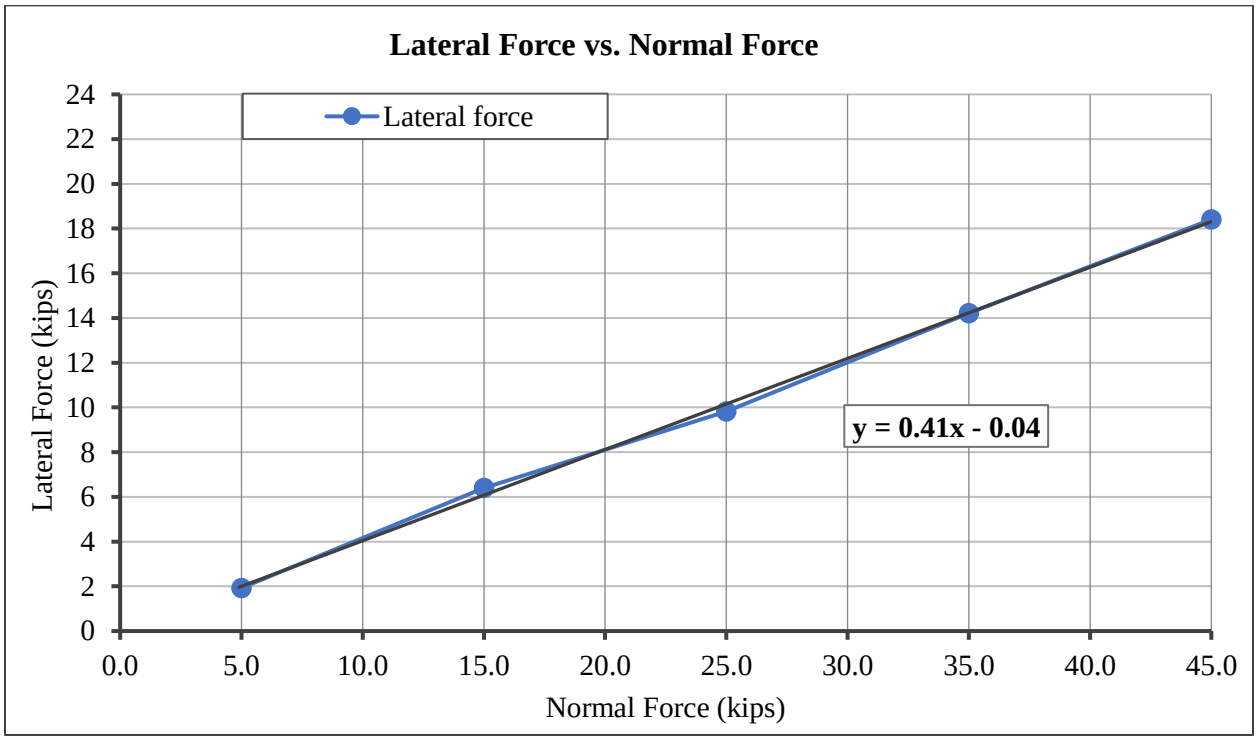

Figure 82: Lateral force graphed as a function of the normal force

Table 11: Lateral loads before slip

Vertical Load (kip)	Horizontal Displacement at Initial Slip (in)	Horizontal Load (kip)
5	0.11	1.93
15	0.17	6.40
25	0.20	9.83
35	0.23	14.21
45	0.32	18.41

The slope of the equation from the graph in Figure 83 was used as a part of the final design equation for determining the overall lateral resistance in a curved bridge that represents the resistance due to friction. The graph in Figure 83 was created using the slope from the graph in Figure 82 and it can be used as a design tool for railroad bridge engineers to determine the lateral resistance contribution from friction at a particular vertical axle load.

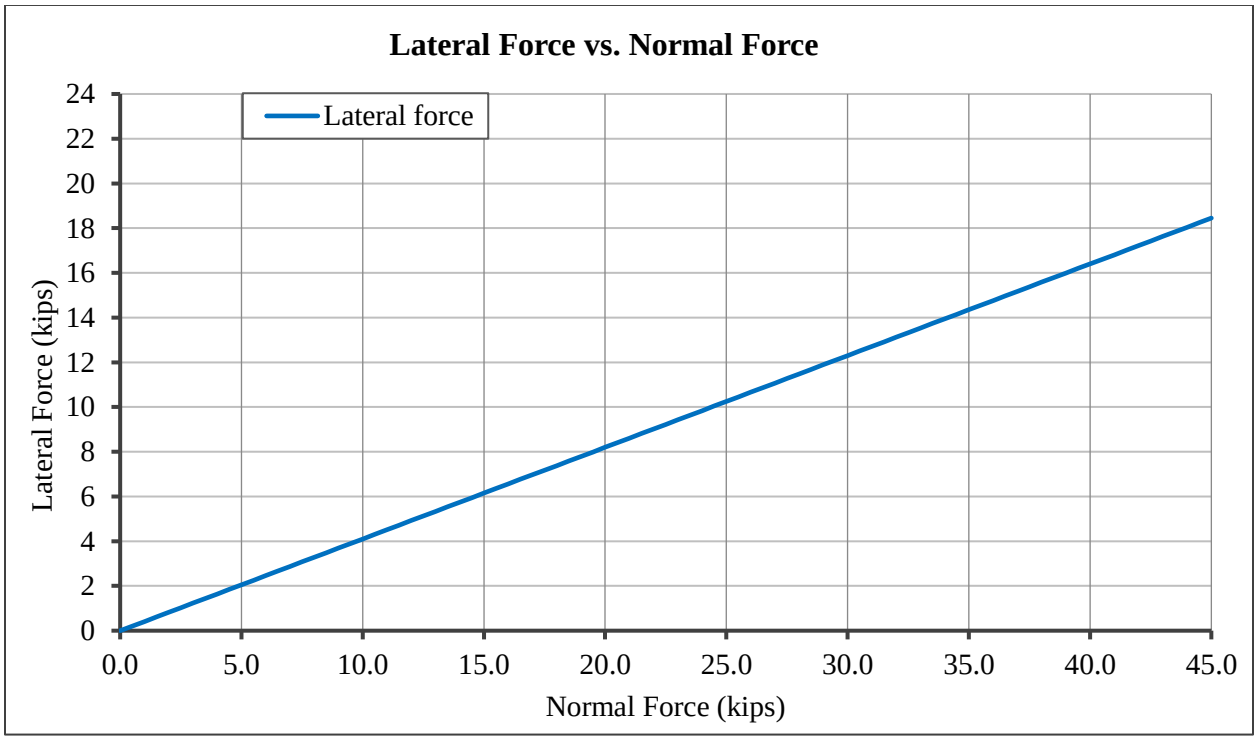

Figure 83: Lateral force as a function of the normal force using a static friction coefficient of 0.4

4.4 Fastener Contribution Results

Results of tests conducted to determine the lateral resistance from fasteners can be found in sections 4.4.1, 4.4.2, and 4.4.3. Similar to data from tests performed for determining the lateral resistance from friction, the data from all the tests which were performed to determine fastener resistance, was analyzed for lateral displacements ranging between 0 – 2 in.

4.4.1 Square body Hook Bolt results

Six square body hook bolts were tested, of which five of them were laterally loaded until a displacement of 2 in. was recorded. The sixth hook bolt was laterally loaded until fastener failure. The lateral load versus lateral displacement graph for all six fasteners can be seen in Figure 84. It was observed that the lateral resistance of the fastener in Tie 8 plateaued at 8.5 kip between 1 in. and 3 in. before failing by slipping over the steel plate. Tensile yielding of the hook portion of the fastener was observed as the edge of the hook climbed over the steel plate when laterally loaded beyond 3 in. of displacement as seen in Figure 85. Uplift of the tie occurred as the hook slipped over the steel plate.

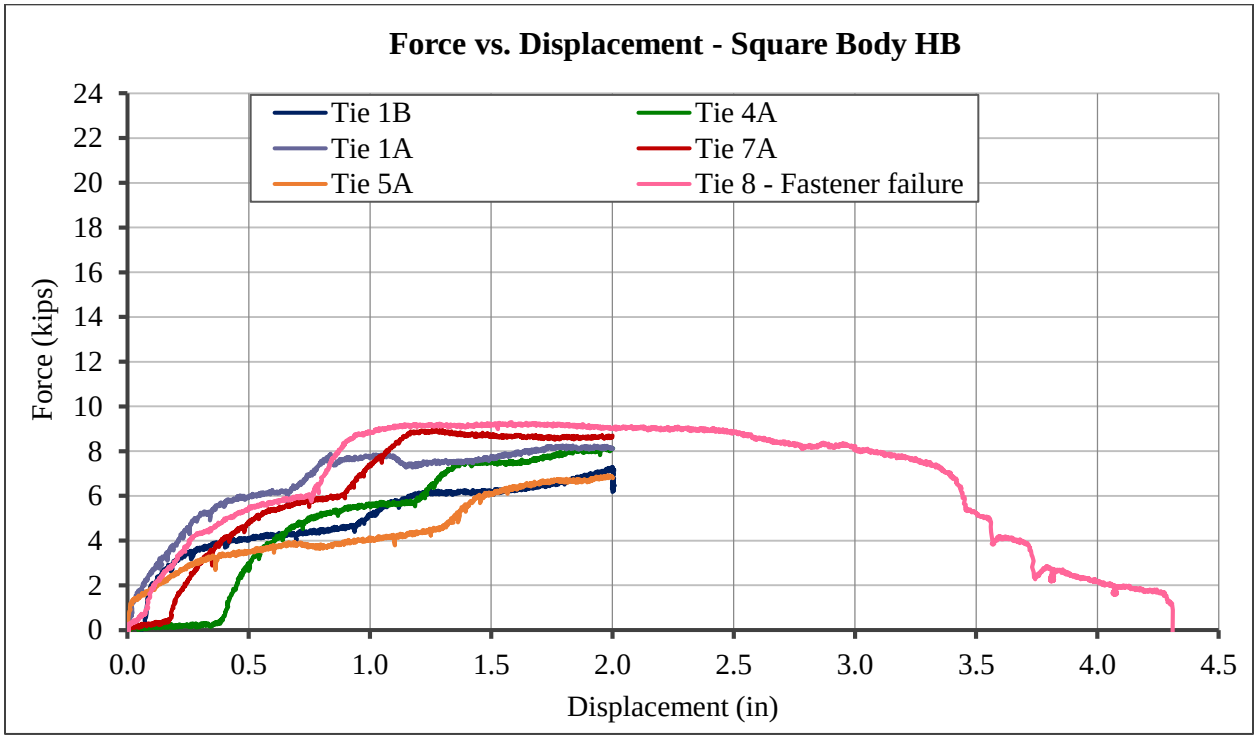

Figure 84: Lateral force vs. lateral displacement for square body hook bolt failure

Figure 85: Tie uplift with fastener climbing over the steel plate

Figure 86 shows the lateral force versus lateral displacement graph for all square body hook bolt until a lateral displacement of 2 in. was achieved. An ultimate lateral resistance within a range of 7 kip - 9 kip was observed for all six fasteners. Local crushing of the wood was also observed where the fastener hook yielded as seen in Figure 87. Figure 88 shows the condition of the failed fasteners. Tensile yielding occurred in the out of plane direction when the hook prevented the tie from displacing laterally. Upon continuous loading, the fastener deformed due to flexure. It was observed that flexural bending was over the length of the square cross section of the hook bolt as seen in Figure 89 where the fastener deformed by 27 degrees.

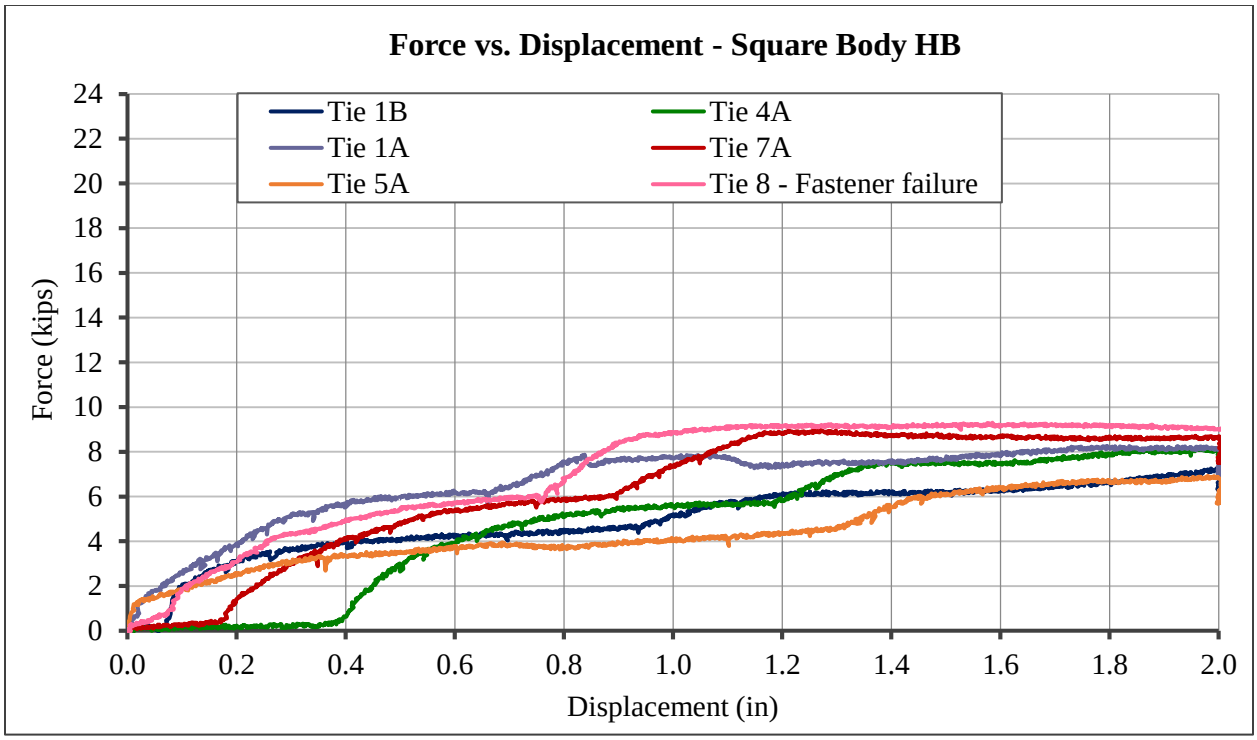

Figure 86: Lateral force vs. lateral displaement for square body hook bolts

Figure 87: Local crushing of the wood near the fastener

Figure 88: Deformed square body hook bolts after testing

Figure 89: Curvature in a deformed Square body hook bolt

Average lateral resistance of the square body hook bolts can be seen in Figure 90 where an ultimate lateral resistance of 8 kips can be observed. A bilinear plot was used to capture the average lateral resistance where the first equation ends and the second equation begins at a lateral

displacement of 1 in. An average slope of 6 kip/in was recorded for the first equation and a slope of 1.4 kip/in was recorded for the second equation as seen in Figure 90. These slope values were used to plot a lateral force versus lateral displacement graph shown in Figure 91 that can be used a design tool by bridge engineers for determining the lateral resistance for square body hook bolts as a function of lateral displacement.

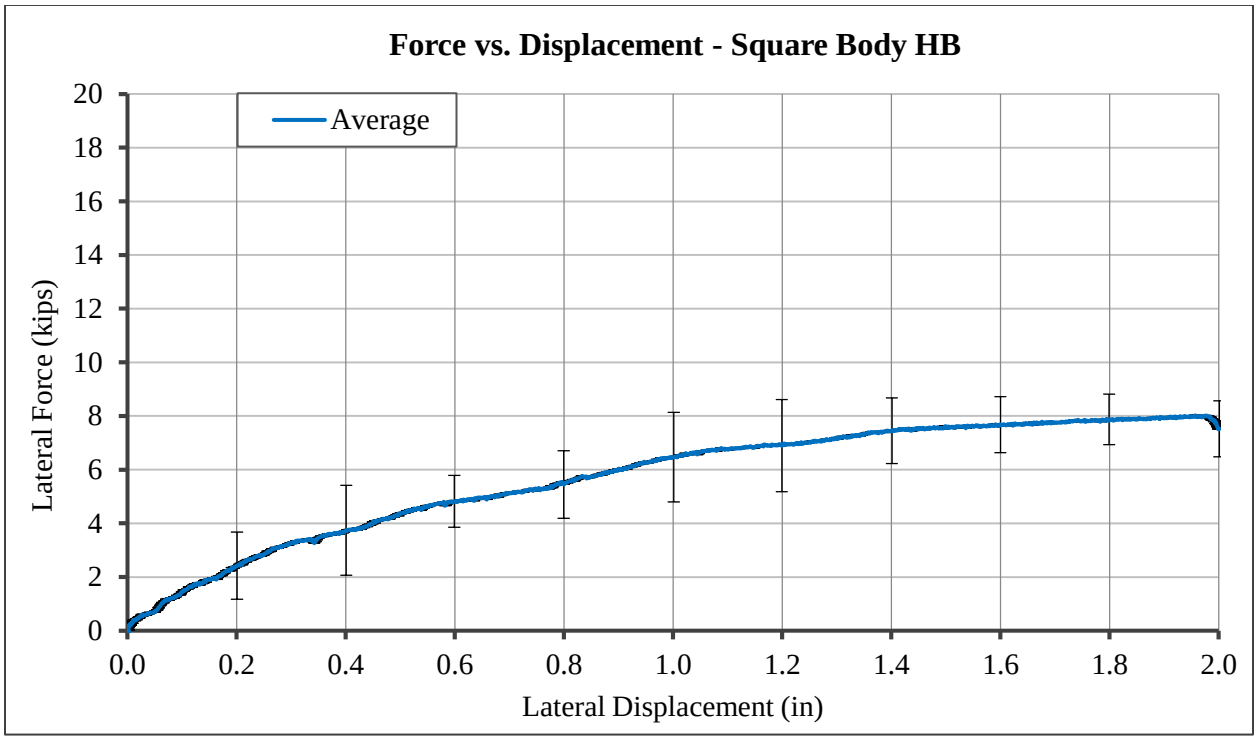

Figure 90: Average lateral resistance of square body hook bolts.

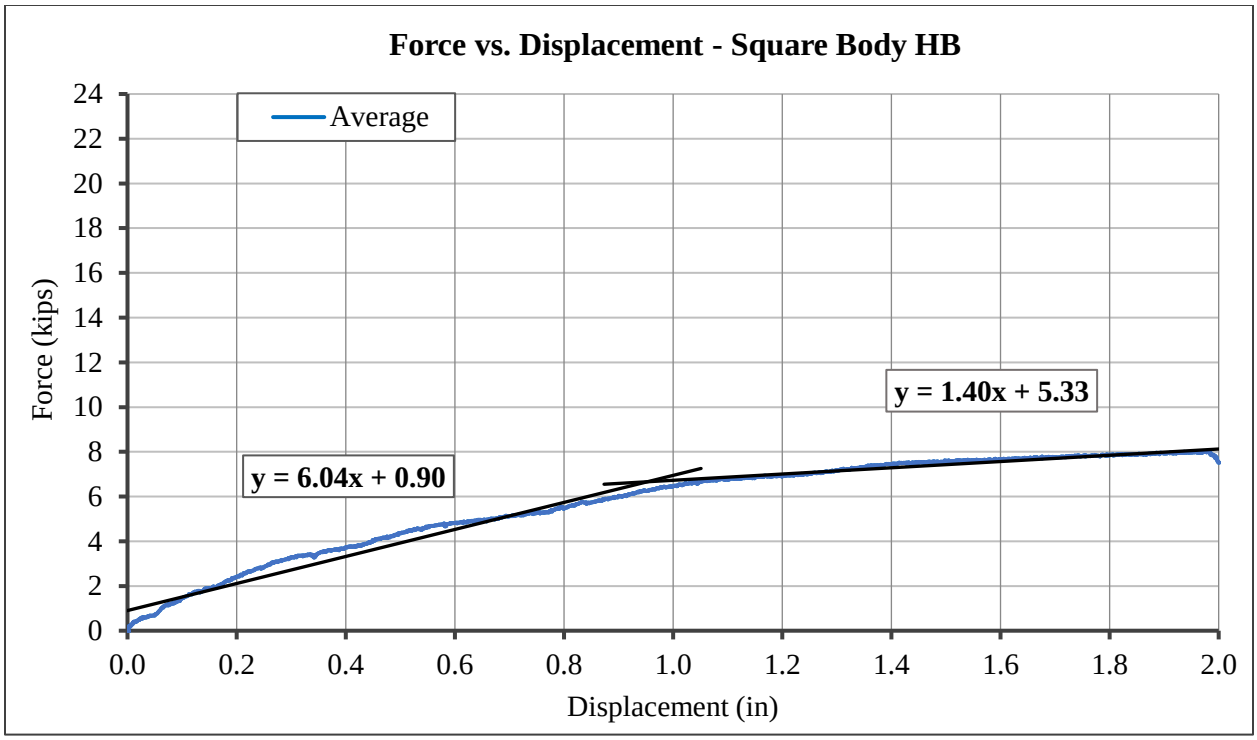

Figure 91: Bilinear curve of average lateral resistance of square body hook bolts.

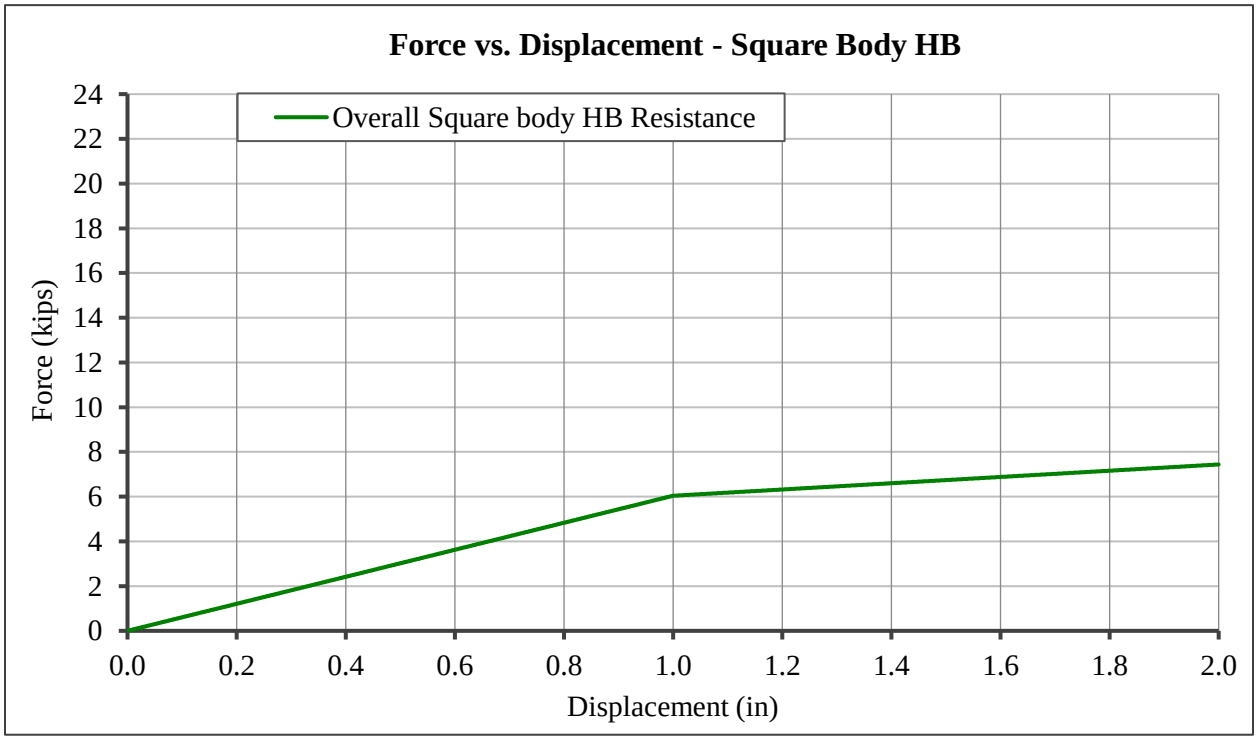

Figure 92: Lateral force as a function of lateral displacement for square body hook bolts.

4.4.2 Lewis Forged Hook Bolt results

Similar to the square body hook bolts, five Lewis Forged hook bolts were laterally loaded until a displacement of 2 in. was recorded in the tie. Fastener 11, however, was loaded until it reached a complete failure. The results from all six tests can be seen in the graph in Figure 93. The fasteners yielded in flexure upon lateral loading until the hook engaged to the edge of the steel plate as shown in Figure 94. It was observed that Fastener 11 failed due to tensile rupture at a lateral displacement of 4.2 in and an ultimate load of 19 kip. The fracture occurred where the cross section of the material changed. It is estimated that stress concentrations in this region caused failure as seen in Figure 95. The tie experienced local crushing near the hook for all six tests and unlike the test involving the square body hook bolt, there was no uplift observed in the tie.

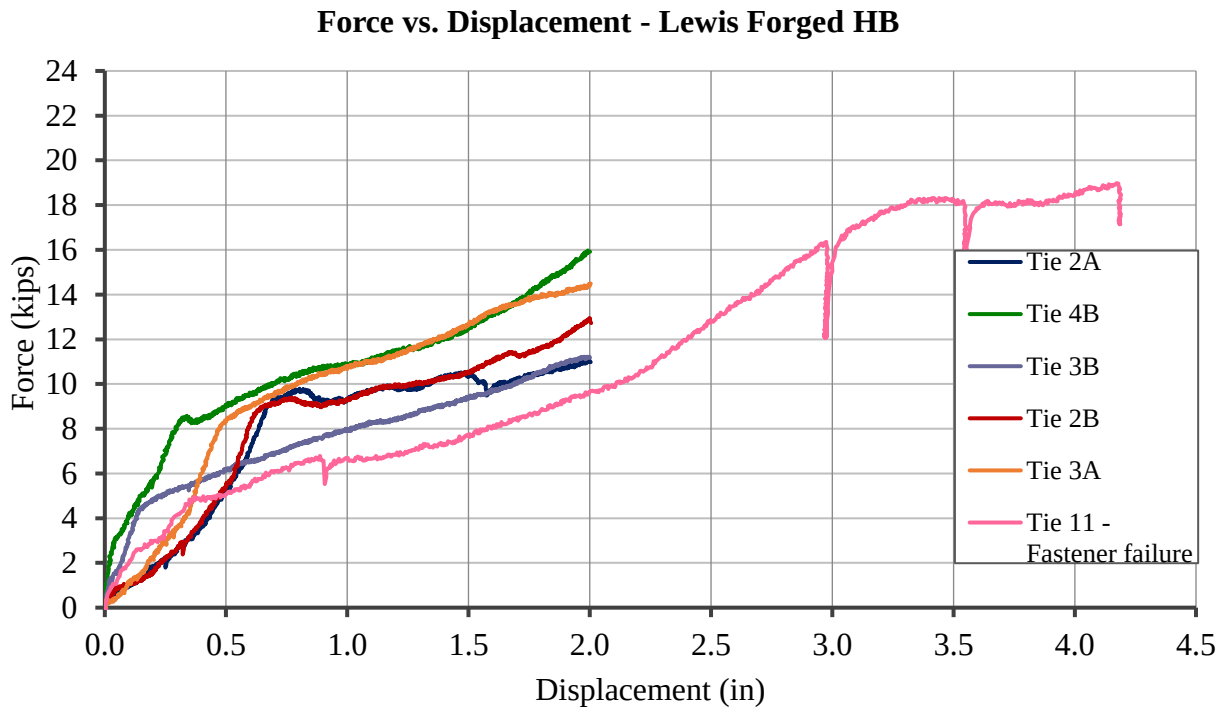

Figure 93: Lateral force vs. lateral displacement for Lewis Forged hook bolt failure

Figure 94: Hook engagement of the Lewis Forged hook bolt with the edge of the steel plate.

Figure 95: Fracture in Lewis Forged hook bolt – Fastener 11

The lateral force versus displacement graph for all fasteners for displacements ranging from 0 - 2 in. can be seen in Figure 96. Lewis Forged hook bolts had a greater lateral resistance in the range of 10 kip – 14 kip as compared to the range of 7 kip – 9 kip for square body hook bolts. All fasteners underwent flexural yielding in the out of plane direction during lateral loading as

shown in Figure 97. Lewis Forged hook bolts experienced more localized flexural yielding near the hook where it deformed by 25 degrees as shown in Figure 98.

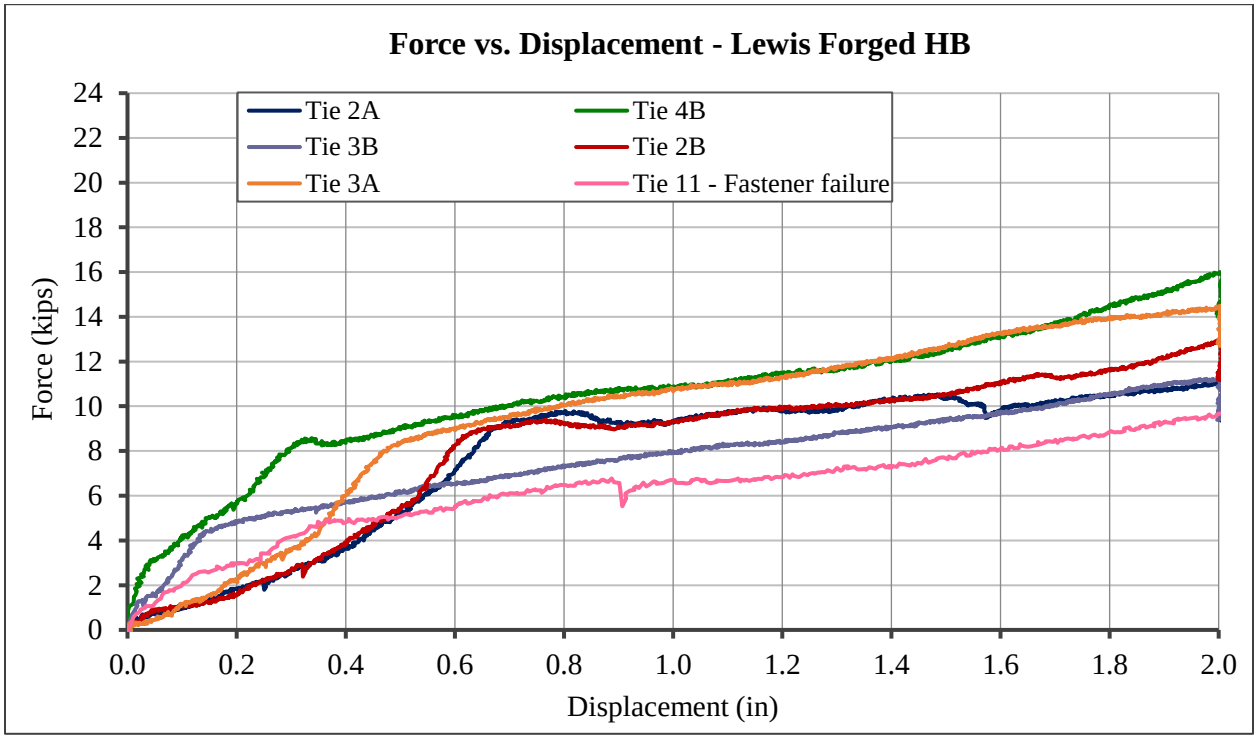

Figure 96: Lateral force vs. lateral displacement for Lewis Forged hook bolts

Figure 97: Deformed Lewis Forged hook bolts after testing

Figure 98: Curvature in a deformed Lewis Forged hook bolt

Average lateral resistance of Lewis Forged body hook bolts can be seen in Figure 99 where an ultimate lateral resistance of 13 kip can be observed at a displacement of 2 in. The average lateral resistance was plotted as a bilinear curve as seen in Figure 100. The first equation having a slope of 13 kip/ in. ends at a lateral displacement of 0.68 in. where the second equation with a

slope of 3 kip/ in. begins. The slope values from both these equations were used to plot a lateral force versus lateral displacement graph shown in Figure 101 that can be used a design tool by bridge engineers for determining the lateral resistance of Lewis Forged hook bolts as a function of lateral displacement.

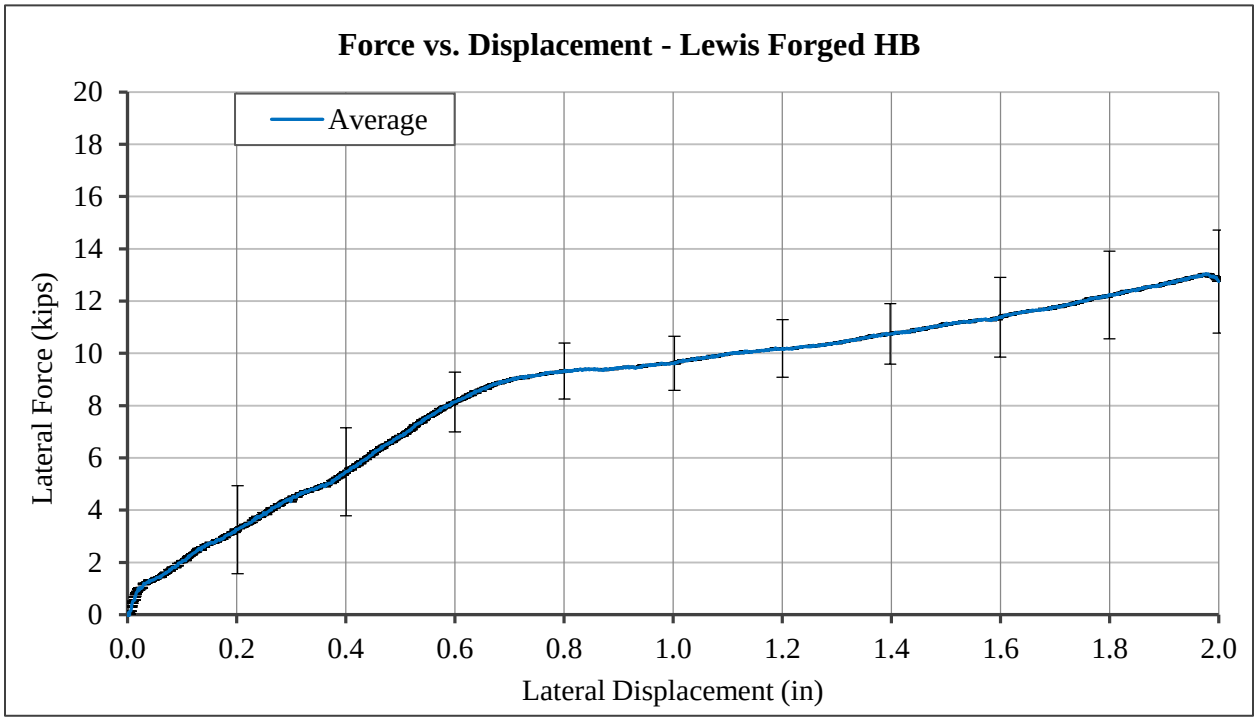

Figure 99: Average lateral resistance of Lewis Forged hook bolts

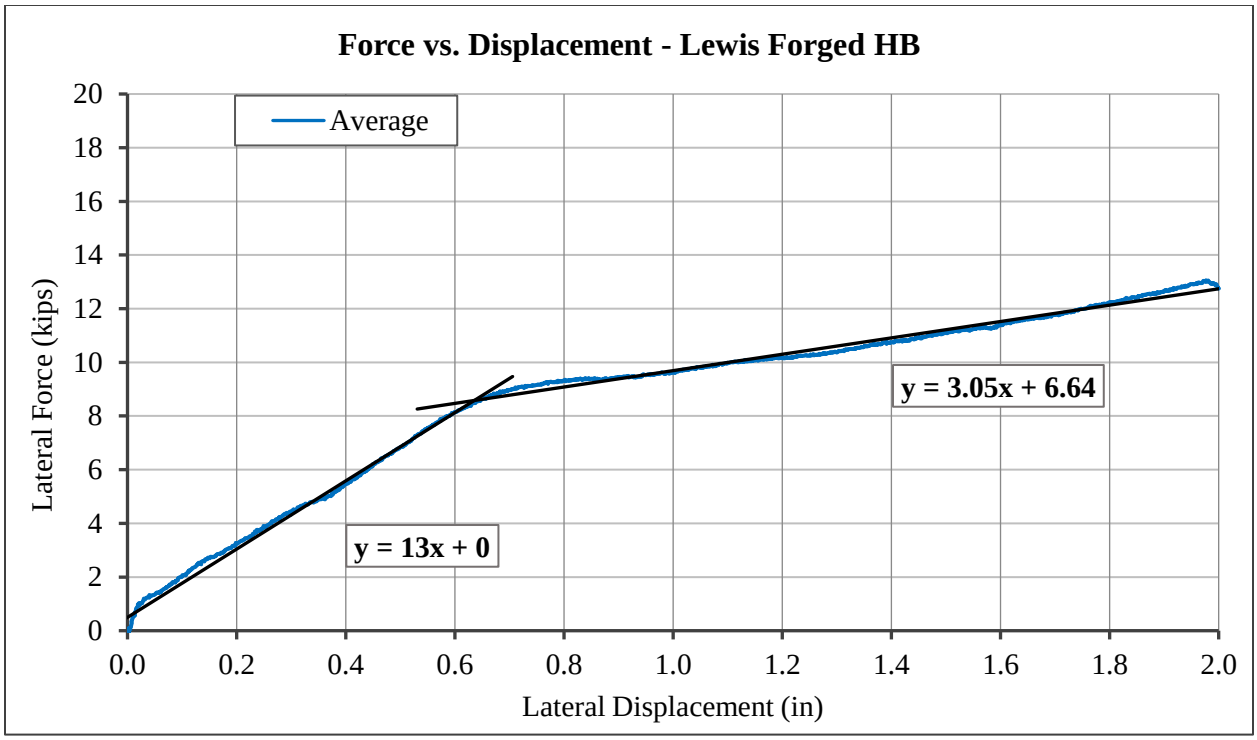

Figure 100: Bilinear curve of average lateral resistance of Lewis Forged hook bolts

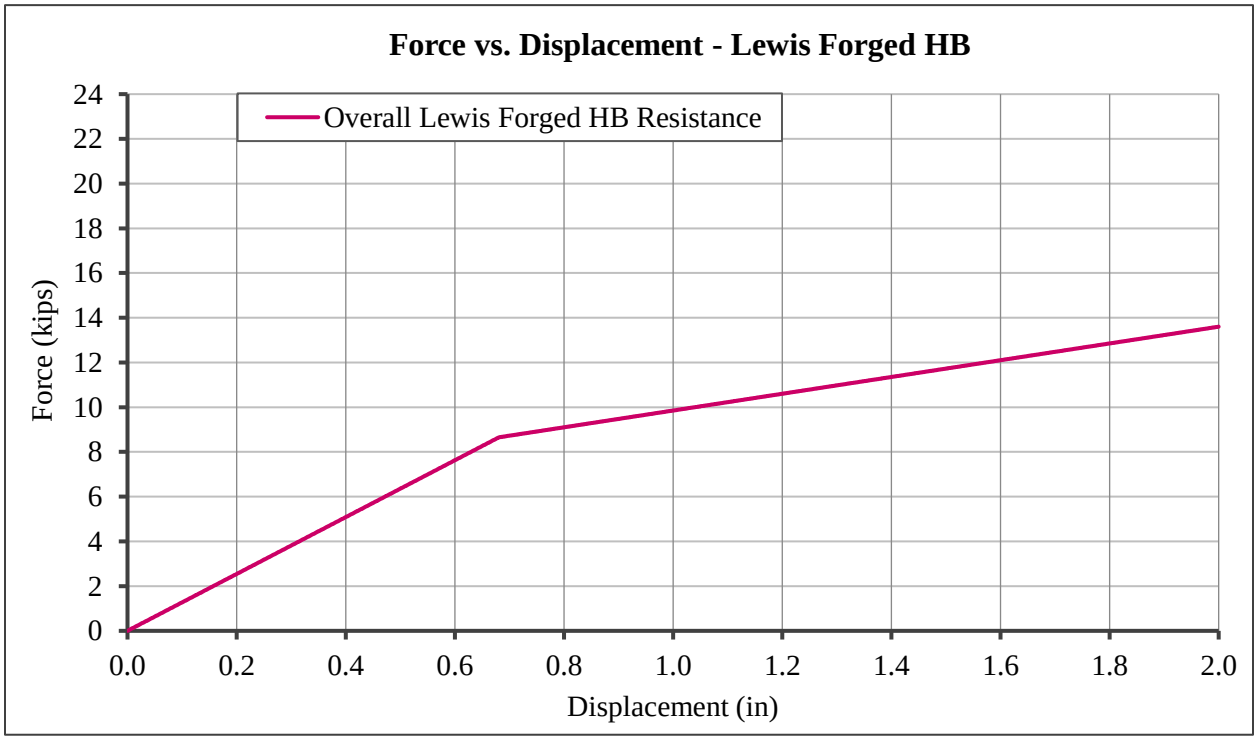

Figure 101: Lateral force as a function of lateral displacement for Lewis Forged hook bolts

4.4.3 Quikset Anchor results

Six Quikset Anchors were tested until failure. One of the fasteners was loaded without a lock plate to investigate the effect of lock plates on hook engagement with the steel plate. The force versus displacement graphs for all the fasteners can be seen in Figure 102. It was observed that the lateral resistance of the Quikset Anchors was influenced by the amount of tension in the bolt which is a function of how well the bolt was tightened. Specimens QS1, QS4, QS6 had an ultimate resistance in the range of 14 kip - 16 kips when they were snug tightened using a crescent wrench. Whereas QS7 and QS9 reached a maximum lateral load of 22 kip before failure when a cheater bar of length 40 in. was used to tighten the bolt.

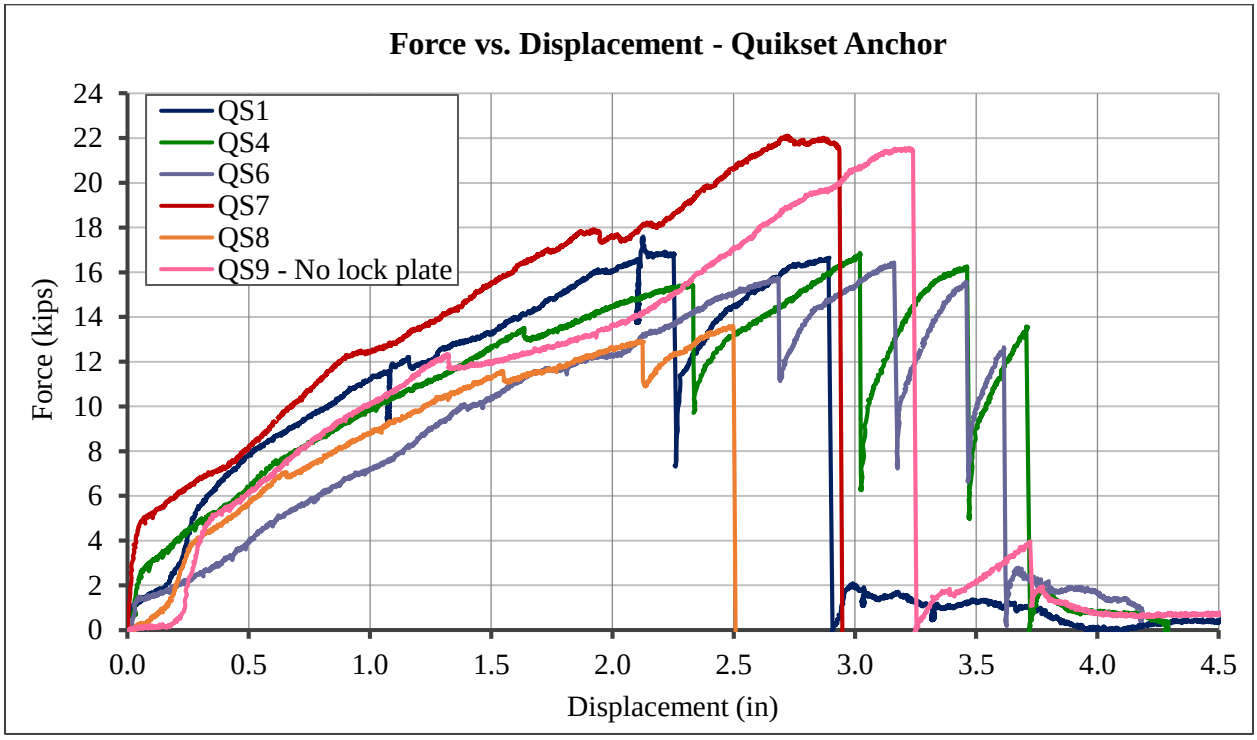

Figure 102: Lateral force vs. lateral displacement for Quikset Anchor failure

Two failure modes were observed for Quikset Anchors. In the first failure mode, the lock plate shown in Figure 103 and Figure 104 fractured and the hook of the fastener climbed over the steel plate. An initial drop in strength occurred when the lock plate fractured at an approximate

displacement of 2 in. as seen in the graph in Figure 102 for fasteners that followed the first failure mode. Figure 105 shows the fractured lock plates for Quikset Anchors that failed in the first failure mode during testing. The lock plate in the extreme left of Figure 105 can be used to compare the fractures in the other lock plates as it was not tested.

Figure 103: Quikset Anchor before testing

Figure 104: Quikset hook climbing over steel plate

Figure 105: Failed Quikset Anchor lock plates

The second failure mode which was observed was tensile rupture of the hook in cases where a cheater bar was used during installation. The hook prevented the fastener from displacing laterally, therefore the fastener continued to bend near the hook as the lateral load was increased. The lateral load steadily increased to 22 kip until a displacement of approximately 3 in. was recorded where the load dropped suddenly as seen in Figure 102 because of fracture of the hook in Quikset Anchors 7 and 8. Some bending in the lock plate was observed when the hook fractured, but there was no fracture in the lock plate. QS9 was tested without a lock plate but it was installed using a cheater bar. The hook of QS9 climbed over the steel plate without an initial drop in strength.

Localized crushing of the wood on the sliding surface was observed for QS7 and QS8 where the tie lifted above the steel plate. No deformation occurred in the Quikset bracket for all specimens. Figure 106 shows the condition of the Quikset Anchors after the test. The first fastener in the left most portion of Figure 106 is an untested Quikset Anchor and it can be compared to the other fasteners in figure that have deformed after testing.

Figure 106: Failed Quikset Anchors after testing

Since the railroads consider 2 in. of lateral displacement as failure, the results from Quikset Anchor testing were only analyzed for displacements within a range of 0 – 2 in. The force versus displacement graphs for all tests until a maximum lateral displacement of 2 in. can be seen in the graph in Figure 107. An average trend of this data can be seen in Figure 108 where the maximum lateral resistance for Quikset Anchors was observed to be 14 kip.

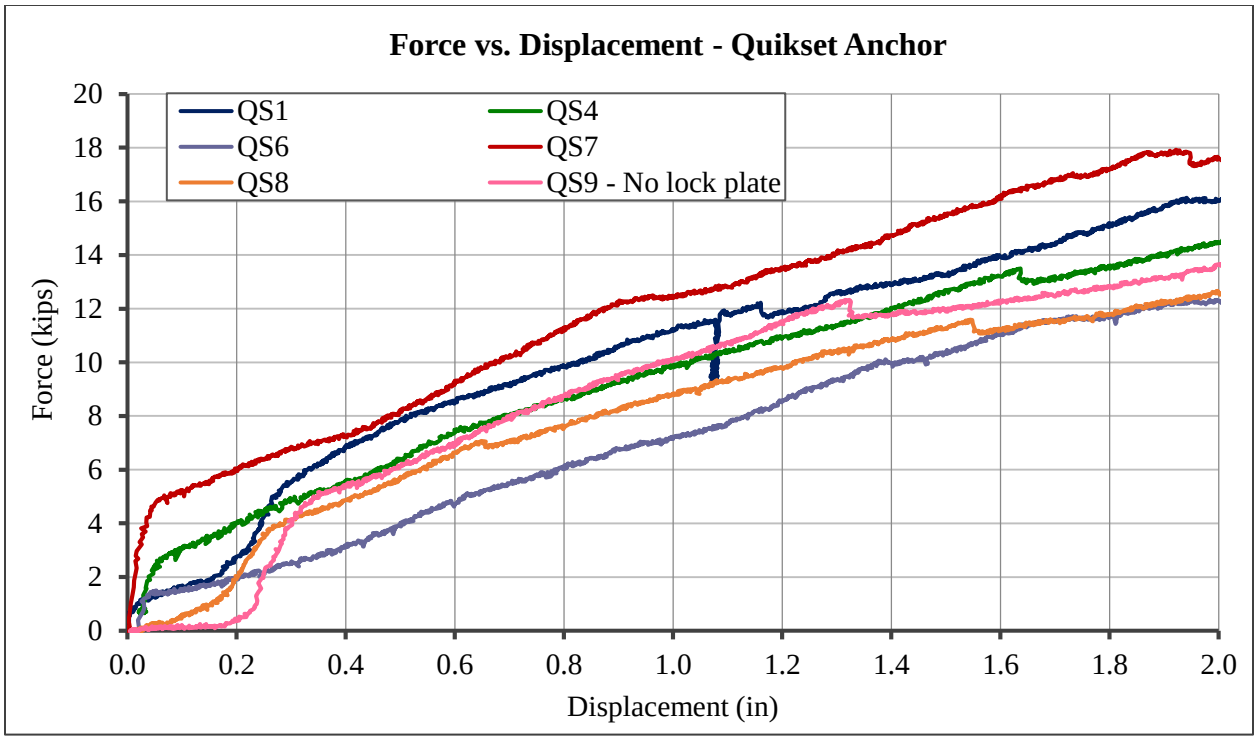

Figure 107: Lateral force vs. lateral displaement Quikset Anchors

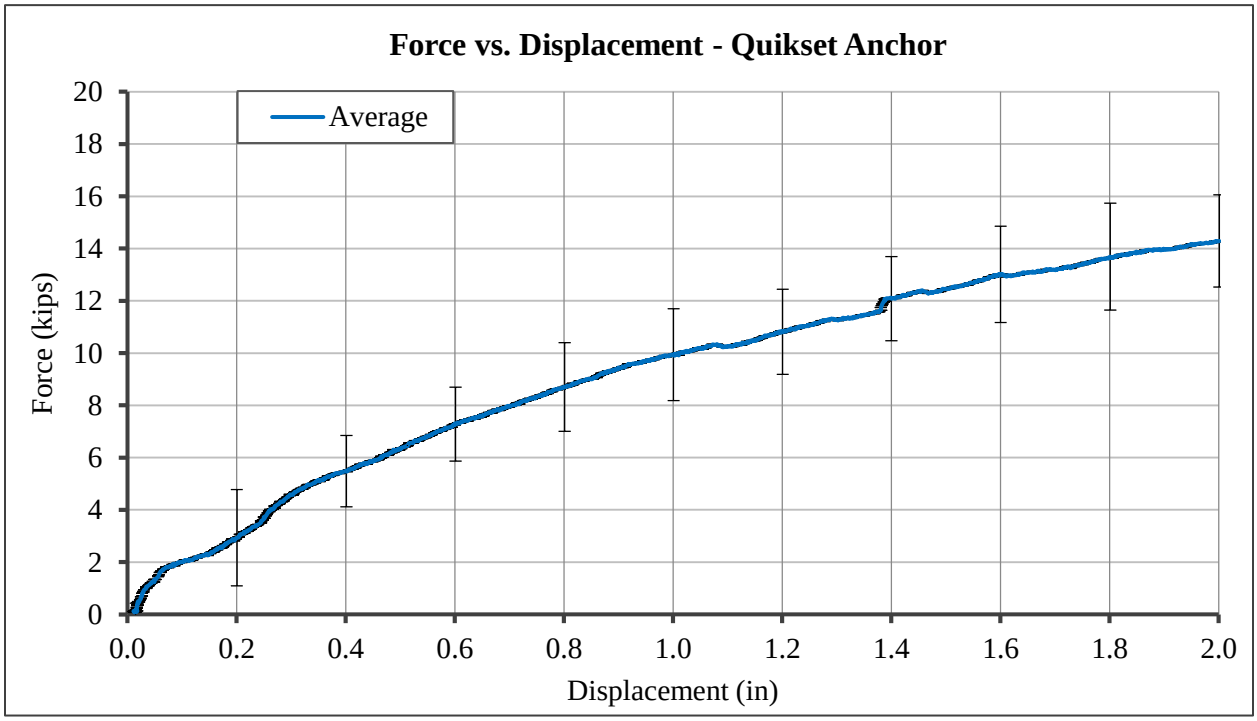

Figure 108: Average lateral resistance of Quikset Anchors.

The average lateral resistance of Quikset Anchors was plotted as a bilinear curve to fit the data as seen in Figure 109 with the first equation capturing the data until a lateral displacement of 0.4 in. and a second equation capturing the data within a displacement range of 0.4 in. – 2 in. The slopes from both these equations was used to create the graph in Figure 110 which can be used as a design tool that calculates the lateral resistance of Quikset Anchors as a function of lateral displacement.

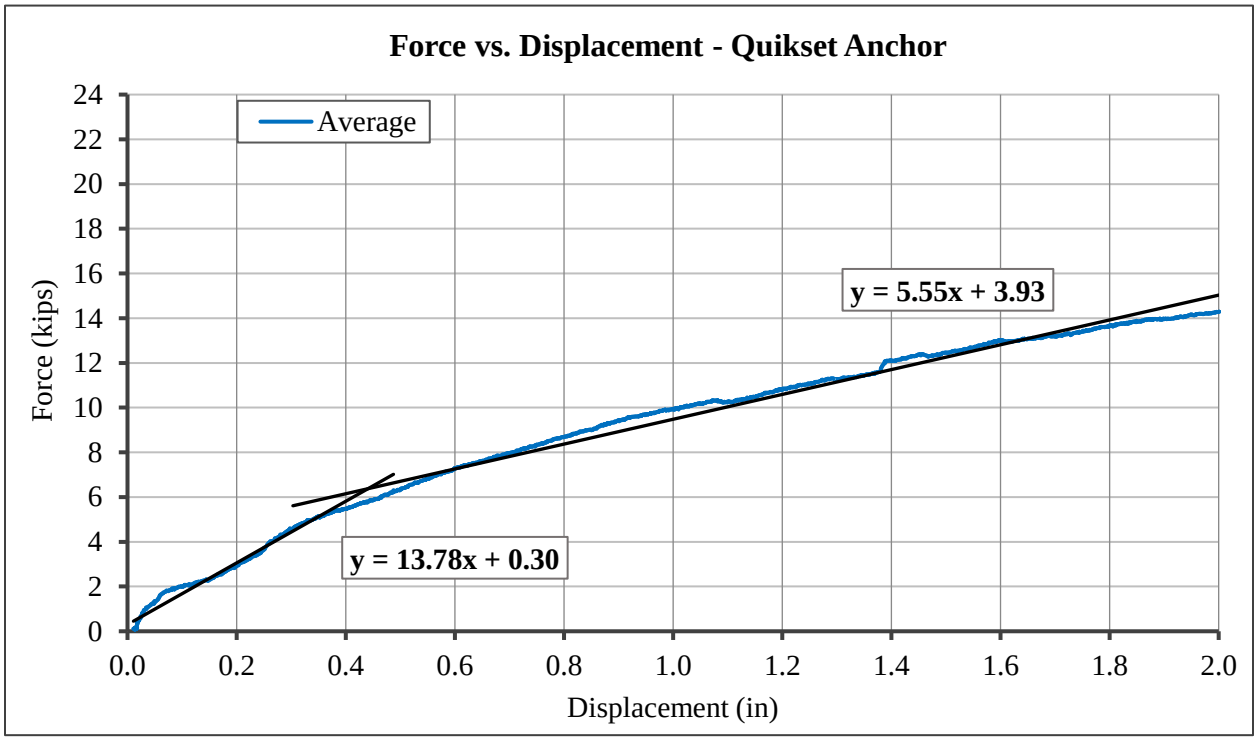

Figure 109: Bilinear curve of average lateral resistance of Quikst Anchors.

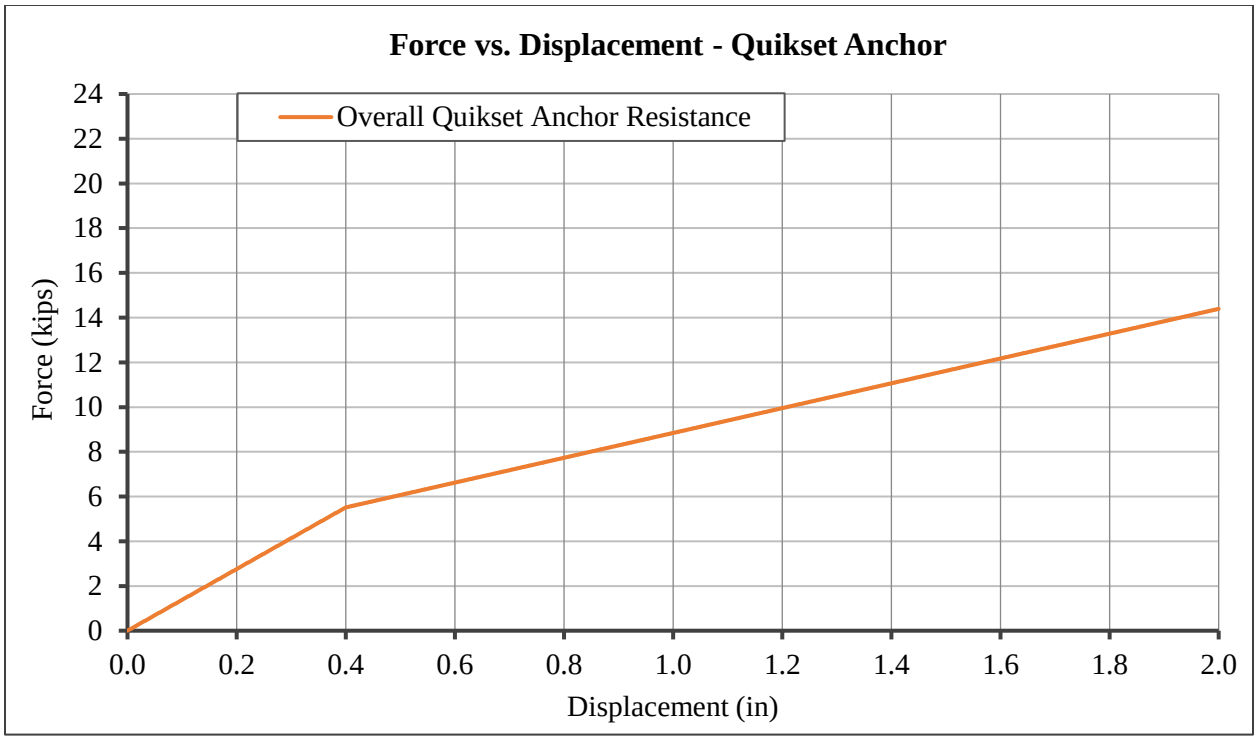

Figure 110: Lateral force as a function of lateral displacement for Quikset Anchors.

4.5 Dap Contribution Results

Five dapped tie specimens were tested to investigate the lateral resistance contribution due to the dap. Lateral force versus lateral displacement plots for each test can be seen in Figure 111. The daps failed in shear parallel to the grain at a lateral force in the range of 50 kip – 60 kip between 0.5 in. – 1.0 in. of lateral displacement. Figure 112 shows the shear failure parallel to grain in dapped specimen D4. It can be seen in Figure 111 that the rate at which lateral load increases with lateral displacement is similar for all five specimens. All specimens have a similar slope before and after a lateral load of 10 kip. Differences in strength gain for each specimen are estimated to be a result of surface irregularities such as the tie surface not being exactly perpendicular to the lateral actuator during lateral loading, and inconsistencies in tie dimensions.

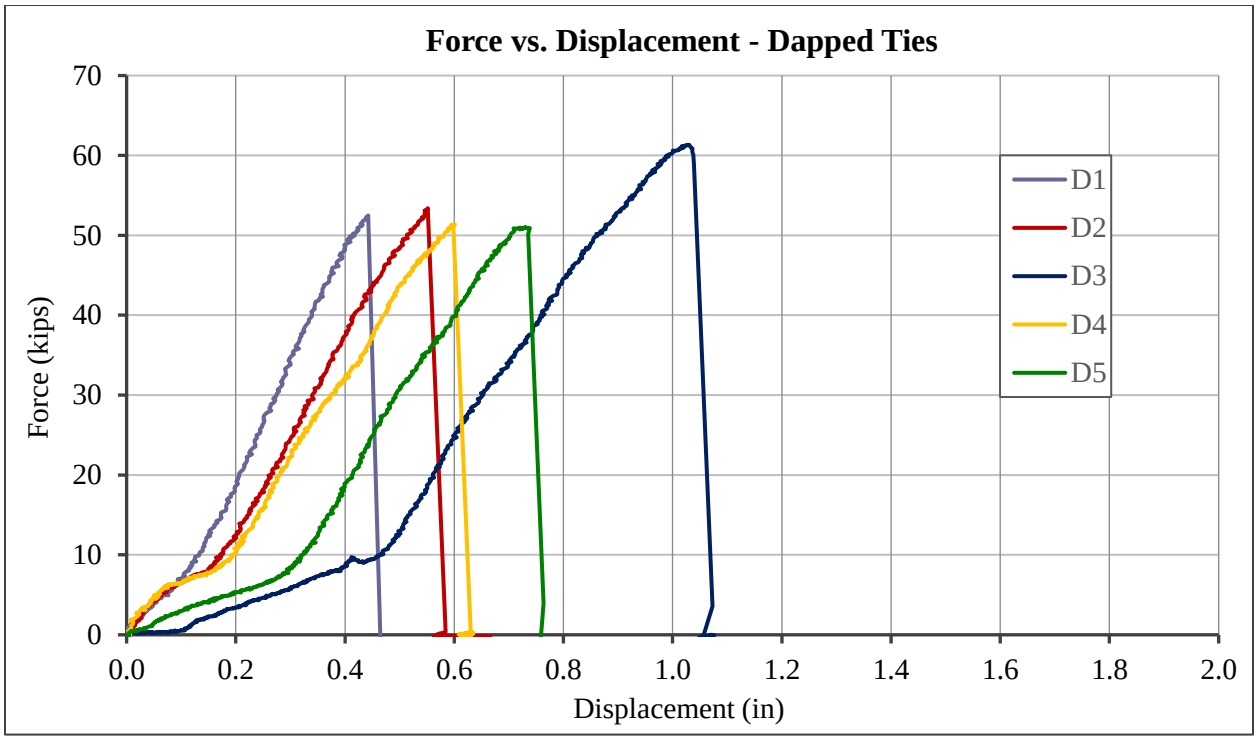

Figure 111: Lateral force vs. lateral displacement graph for dapped tie samples

Figure 112: Dap shear failure in tie specimen D4

The data for each test fit a bilinear curve as seen in Figure 113 which shows the results of dapped specimen D3. Refer to Appendix B for bilinear curves for each dapped sample. The slope calculated for the portion of the curve below a lateral load of 10 kip is referred to as S1 and the slope for the portion of the curve above a lateral load of 10 kip is referred to as S2. S1 and S2 values which were calculated for all five dapped specimens are summarized in Table 12.

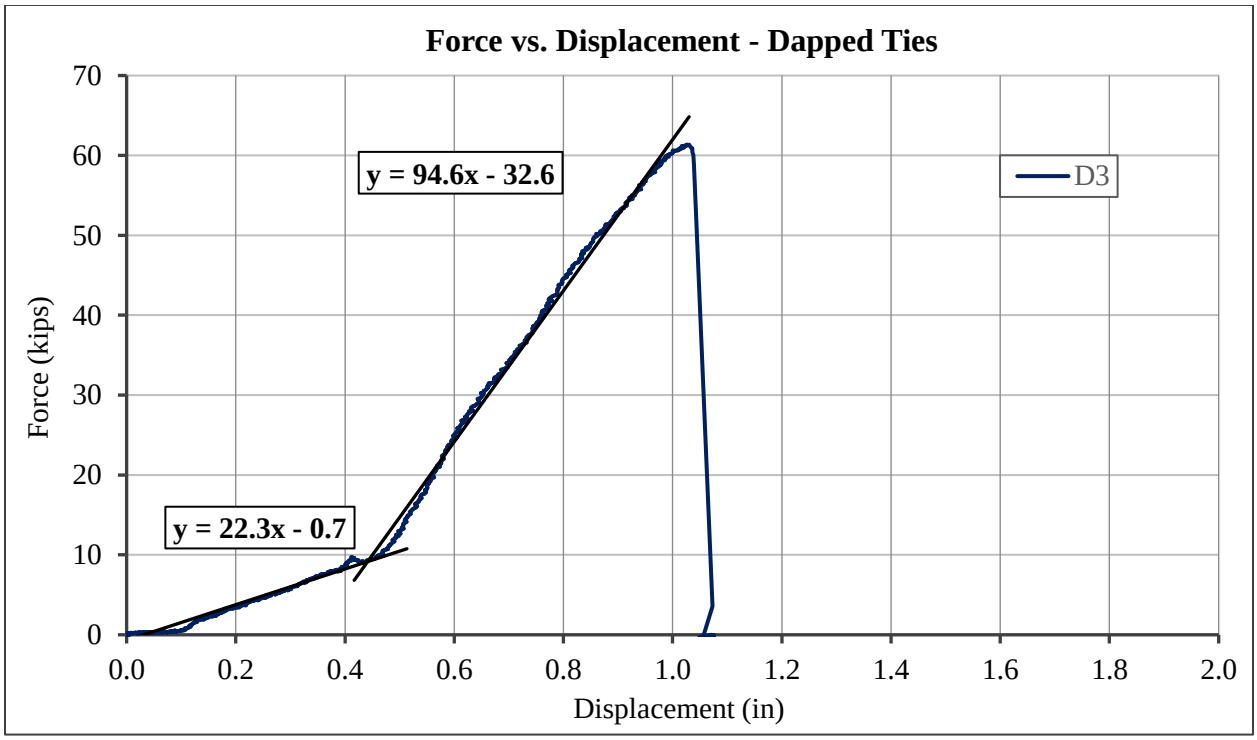

Figure 113: Bilinear curve for dapped specimen D3

Table 12: S1 and S2 slope values for dapped specimens

Sample	Slope (kip/in)	
	S1	S2
D1	70.3	145.2
D2	55.4	119.8
D3	22.3	94.5
D4	50.1	104.5
D5	27.0	105.1
Average Slope	**45.0**	**113.8**

The slope values from all the dapped samples were averaged to obtain the overall contribution towards lateral resistance as shown in the graph in Figure 114 which can be used as a design tool to estimate the lateral resistance from the dap based on lateral displacement of the tie. The average S1 and S2 values for dapped specimens that were used to plot the graph in Figure 114 were compared to the results from material testing that was done to determine the compressive strength of the wood parallel to grain.

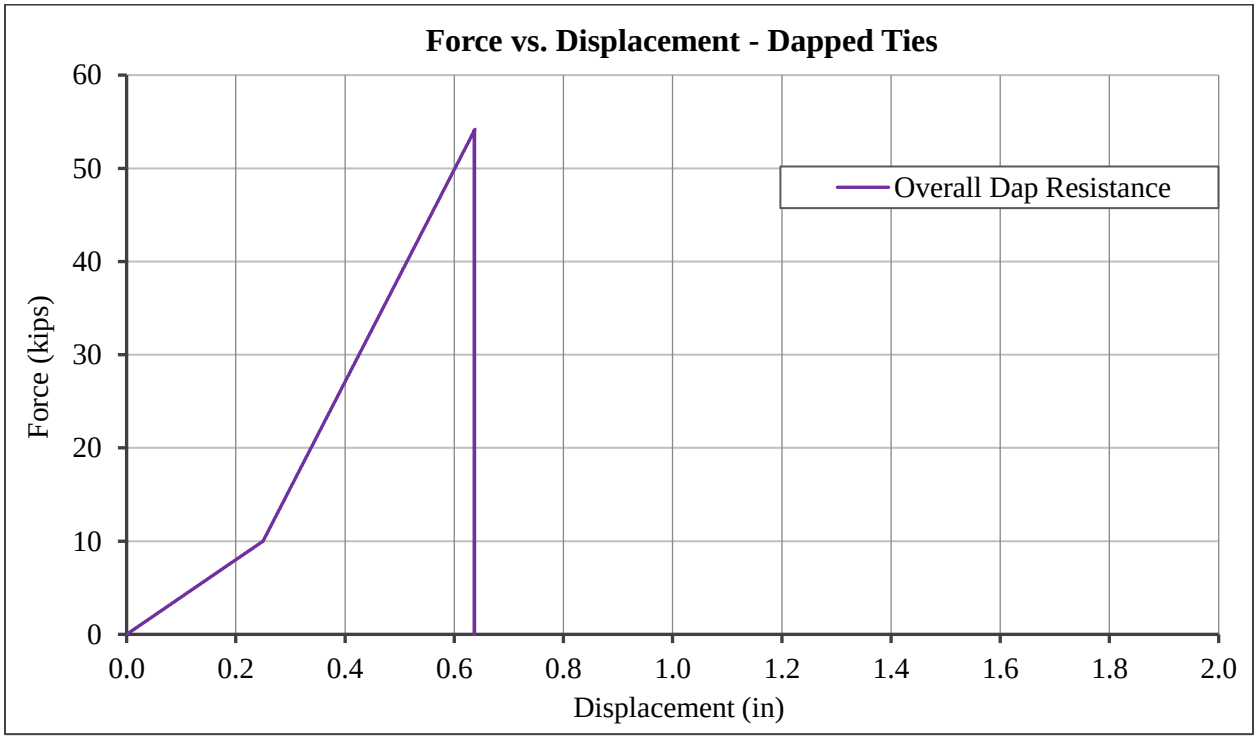

Figure 114: Average lateral resistance due to dap as a function of lateral displacement

A force versus displacement graph was also plotted for all the samples that were tested in compression parallel to grain as can be seen in Figure 115. Similar to the graph in Figure 114, the graph in Figure 115 uses a bilinear curve to calculate the average slope of small scale samples. It was observed that the average slope values, S1 (45 kip/in) and S2 (113 kip/in) of the dapped tie specimens was similar to the average slope values S1 (47.5 kip/in) and S2 (133 kip/in) respectively, which were obtained from material testing.

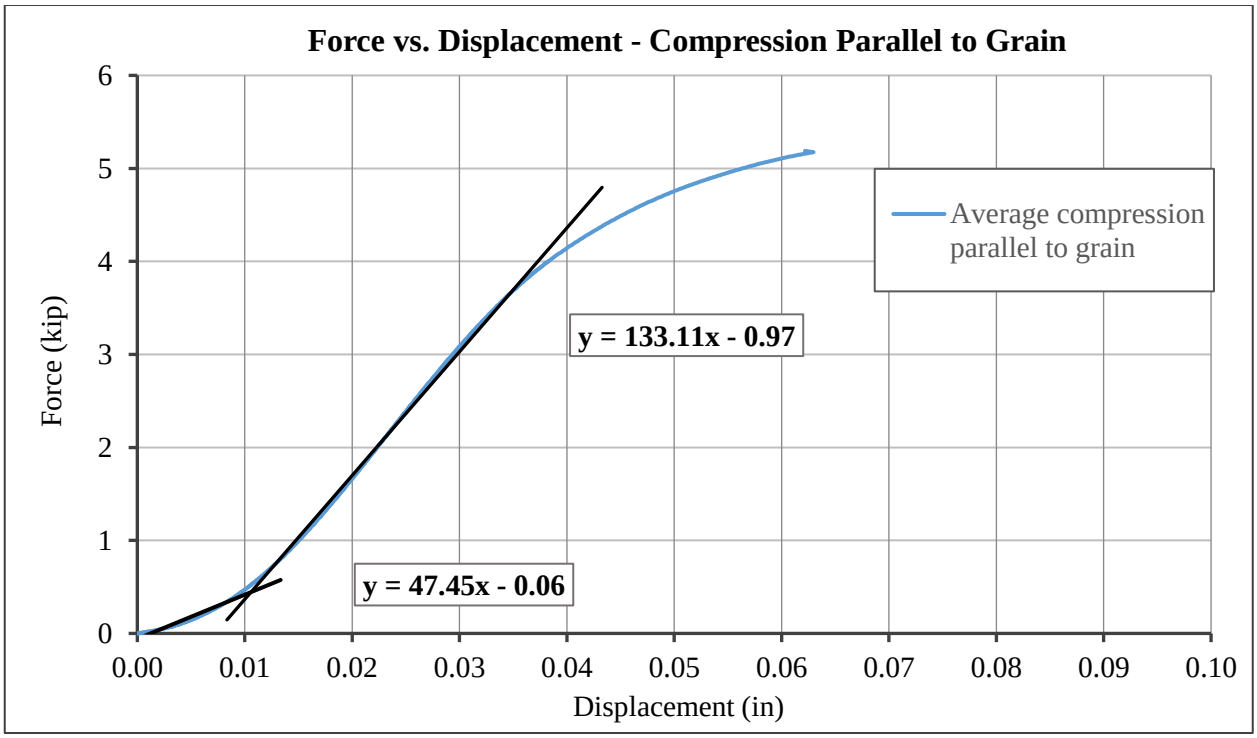

Figure 115: Force vs. displacement for average compressive strength parallel to grain

Dimensions of each tie specimen were recorded prior to testing as seen in Table 13. The height of the dap measured closer to the notch is referred to as dap height A, and the dap height away from the notch is referred to as dap height B as seen in Figure 116. The area of the horizontal shear plane was calculated by multiplying the width of the tie with the distance between the notch and the edge of the dap bearing against the steel plate as seen in Figure 116. The horizontal shear stress at this plane was determined by dividing the ultimate lateral load in kips with the area of the shear plane. It can be observed that all the dapped specimens failed at an average horizontal shear stress of 0.46 ksi. This appears to indicate that the resulting shear stress parallel to grain is similar for all dapped ties.

Table 13: Dimensions of tested tie samples

Tie Dimensions							
Sample	**Dap height (A)** *in.*	**Dap height (B)** *in.*	**Width** *in.*	**Length of shear plane** *in.*	**Area** *in²*	**Ultimate force** *kip*	**Shear stress** *ksi*
D1	1.5	1.5	9.5	12	114	52.5	0.46
D2	1.75	1.75	10	12	120	53.4	0.44
D3	2	1	9.5	12	114	61.3	0.54
D4	2	1.6	10	12	120	51.4	0.43
D5	2	1	9.5	12	114	51.0	0.45
					Average Shear Stress		**0.46**

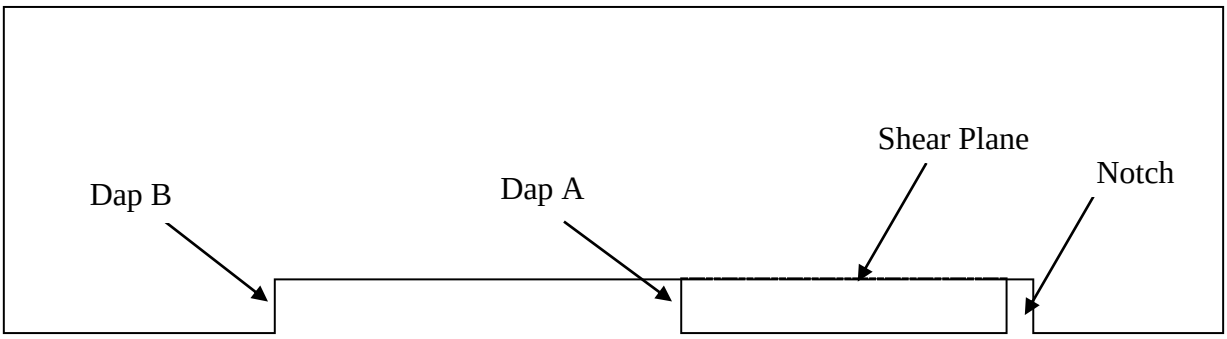

Figure 116: Dapped tie specimen

4.6 Total Lateral Resistance

The structural test set up for this research project involved looking at a tie, fastener and girder assembly for one half of the track on a railroad bridge. In an actual open deck railroad bridge with plate girders, there are two bridge girders and two fasteners that act as one system with a full length bridge tie as seen in Figure 117. Assuming that the railroad bridge is curving to the right, the lateral forces generated for this system act towards the left as indicated in Figure 117.

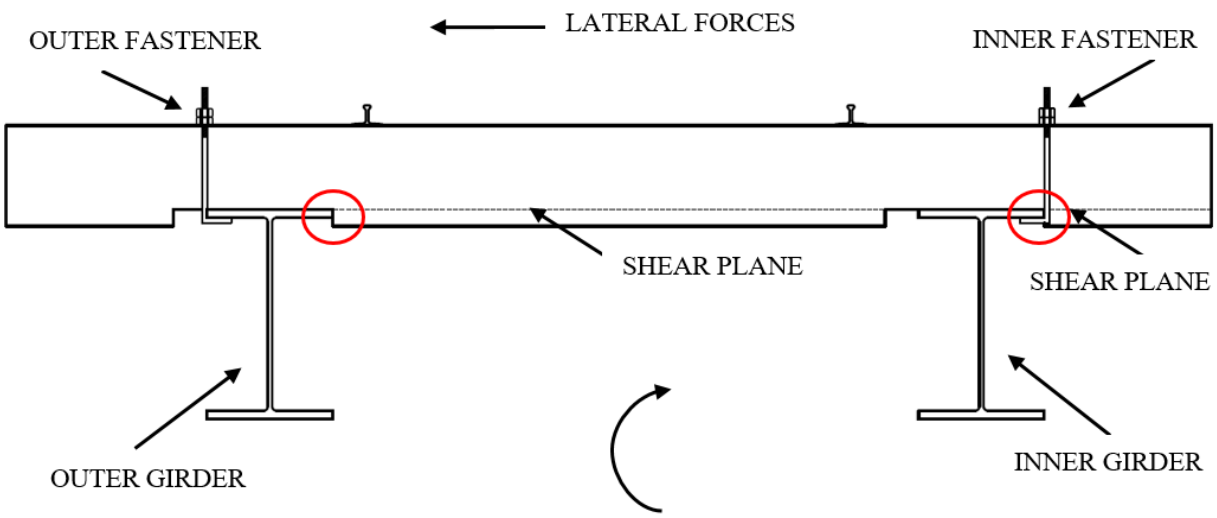

Figure 117: Full track assembly in a railroad bridge, with both inner and outer daps being engaged

In such a case, it can be observed that only the fastener on the inner rail contributes towards overall lateral resistance by bearing against the girder flange. Because of the orientation of the fastener on the outer rail, it does not provide any lateral resistance against lateral forces that are generated at the outer rail as it does not bear against the top flange of the bridge girder. Since only one fastener is engaged, it is recommended that the contribution from only one fastener in the system shown in Figure 117 be included for determining the total lateral resistance. The fastener on the outer rail may provide lateral resistance if it is not loose and if there is tension in the bolt.

In the railroad industry, daps are typically oversized to be greater than the width of the bridge girder flange so that they can be installed easily in the field. Dap lateral resistance is a function of the area of the horizontal shear plane. Therefore, dap strength depends the portion of the dapped tie which is engaged by bearing against a girder flange. In Figure 117, the outer dap and the inner dap are engaged with the outer and inner girder flanges respectively. In such a case, the center portion of the tie between both the girders, and the portion of the tie to the right of the inner girder will comprise of the shear plane. It is also possible that only the inner dap is engaged

as shown in Figure 118 where the shear plane will be over the length of the tie overhang to the right of the inner girder. It is possible that only the outer dap is engaged as shown in Figure 119 with the shear plane forming at the center portion of the tie. The lateral strength contribution from the dap changes, depending on which portion of the bridge tie is subject to bearing. Therefore, the slope of the graph shown in Figure 114 for the average resistance from the dap can increase or decrease as a function of the area of the shear plane.

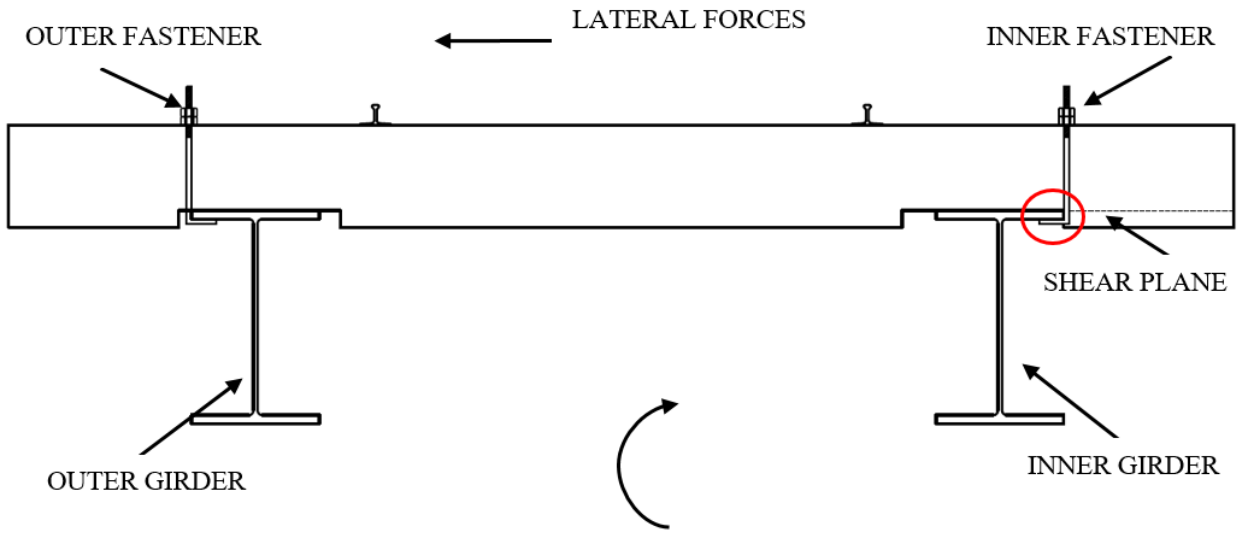

Figure 118: Full track assembly in a railroad bridge, with only the inner dap being engaged

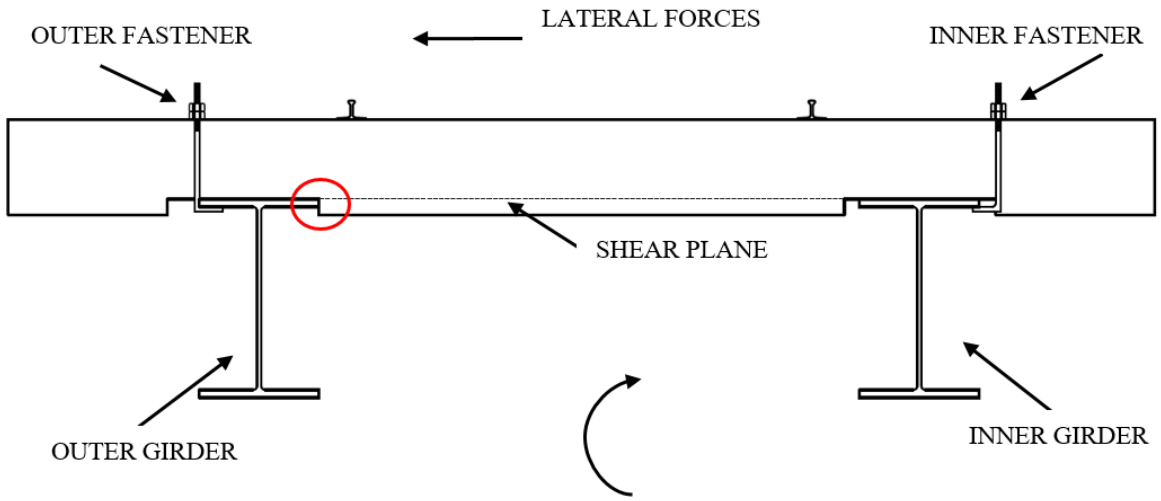

Figure 119: Full track assembly in a railroad bridge, with only the outer dap being engaged

From Figure 117 it can also be observed that wheel loads applied to the rails may not align with the axis of the bridge girders. For research purposes, the structural test set up for this project ignored the effect of load eccentricity between the rails and the bridge girders and assumed that the vertical loads were applied directly to the girder section. In an actual railroad bridge, the vertical loads are distributed to the ties from the rails and transferred to the girders from the tie.

4.7 Preliminary Guide for Calculating Lateral Resistance

Figure 120 shows the force versus displacement graph with the average lateral resistance from the dap and each of the three fasteners. In this research project, superposition was used as the primary approach to obtain the total lateral resistance of the system shown in Figure 117 by summing the lateral resistance contributions from friction, fasteners and from the dap. The plots representing the average resistance contributions from the dap and from each type of fastener in Figure 120 can be superimposed based on the type of fastener and the availability of the dap. The friction resistance contribution was calculated as a function of the vertical load applied on the

system. The steps for calculating overall lateral resistance for one potential case of a railroad bridge with square body hook bolts and a normal force of 45 kip from the train wheels are described in this section.

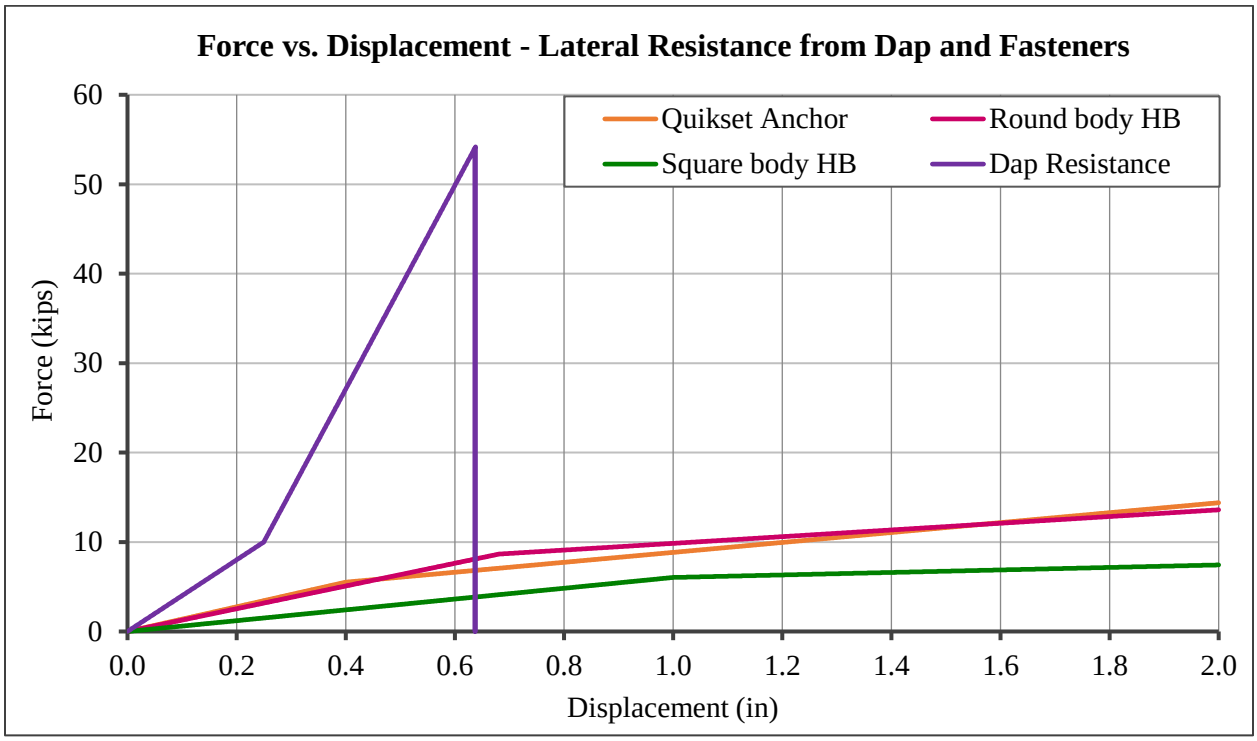

Figure 120: Lateral force vs. lateral displacement with average resistance from the dap and from fasteners

The lateral resistance due to friction is a function of the normal force. For a vertical wheel load of 45 kip, the average lateral resistance due to friction is obtained as 18 kip from Figure 82 or by multiplying the magnitude of the normal force by the static friction coefficient of 0.41. Superposition of average lateral resistance from friction, from the dap and from square body hook bolts can be seen in the lateral force versus lateral displacement graph shown in Figure 121. From Figure 121 it can be observed that the ultimate overall lateral resistance for this particular system is 75 kip if the dap is engaged. For cases where there is no dap engagement because of the dap being oversized or if undapped bridge ties are used, the superimposed lateral resistance from

friction and from square body hook bolts can be obtained from Figure 122. Since a single bridge tie only carries a percentage of the lateral wheel load, it was assumed that a single tie carried a maximum load distribution of 60% as discussed previously in Chapter 2. 60% of the AREMA maximum lateral load is plotted in the graphs in Figure 121 and Figure 122.

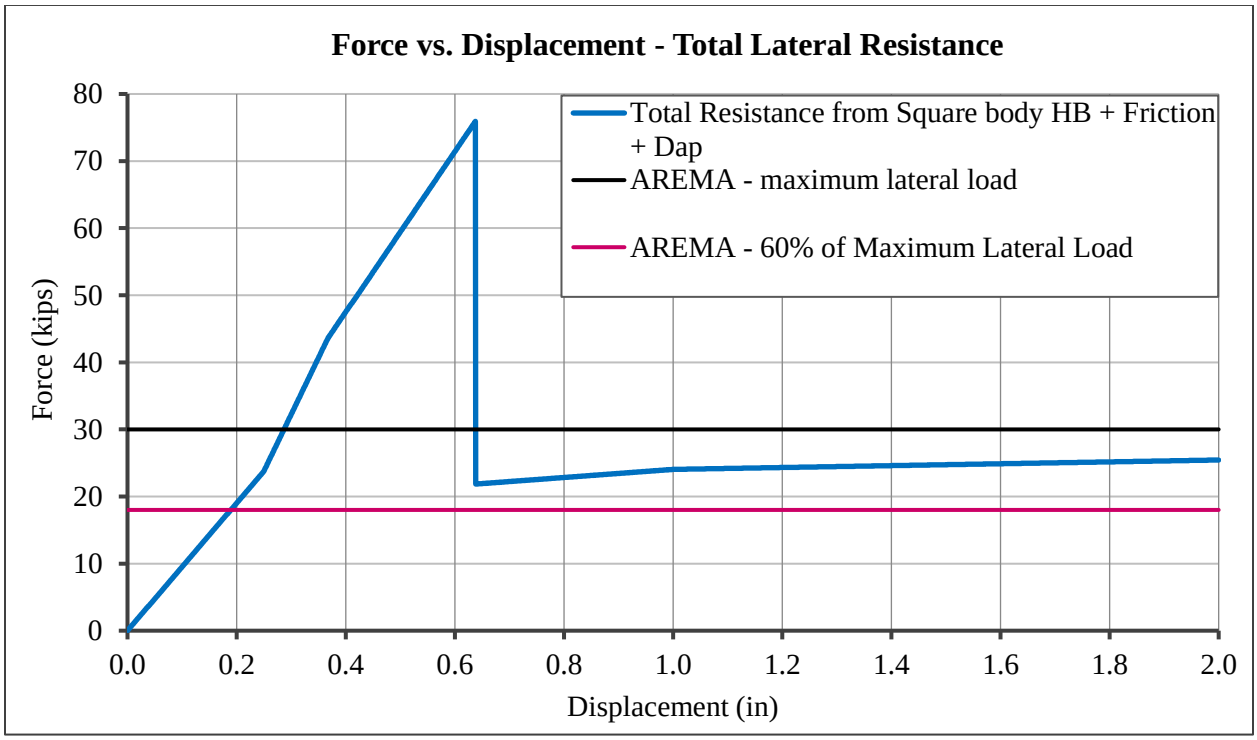

Figure 121: Lateral force vs. lateral displacement for superposition of average lateral resistance from the dap, from friction and from the fasteners

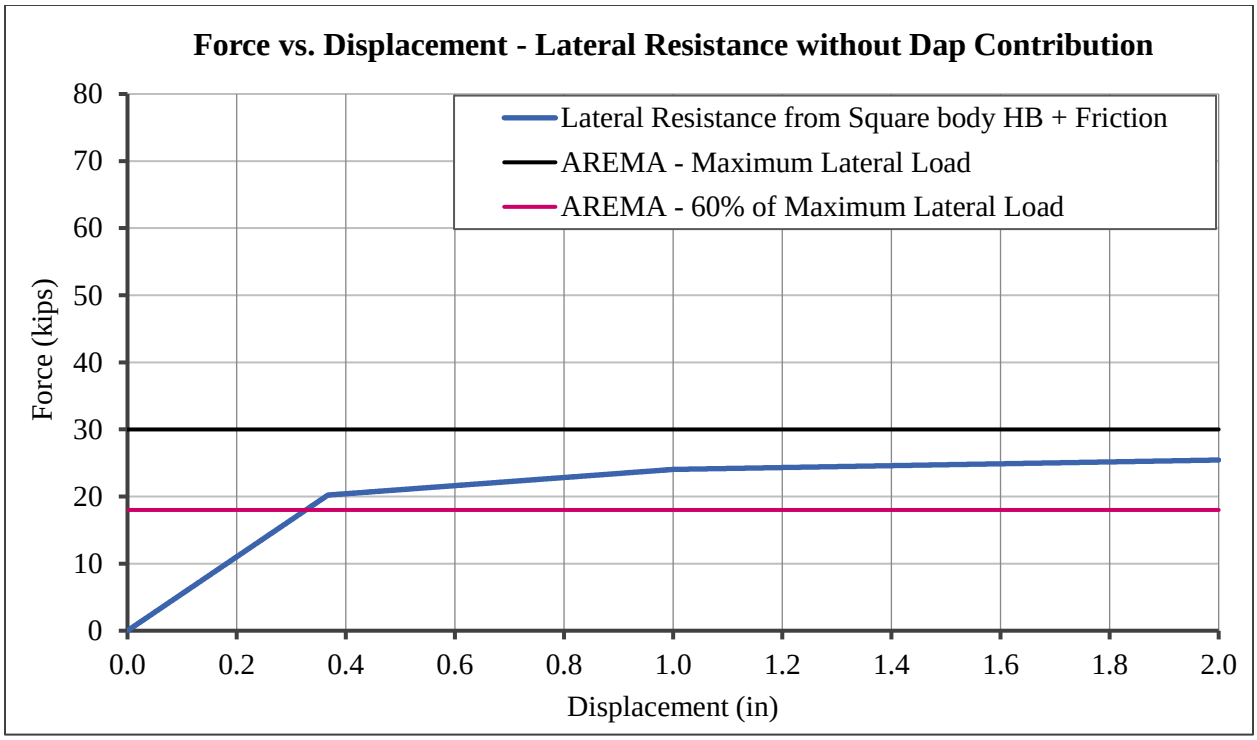

Figure 122: Lateral force vs. lateral displacement for average lateral resistance from friction and from the fasteners

A maximum lateral wheel to rail load of 30 kip of the rail was recorded from the load provisions given by AREMA as earlier described in Figure 28. Assuming that a single bridge carries the 30 kip lateral load, it can be seen in Figure 121 that with contribution from the dap there is sufficient lateral resistance. It can be seen in Figure 122 that there is sufficient lateral resistance without the dap which is beneficial for bridges that have undapped ties, assuming that each bridge tie carries 60% of the maximum load. In a condition where the vertical load is as low as 5 kip, it is estimated that the resistance from friction as well as the demand lateral loads will also be reduced. Therefore, it can be concluded that there is sufficient lateral resistance capacity from the superposition of lateral resistance from the friction, the fastener and the dap to meet the demand in an actual open deck railroad bridge with smooth top girders.

4.7.1 Sample calculation for determining lateral resistance

Equation 14 was used to plot Figure 121 and Figure 122 which can be used to calculate the lateral resistance as a function of lateral displacement. For this research project a displacement of 0.5 in. has been used as the primary value for determining the lateral resistance contribution from the dap and from the fastener. The sample calculation for the lateral capacity of a railroad bridge with smooth top girders, having dapped ties with square body hook bolts under the application of a train wheel load of 45 kip is shown below. It was assumed that only the inner dap was engaged as shown in Figure 118.

$LR_u = F_f + F_B + F_D$		Equation 14
$F_f(N) = \mu N$	$\mu = 0.41$	-
$F_B(x) = F_{B1}, F_{B2}\ or\ F_{B3}$	$F_{B1}(x) = 6.04x$ $F_{B1}(x) = 1.4x + 4.64$	For $x < 1.0$ $x \geq 1.0$
	$F_{B2}(x) = 12.71x$ $F_{B2}(x) = 3.75x + 6.1$	For $x < 0.68$ $x \geq 0.68$
	$F_{B3}(x) = 13.78x$ $F_{B3}(x) = 5.55x + 3.29$	For $x < 0.4$ $x \geq 0.4$
$F_D(A_{shear}) = A_{shear}\sigma$	$\sigma = 0.46$	-

Where:

LR_u = Ultimate lateral resistance capacity of the system (kip)

F_f = Lateral resistance capacity due to friction (kip)

μ = Coefficient of Static Friction (0.41)

N = Normal force or the vertical wheel load applied to a single rail (kip)

F_B = Lateral resistance capacity due to the fastener (kip)

F_{B1} = Lateral resistance capacity due to Square body hook bolts (kip)

F_{B2} = Lateral resistance capacity due to Lewis Forged hook bolts (kip)

F_{B3} = Lateral resistance capacity due to Quikset Anchors (kip)

F_D = Lateral resistance capacity due to the dap (kip)

x = Lateral displacement (in.)

A_{shear} = Area of the shear plane depending on dap engagement (in^2)

σ = Shear stress in the shear plane (0.46 ksi)

Friction resistance:

N = 45 kip (Applied vertical wheel load)
$F_f(N) = 0.41 * 45$
$\boldsymbol{F_f(N) = 18.45\ kip}$

Fastener resistance:

$F_B = F_{B1}$
$F_{B1} = 6.04 * 0.5$ (Assuming x = 0.5 in.)
$\boldsymbol{F_B = 3.02\ kip}$

Resistance from the inner dap:

$A_{shear} = Tie\ width\ x\ Length\ of\ shear\ plane$
$A_{shear} = 10x\ 20$
$A_{shear} = 200in^2$
$F_D(A_{shear}) = 200 * 0.46$
$\boldsymbol{F_D(A_{shear}) = 92\ kip}$

Total lateral resistance:

$LR_u = F_f + F_B + F_D$
$LR_u = 18.45 + 3.02 + 92$
$\boldsymbol{LR_u = 113.5\ kip}$

4.8 Preliminary Guide for Fastener spacing

There are multiple ways that a fastener can be spaced on an open deck railroad bridge. One potential case is described in this section with square body hook bolts spaced at every third tie. One half of the railroad track was analyzed using a free body diagram with the lateral demand loads generated in a curved bridge and the lateral resistance forces due to friction F_f, and due to the fastener F_B. Mastan2 was used to analyze reaction forces from the ties that did not have a fastener and reaction forces from ties that had a fastener. Eight ties were analyzed as reaction forces spaced at a nominal spacing of 16 in. center to center for bridge ties, with a fastener at every fourth tie. The first tie had a pin support and the other seven ties had roller supports. Two cases were analyzed by varying the point of application of the demand lateral load, F_{lat}.

Case 1 was chosen because it represented the worst case scenario for the second and third tie by generating the maximum reaction at the second or the third tie. It was also the point which was farthest away from the first tie and the fourth tie, which had fasteners as shown in Figure 123. In Case 1, F_{lat} of 30 kip was applied at the halfway point between the first and the fourth tie as shown in Figure 123. The maximum reaction for this case was analyzed as 15.2 kip at the third tie as seen in Figure 124. Assuming a maximum lateral load distribution of 60% to a single tie, when a load of 18 kip was applied for Case 1, it was observed that the maximum reaction reduced to 9.1 kip as shown in Figure 125.

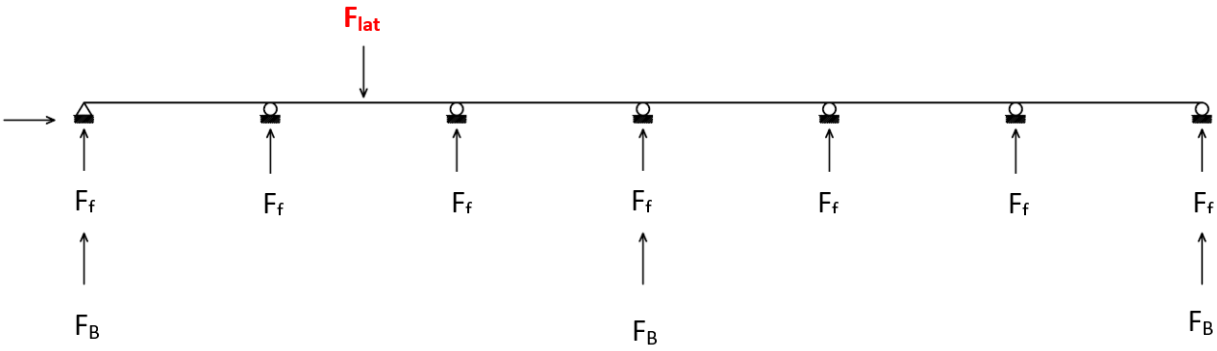

Figure 123: Case 1 - Lateral demand load (F_{lat}) at the midpoint between the first tie and the fourth tie that had fasteners

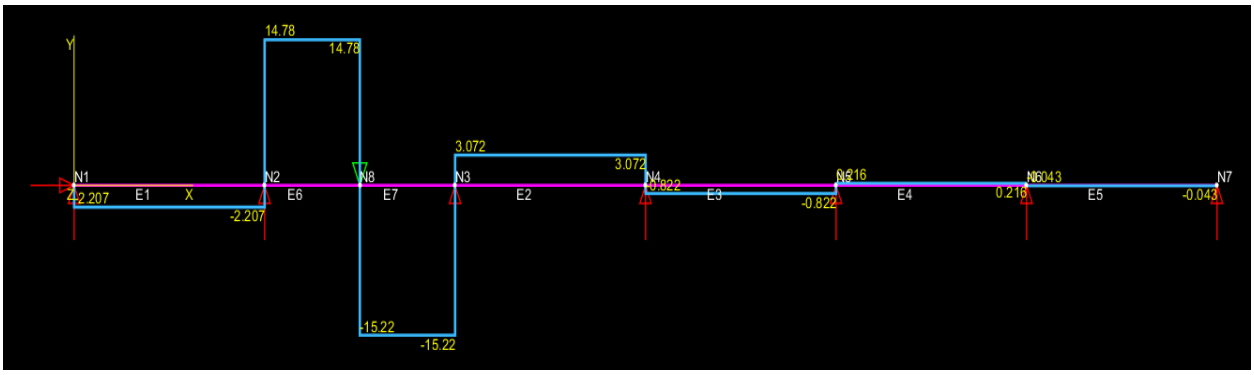

Figure 124: Case 1 – F_{lat} of 30 kip applied at the midpoint between the first tie and the fourth tie

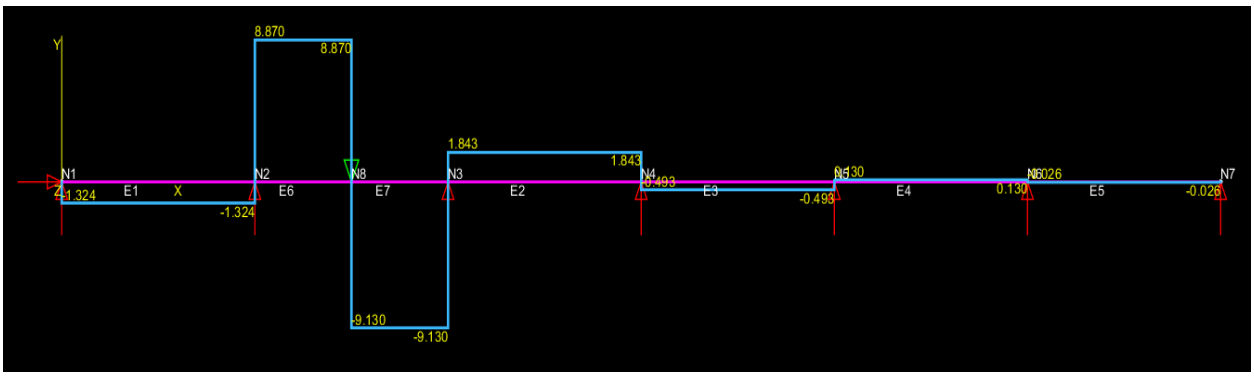

Figure 125: Case 1 – 18 kip (60% of F_{lat}) applied at the midpoint between the first tie and the fourth tie

For Case 2, F_{lat} of 30 kip was applied at the fourth tie which had a fastener as shown in Figure 126. This case was chosen because it represented the worst case scenario for the fourth tie by generating the largest reaction at the fourth tie. A maximum reaction of 29.3 kip was calculated at the fourth tie as seen in Figure 127. Assuming a 60% distribution of demand lateral load, when F_{lat} of 18 kip was applied at the fourth tie, the maximum reaction reduced to 17.6 kip as seen in Figure 128.

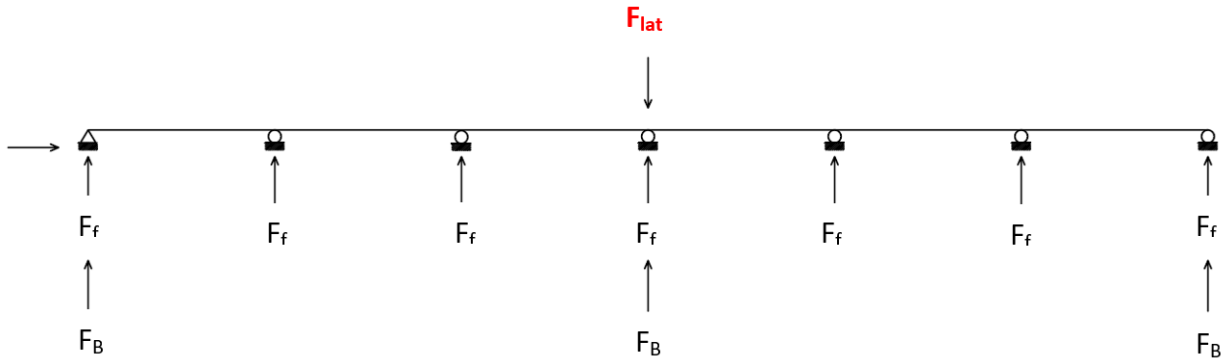

Figure 126: Case 2 - Lateral demand load (F_{lat}) at the fourth tie having a sqaure body hook bolt

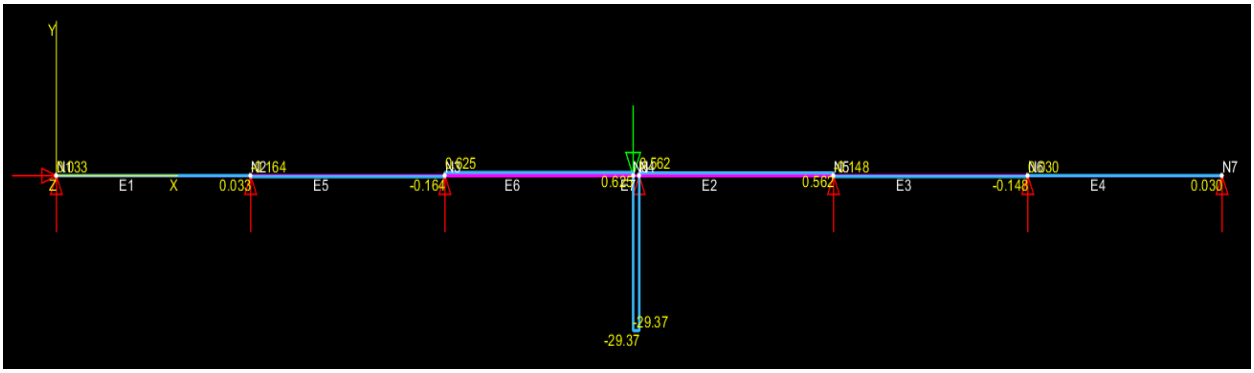

Figure 127: Case 2 – F_{lat} of 30 kip applied at the fourth tie having a sqaure body hook bolt

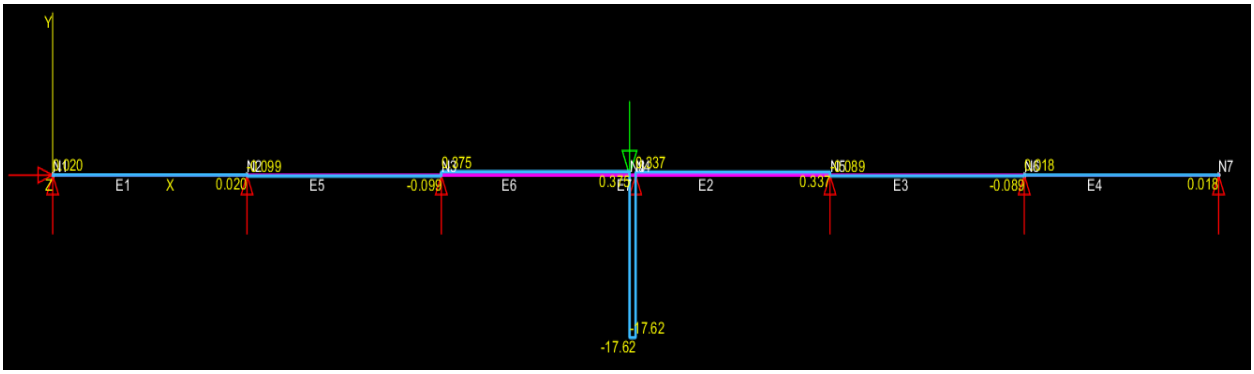

Figure 128: Case 2 – 18 kip (60% of F_{lat}) applied at the fourth tie having a sqaure body hook bolt

The lateral demand loads described in Case 1 and Case 2 and the reaction forces at each tie were compared to the lateral resistance capacity using Equation 15. The maximum reaction force due to F_{lat} can be obtained from the structural analysis model for Case 1 and Case 2. The total lateral resistance capacity can be calculated using Equation 14. If Equation 15 is satisfied, it can be concluded that the system has sufficient lateral resistance from a combination of friction and fasteners. If the reactions generated from the demand loads were less than or equal to the sum of the resistance from friction and from the fastener, it can be proved that the system has adequate lateral resistance from friction and that additional lateral resistance from the dap is not required. Therefore, for the forces described in Case 1 and Case 2, it can be assumed that the fastener spacing which was used is adequate if Equation 15 is satisfied.

$$R_u \leq LR_u \qquad \text{Equation 15}$$

Where:

R_u = Ultimate reaction due to F_{lat} from structural analysis (kip)

LR_u = Ultimate lateral resistance capacity of the system (kip)

R_u was calculated as 29.3 kip from Case 2 and LR_u was calculated as 113.5 kip in 4.7.1. Since LR_u is greater than R_u it can be concluded that square body hook bolts spaced at every third tie provide adequate lateral resistance against lateral loads generated by a wheel load of 45 kip.

CHAPTER 5: CONCLUSIONS AND RECOMMENDATIONS

This chapter describes important conclusions drawn from this research study and presents recommendations for future work. Conclusions from each phase of testing are described in sections 5.1, 5.2 and 5.3. Total lateral resistance conclusions for system having two bridge girders, one bridge tie and one fastener are explained in 5.4. Recommendations can be found in section 5.5.

5.1 Friction Resistance

1. The coefficient of static friction was calculated as 0.41 and the coefficient of kinetic friction was calculated as 0.42. The static friction coefficient was used to develop the equation for lateral resistance due to friction shown below as it was more conservative.

$$F_f(N) = \mu N$$

   Where:

   F_f = Lateral resistance capacity due to friction (kip)

   μ = Coefficient of Static Friction (0.41)

   N = Normal force or the vertical wheel load applied to a single rail (kip)

2. Lateral resistance was found to be directly proportionate to the magnitude of the applied vertical load.
3. It was observed that relaxation of the wood fibers in the ties does not affect lateral resistance due to friction of the tie. Therefore, ties can be reused for multiple tests.
4. Presence of grease or dried rail lubricant on the sliding surface of the tie increased the lateral resistance of the tie by 1 - 2 kip after initial slip in the presence of a vertical load.
5. Stick slip behavior can be expected when the surface of the tie is clean of grease or rail lubricant. Stick slip behavior also appears to be during the application of a higher vertical load.

6. Imperfections in the sliding surface of the tie caused minor variations in lateral load.

5.2 Fastener Resistance

1. Lateral resistance from the fastener was calculated based on the type of fastener (Square body hook bolt, Lewis Forged hook bolt or the Quikset Anchor) which is used. Lateral resistance for each type of fastener was calculated as a function of the lateral displacement in inches. For the purposes of this research project, a lateral displacement of 0.5 in. was used.

$F_B(x) = F_{B1}, F_{B2}\ or\ F_{B3}$	$F_{B1}(x) = 6.04x$ $F_{B1}(x) = 1.4x + 4.64$	For $x < 1.0$ $x \geq 1.0$
	$F_{B2}(x) = 12.71x$ $F_{B2}(x) = 3.75x + 6.1$	For $x < 0.68$ $x \geq 0.68$
	$F_{B3}(x) = 13.78x$ $F_{B3}(x) = 5.55x + 3.29$	For $x < 0.4$ $x \geq 0.4$

Where:

F_B = Lateral resistance capacity due to the fastener (kip)

F_{B1} = Lateral resistance capacity due to Square body hook bolts (kip)

F_{B2} = Lateral resistance capacity due to Lewis Forged hook bolts (kip)

F_{B3} = Lateral resistance capacity due to Quikset Anchors (kip)

x = Lateral displacement (in.)

2. Square body hook bolts had a lateral resistance in the range of 7 kip – 9 kip.
3. During lateral loading, the square body hook bolt did not engage with the edge of the steel plate and the tie lifted up over the steel plate when laterally loaded beyond 2 in. of

displacement. Failure in square body hook bolts occurred due to bending near the hook under lateral loading.

4. Square body hook bolts showed yielding over the length of the fastener having a square cross section which did not include the threaded portion of the bolt. The fastener deformed by 21 degrees under later loading.
5. Lewis Forged hook bolts had a lateral resistance in the range of 10 kip – 14 kip.
6. The hook of the Lewis Forged hook bolt engaged with the steel plate before fracture in the fastener. As a result of fastener engagement with the steel plate, there was no tie uplift during fastener failure in the case of the Lewis Forged hook bolt.
7. Lewis Forged hook bolts exhibited more localized flexural yielding near the hook at an average angle of 29 degrees.
8. Quikset Anchors had lateral resistance in the range of 12 kip – 16 kip.
9. Quikset Anchors exhibited two failure modes with the first being the hook climbing over the steel plate under lateral loading in cases where a cheater bar was not used to tighten the bolt. The second failure mode was fracture of the fastener when the Quikset Anchor was tightened using a cheater bar of length 40 in. Tests proved that failure modes depend on the method of installation.
10. The lock plate did not affect lateral resistance of the fastener. It prevented sideways movement of the hook by locking it in position during loading.

5.3 Dap Contribution

1. Lateral resistance from a dapped tie can be calculated using the following equation:

$$F_D(A_{shear}) = A_{shear}\sigma$$

Where,

F_D = Lateral resistance capacity due to the dap (kip)

A_{shear} = Area of the shear plane depending on dap engagement (in^2)

σ = Shear stress in the shear plane equal to 0.46 ksi

2. Dap strength was found to be a function of the shear stress in the wood which depends on the area of the shear plane. The area of the shear plane for a tie can be calculated by multiplying the length of the shear plane with the width of the tie.
3. The length of the shear plane depends on dap engagement in the bridge tie due to the dap bearing against the girder flange.
4. Daps have a considerable amount of lateral resistance when engaged, in the range of 55 kip – 65 kip.
5. The slope of the data from the average lateral resistance of the dap was found to be similar to the stiffness of the wood in compression parallel to grain from the time of initial engagement of the lateral load in the dapped tie until failure of the dap.

5.4 Total Lateral Resistance

The total lateral resistance of a system consisting of a bridge tie, fasteners and two bridge girders on an open deck railroad bridge can be calculated using the following equation:

$$LR_u = F_f + F_B + F_D$$

Where:

F_f = Lateral resistance capacity due to friction (kip)

F_B = Lateral resistance capacity due to the fastener (kip)

F_D = Lateral resistance capacity due to the dap (kip)

5.5 Recommendations for Future Work

1. Current structural testing involved simulating just one half of the track on a railroad bridge containing one portion of a bridge tie and a single bridge girder. Lateral testing with a full length bridge tie resting on two bridge girders is recommended in order to investigate the behavior of the full track system.
2. Investigate dap strength as a function of the area of the shear plane in a full track system by using a full length bridge tie with oversized daps and changing the location of dap engagement against the bridge flanges. Conduct lateral testing to observe multiple failure modes in a dapped bridge tie and identify the length of the shear plane during various dap engagement scenarios to study dap limit states.
3. Conduct material testing to determine shear strength parallel to grain for the wood species used in the bridge ties. Analyze dap failure limit states of crushing in the direction parallel to grain and horizontal shear parallel to grain by comparing material strength properties.
4. Study the effect of longitudinal forces generated during train braking and acceleration on lateral resistance by conducting experimental tests and loading bridge ties in the longitudinal and lateral direction.
5. Preliminary bridge surveys revealed that fasteners on existing railroad bridges were loose. Investigate if loose fasteners on a railroad bridge are a cause for concern, by studying the lateral resistance capacity of loose fasteners through structural testing on fasteners that have been installed without a nut and washer to ensure there is no tension in the bolt.
6. Study the effect of riveted top girders on lateral resistance of the railroad bridge track. Perform lateral testing of ties resting on a riveted top flange to study variations in resistance due to friction under application of a simultaneous vertical load.

7. Study how changing the material of the tie affects lateral resistance. Perform structural tests by changing the species of the wood used in the bridge tie. Also investigate how glulam ties or composite ties affect lateral resistance.
8. Create finite element models to determine the force distribution in a bridge tie during the simultaneous application of vertical and lateral loads. Analyze a section of a railroad bridge track as a beam on an elastic foundation to determine spacing requirements for fasteners.

CHAPTER 6: BIBLIOGRAPHY

AREMA. (2003a). Introduction to Railway Structures. In *Practical Guide To Railway Engineering* (pp. 320–388). AREMA. Retrieved from http://www.arema.org/files/pubs/pgre/PGChapter8.pdf

AREMA. (2003b). Railway Track Design. In *Practical Guide To Railway Engineering* (pp. 217–234). Retrieved from http://www.arema.org/files/pubs/pgre/PGChapter6.pdf

AREMA. (2010). *AREMA Manual for Railway Engineering: Chapter 30 Ties*.

AREMA. (2017a). *AREMA Manual for Railway Engineering: Chapter 15 Steel Structures*. https://doi.org/10.1163/ej.9789004155947.i-937.23

AREMA. (2017b). *AREMA Manual for Railway Engineering: Chapter 30 Ties*.

ASTM Standard. (2013). ASTM G115 - 10: Standard Guide for Measuring and Reporting Friction Coefficients. *ASTM Standards*, *10*(Reapproved 2013), 13. https://doi.org/10.1520/G0115-10R13.2

ASTM Standard. (2014). Standard Test Methods for Small Clear Specimens of Timber - D143. *ASTM International*, (0), 31. https://doi.org/10.1520/D0143-09.2

Choros, J., Zarembski, A. M., & Gitlin, I. (1980). *Laboratory Investigation of Lateral Track Shift*.

Igwemezie, J. (1987). *Dynamic Response and Impact Effects In Precast, Prestressed Concrete Bridge Ties*. McGill University.

Igwemezie, J. (2014). Understanding Stresses in Rails (Part 1 of 2). *Interface Journal*. Retrieved from http://interfacejournal.com/archives/532

Igwemezie, J., & Mirza, S. (1989). Impact Load Distribution In Concrete Bridge Ties. *Journal of Structural Engineering*, *115*(3), 526–542.

Iwnicki, S., Wickens, A. H., Orlova, A., & Boronenko, Y. (2006). *Handbook of Railway Vehicle Dynamics*. (S. Iwnicki, Ed.). Boca Raton, FL: Taylor and Francis Group, LLC. https://doi.org/10.1201/9781420004892

Kratville, W. (1997). *The Car and Locomotive Cyclopedia of American Practices, Sixth Edition*. Simmons-Boardman Books, Inc.

Nilmani. (2011). Tracking and Curving by Railway Vehicle : Issues in Heavy Haul, 18. Retrieved from http://www.iricen.gov.in/iricen/ipwe_seminar/2011/nilmani.pdf

Oldknow, K. (2017). Wheel-Rail Interaction Fundamentals. Retrieved from https://www.wheel-rail-seminars.com/archives/2017/pc-papers/presentations/PC 1-3 Wheel-Rail Interaction

Fundamentals WRI 2017 - 20170604.pdf

Otter, D., Doe, B., & Belport, S. (2005). Rail Car Lateral Forces for Bridge Design and Rating. *Technology Digest*, (05), 002.

Railway Tie Association. (2018a). RTA-Frequently Asked Questions. Retrieved February 4, 2018, from https://www.rta.org/faqs-main

Railway Tie Association. (2018b). *TieReport 6*. Fayetteville, GA 30214. Retrieved from https://www.rta.org/assets/docs/TieReports/tiereport6.pdf

Webb, D. A., Webb, G. V, Zarembski, D. A., Smith, S., & Gauntt, J. C. (2016). *The Tie Guide*. Retrieved from https://www.rta.org/assets/docs/TieGuide/2016_tie guide for web.pdf

Zarembski, A. (n.d.). Dynamic Loading Track Structure Part II - Lateral Loads. Retrieved from https://www.rta.org/assets/docs/ComprehensiveRail/sec8/dynamic loading track structure part ii.pdf

Zarembski, A. M. (n.d.). Vertical Wheel Loads: The Distribution on Cross-Ties. Retrieved from http://www.rta.org/comprehensive-rail-and-track-related-research

APPENDIX A : SPECIFICATIONS FOR MATERIALS

This section includes data sheets for materials that were used in preparing and testing specimens for this project such as the Heavy Duty Hole Hawg drill and Teflon grease. This section also has specifications for each type of deck tie fastener used for testing.

DuPont® Heavy Equipment Grease
with Teflon® fluoropolymer

PRODUCT INFORMATION SHEET

Formulated for extreme conditions encountered in highway construction, farming, mining and trucking

For highly loaded bearings, gears, joints, chassis and more. Fortified with 3% Molybdenum.

Product Description

DuPont® Heavy Equipment Grease with Teflon® fluoropolymer is formulated to meet the extreme conditions encountered on off-highway construction equipment, as well as the demands of heavy equipment used in farming, mining and trucking. Formulated with high viscosity base oils, thickened with a lithium complex binder, and fortified with both molybdenum disulfide and Teflon® fluoropolymer to deliver load carrying and anti-wear performance.

DuPont® Heavy Equipment Grease with Teflon® fluoropolymer contains a blend of extreme pressure and anti-wear additives, and rust and oxidation inhibitors for wet conditions. A dropping point of 500°F (260°C) ensures retention in high temperature applications. Recommended operating temperature range: -10°F (-23°C) to 350°F (177°C).

Note: not recommended for automotive applications.

Features

- Film strength & mechanical stability
- Protection against wear & shock loads
- Low water washout (5%)
- Operating temperature range: -10°F (-23°C) to 350°F (177°C)
- Contains 3% molybdenum
- Meets NLGI #2

Directions For Use

For best results, remove old grease before applying.

Grease Specifications

Thickener Type	**Lithium Complex**		Timken OK Load (ASTM D-2509) lbs	**55 Min**
NLGI Grade	**#2**		Water Washout (ASTM D-1264) @ 79° C (175° F) % Loss Max	**5**
Texture	**Tacky**		Copper Strip Corrosion (ASTM D-4048) Rating	**1lb Max**
Color	**Grey**		Molybdenum Disulfide, %	**3.0 Min**
Odor	**Mild Petroleum**		Teflon® fluoropolymer % Min	**1.0**
Solubility in Water	**Insoluble**		**Base Oil Characteristic**	
Penetration @ 25°C (77°F) (ASTM D-217), mm/10, Worked 60 strokes	**265-295**		Base Fluid Type	**Petroleum Mineral Oil**
Dropping Point (ASTM D-2265) °F (°C) Min	**500 (260)**		Viscosity SUS @ 104°F / 40°C	**1,715 - 1,875**
Rust & Corrosion Test Rating (ASTM D-1743)	**Pass**		Viscosity SUS @ 212°F / 100°C	**110 - 122**
Four Ball Wear Test, Scar Diameter (ASTM D-2266) mm scar, 40kg, 1200 RPM 75°C, 1 H	**0.50**		Viscosity cSt @ 104°F / 40°C	**327 - 350**
Four Ball EP Test (ASTM D-2596) Load Wear Index, kg	**70**		Viscosity cSt @ 212°F / 100°C	**22 - 24.5**
Weld Point, Kg	**400**		Viscosity Index, Min	**80**

Ordering Information

Part Number	Container Size
DGE614101	**14 oz.** Cartridge
DGE616101	**16 oz.** Tub
DGE035101	**35 lb** Pail

For information on availability at specific retailers, visit the "Where to Buy" section of www.PerformanceLubricantsUSA.com

Handling - For safe handling information, consult the SDS.

For damage, sales or directions for use, call Finish Line at 631-666-4186 who assumes all liability in the manufacture of this product.

Finish Line Technologies, Inc.
50 Wireless Boulevard • Hauppauge, NY 11788 USA
Tel: 631 666-7300 • Fax: 631 666-7391
www.PerformanceLubricantsUSA.com

Specifications sheet for Heavy Duty Hole Hawg Drill:

Milwaukee®

OPERATOR'S MANUAL
MANUEL de L'UTILISATEUR
MANUAL del OPERADOR

Catalog No.
No de Cat.
1670-1
1675-1
1675-6
1676-6

HEAVY-DUTY HOLE HAWG®
FOREUSE EXTRA-ROBUSTE HOLE HAWG®
TALADRO HEAVY-DUTY HOLE HAWG®

TO REDUCE THE RISK OF INJURY, USER MUST READ AND UNDERSTAND OPERATOR'S MANUAL.

AFIN DE RÉDUIRE LE RISQUE DE BLESSURES, L'UTILISATEUR DOIT LIRE ET BIEN COMPRENDRE LE MANUEL DE L'UTILISATEUR.

PARA REDUCIR EL RIESGO DE LESIONES, EL USUARIO DEBE LEER Y ENTENDER EL MANUAL DEL OPERADOR.

GENERAL POWER TOOL SAFETY WARNINGS

WARNING **READ ALL SAFETY WARNINGS AND ALL INSTRUCTIONS. Failure to follow the warnings and instructions may result in electric shock, fire and/or serious injury. *Save all warnings and instructions for future reference.* The term "power tool" in the warnings refers to your mains-operated (corded) power tool or battery-operated (cordless) power tool.**

WORK AREA SAFETY

- **Keep work area clean and well lit.** Cluttered or dark areas invite accidents.
- **Do not operate power tools in explosive atmospheres, such as in the presence of flammable liquids, gases or dust.** Power tools create sparks which may ignite the dust or fumes.
- **Keep children and bystanders away while operating a power tool.** Distractions can cause you to lose control.

ELECTRICAL SAFETY

- **Power tool plugs must match the outlet. Never modify the plug in any way. Do not use any adapter plugs with earthed (grounded) power tools.** Unmodified plugs and matching outlets will reduce risk of electric shock.
- **Avoid body contact with earthed or grounded surfaces such as pipes, radiators, ranges and refrigerators.** There is an increased risk of electric shock if your body is earthed or grounded.
- **Do not expose power tools to rain or wet conditions.** Water entering a power tool will increase the risk of electric shock.
- **Do not abuse the cord. Never use the cord for carrying, pulling or unplugging the power tool. Keep cord away from heat, oil, sharp edges or moving parts.** Damaged or entangled cords increase the risk of electric shock.
- **When operating a power tool outdoors, use an extension cord suitable for outdoor use.** Use of a cord suitable for outdoor use reduces the risk of electric shock.
- **If operating a power tool in a damp location is unavoidable, use a ground fault circuit interrupter (GFCI) protected supply.** Use of an GFCI reduces the risk of electric shock.

PERSONAL SAFETY

- **Stay alert, watch what you are doing and use common sense when operating a power tool. Do not use a power tool while you are tired or under the influence of drugs, alcohol or medication.** A moment of inattention while operating power tools may result in serious personal injury.
- **Use personal protective equipment. Always wear eye protection.** Protective equipment such as dust mask, non-skid safety shoes, hard hat, or hearing protection used for appropriate conditions will reduce personal injuries.
- **Prevent unintentional starting. Ensure the switch is in the off-position before connecting to power source and/or battery pack, picking up or carrying the tool.** Carrying power tools with your finger on the switch or energising power tools that have the switch on invites accidents.
- **Remove any adjusting key or wrench before turning the power tool on.** A wrench or a key left attached to a rotating part of the power tool may result in personal injury.
- **Do not overreach. Keep proper footing and balance at all times.** This enables better control of the power tool in unexpected situations.
- **Dress properly. Do not wear loose clothing or jewellery. Keep your hair, clothing and gloves away from moving parts.** Loose clothes, jewellery or long hair can be caught in moving parts.
- **If devices are provided for the connection of dust extraction and collection facilities, ensure these are connected and properly used.** Use of dust collection can reduce dust-related hazards.

POWER TOOL USE AND CARE

- **Do not force the power tool. Use the correct power tool for your application.** The correct power tool will do the job better and safer at the rate for which it was designed.
- **Do not use the power tool if the switch does not turn it on and off.** Any power tool that cannot be controlled with the switch is dangerous and must be repaired.
- **Disconnect the plug from the power source and/or the battery pack from the power tool before making any adjustments, changing accessories, or storing power tools.** Such preventive safety measures reduce the risk of starting the power tool accidentally.
- **Store idle power tools out of the reach of children and do not allow persons unfamiliar with the power tool or these instructions to operate the power tool.** Power tools are dangerous in the hands of untrained users.
- **Maintain power tools. Check for misalignment or binding of moving parts, breakage of parts and any other condition that may affect the power tool's operation. If damaged, have the power tool repaired before use.** Many accidents are caused by poorly maintained power tools.
- **Keep cutting tools sharp and clean.** Properly maintained cutting tools with sharp cutting edges are less likely to bind and are easier to control.
- **Use the power tool, accessories and tool bits etc. in accordance with these instructions, taking into account the working conditions and the work to be performed.** Use of the power tool for operations different from those intended could result in a hazardous situation.

SERVICE

- **Have your power tool serviced by a qualified repair person using only identical replacement parts.** This will ensure that the safety of the power tool is maintained.

SPECIFIC SAFETY RULES

- **Use auxiliary handle(s), if supplied with the tool.** Loss of control can cause personal injury.
- **Hold power tool by insulated gripping surfaces, when performing an operation where the cutting accessory may contact hidden wiring or its own cord.** Cutting accessory contacting a "live" wire may make exposed metal parts of the power tool "live" and could give the operator an electric shock.
- **Maintain labels and nameplates.** These carry important information. If unreadable or missing, contact a *MILWAUKEE* service facility for a free replacement.
- **WARNING** Some dust created by power sanding, sawing, grinding, drilling, and other construction activities contains chemicals known to cause cancer, birth defects or other reproductive harm. Some examples of these chemicals are:
  - lead from lead-based paint
  - crystalline silica from bricks and cement and other masonry products, and
  - arsenic and chromium from chemically-treated lumber.

Your risk from these exposures varies, depending on how often you do this type of work. To reduce your exposure to these chemicals: work in a well ventilated area, and work with approved safety equipment, such as those dust masks that are specially designed to filter out microscopic particles.

SYMBOLOGY

A	Amps
V	Volts
~	Alternating Current Only
n_0 xxxxmin.$^{-1}$	No Load Revolutions per Minute (RPM)
c UL us	Underwriters Laboratories, Inc. United States and Canada
NOM ANCE	Mexican Approvals Marking

FUNCTIONAL DESCRIPTION

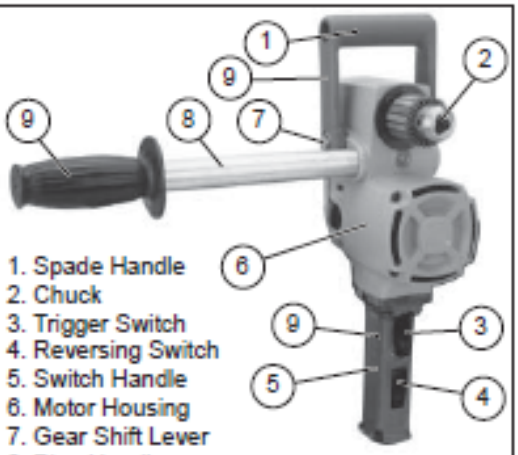

1. Spade Handle
2. Chuck
3. Trigger Switch
4. Reversing Switch
5. Switch Handle
6. Motor Housing
7. Gear Shift Lever
8. Pipe Handle
9. Insulated Gripping Surfaces

SPECIFICATIONS

				Steel Capacity	Wood Capacity		
Cat. No.	Volts AC	Speed	No Load RPm	Twist Bit	Auger Bits	Ship Auger Bits	Selfeed Bit
1670-1	120	-	900	7/16"	1-1/2"	1-1/2"	2-9/16"
1675-1	120	High	1200	5/16"	1-1/8"	1-1/4"	1-3/8"
		Low	300	1/2"	1-1/2"	1-1/2"	4-5/8"
1675-6	120	High	1200	5/16"	1-1/8"	1-1/4"	1-3/8"
		Low	300	1/2"	1-1/2"	1-1/2"	4-5/8"
1676-6	120	High	1200	5/16"	1-1/8"	1-1/4"	1-3/8"
		Low	300	1/2"	1-1/2"	1-1/2"	4-5/8"

GROUNDING

⚠ *WARNING* Improperly connecting the grounding wire can result in the risk of electric shock. Check with a qualified electrician if you are in doubt as to whether the outlet is properly grounded. Do not modify the plug provided with the tool. Never remove the grounding prong from the plug. Do not use the tool if the cord or plug is damaged. If damaged, have it repaired by a *MILWAUKEE* service facility before use. If the plug will not fit the outlet, have a proper outlet installed by a qualified electrician.

Grounded Tools: Tools with Three Prong Plugs
Tools marked "Grounding Required" have a three wire cord and three prong grounding plug. The plug must be connected to a properly grounded outlet (See Figure A). If the tool should electrically malfunction or break down, grounding provides a low resistance path to carry electricity away from the user, reducing the risk of electric shock.
The grounding prong in the plug is connected through the green wire inside the cord to the grounding system in the tool. The green wire in the cord must be the only wire connected to the tool's grounding system and must never be attached to an electrically "live" terminal.
Your tool must be plugged into an appropriate outlet, properly installed and grounded in accordance with all codes and ordinances. The plug and outlet should look like those in Figure A.

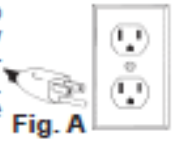
Fig. A

Double Insulated Tools:
Tools with Two Prong Plugs
Tools marked "Double Insulated" do not require grounding. They have a special double insulation system which satisfies OSHA requirements and complies with the applicable standards of Underwriters Laboratories, Inc., the Canadian Standard Association and the National Electrical Code. Double Insulated tools may be used in either of the 120 volt outlets shown in Figures B and C.

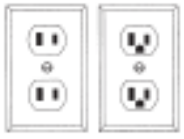
Fig. B Fig. C

EXTENSION CORDS

Grounded tools require a three wire extension cord. Double insulated tools can use either a two or three wire extension cord. As the distance from the supply outlet increases, you must use a heavier gauge extension cord. Using extension cords with inadequately sized wire causes a serious drop in voltage, resulting in loss of power and possible tool damage. Refer to the table shown to determine the required minimum wire size.
The smaller the gauge number of the wire, the greater the capacity of the cord. For example, a 14 gauge cord can carry a higher current than a 16 gauge cord. When using more than one extension cord to make up the total length, be sure each cord contains at least the minimum wire size required. If you are using one extension cord for more than one tool, add the nameplate amperes and use the sum to determine the required minimum wire size.

Guidelines for Using Extension Cords
- If you are using an extension cord outdoors, be sure it is marked with the suffix "W-A" ("W" in Canada) to indicate that it is acceptable for outdoor use.
- Be sure your extension cord is properly wired and in good electrical condition. Always replace a damaged extension cord or have it repaired by a qualified person before using it.
- Protect your extension cords from sharp objects, excessive heat and damp or wet areas.

Recommended Minimum Wire Gauge For Extension Cords*

	Extension Cord Length				
Nameplate Amperes	25'	50'	75'	100'	150'
0 - 2.0	18	18	18	18	16
2.1 - 3.4	18	18	18	16	14
3.5 - 5.0	18	18	16	14	12
5.1 - 7.0	18	16	14	12	12
7.1 - 12.0	16	14	12	10	
12.1 - 16.0	14	12	10		
16.1 - 20.0	12	10			

* Based on limiting the line voltage drop to five volts at 150% of the rated amperes.

READ AND SAVE ALL INSTRUCTIONS FOR FUTURE USE.

ASSEMBLY

WARNING To reduce the risk of injury, always unplug tool before attaching or removing accessories or making adjustments. Use only specifically recommended accessories. Others may be hazardous.

Installing Bits into Keyed Chucks

1. Unplug tool.
2. Open the chuck jaws wide enough to insert the bit. Be sure the bit shank and chuck jaws are clean. Dirt particles may prevent the bit from lining up properly.
3. Insert the bit into the chuck. Center the bit in the chuck jaws and lift it about 1/16" off of the bottom. Tighten the chuck jaws by hand to align the bit.
4. Place the chuck key in each of the three holes in the chuck, turning it clockwise. Tighten securely.
5. To remove the bit, insert the chuck key into one of the holes in the chuck and turn it counterclockwise.

Bit Selection

- Use sharp bits. Sharp bits are less likely to bind when drilling.
- Use the proper bit for the job. There are many types of bits designed for specific purposes. Check the information on the bit's packaging for proper usage.
- Do not use bits larger than the rated capacity of the drill. Gear damage or motor overload may result.

Pipe Handle

The pipe handle may be used on either side of the tool. Thread pipe handle into one of the threaded holes in the motor housing.

Spade Handle

The spade handle can be attached to the tool in three positions. Remove the hex head screws which secure the handle. Remove the handle and move it to the desired position. To mount the handle in position C, it is necessary to reverse the mounting holes by turning the handle around.

Fig. 2

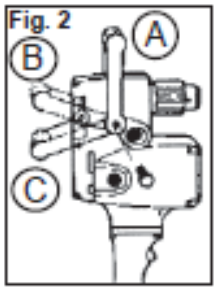

OPERATION

WARNING To reduce the risk of injury, wear safety goggles or glasses with side shields.

WARNING To reduce the risk of personal injury when drilling, hold tool by insulated gripping surfaces when performing an operation where the cutting tool may contact hidden wiring or its own cord. Contact with a "live" wire will make exposed metal parts of the tool "live" and shock the operator.

WARNING When drilling with a single speed drill or in HI with a two speed drill, always hold the drill securely using the pipe handle, or brace the drill against a solid fixed object in preparation for a sudden reaction. When drilling in LO with a two speed drill, always brace the drill against a solid fixed object in preparation for a sudden reaction. When drilling, never use your body to brace drill.
Never put your hands (or other body parts) between the part of the drill being braced and the object it is being braced against. Hands (or other body parts) that are in the path of the reaction can be pinched, crushed and broken.

Bit binding

Fig. 3

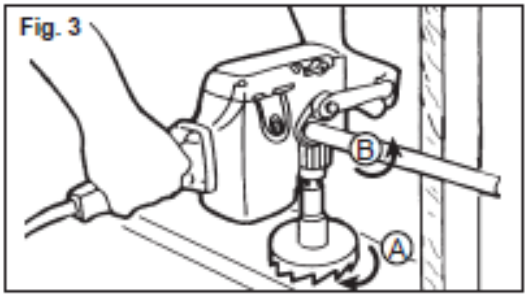

If the bit binds, the drill will suddenly react in the opposite direction of the rotation of the bit. Figure 3 shows the path of reaction (B) if the drill bit binds while being driven in forward (A). The operator should reduce the chances of a sudden reaction by following the instructions listed below.

The operator should also prepare for a sudden reaction by holding securely using the pipe handle or bracing against a solid fixed object.

To reduce the chance of bit binding

- Use sharp bits. Sharp bits are less likely to bind when drilling.
- Use the proper bit for the job. There are many types of bits designed for specific purposes.
- Use the proper speed for the size bit. Larger bits should be run at the lower speed. Driving larger bits at high speeds will increase the chance of the bit binding and increase the chance of reaction.
- Avoid drilling warped, wet, knotty, and or pitchy material if possible.
- Avoid drilling in material that you suspect contains hidden nails or other things that may cause the bit to bind.

The direction of reaction is always opposite of the direction of bit rotation.
Reaction is even more likely to occur when enlarging already existing holes and at the point when the bit breaks through the other side of the material.

Bracing for forward rotation

Fig. 4

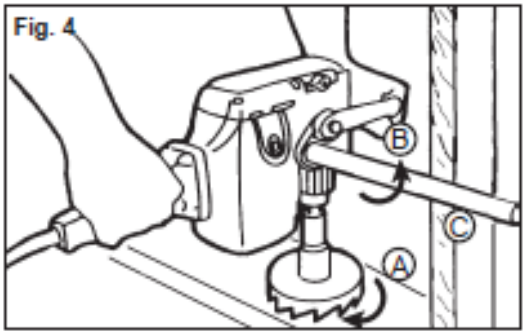

Fig. 5

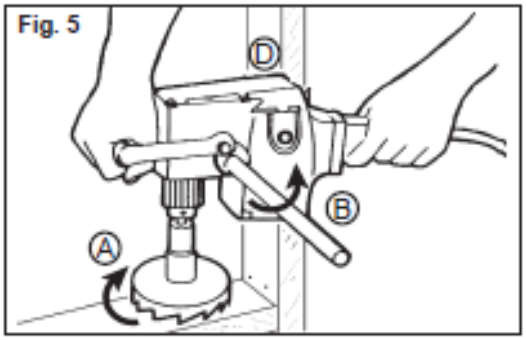

When drilling in forward, the bit will **rotate** in a clockwise direction. If the bit binds in the hole, the bit will come to a sudden stop and drill will suddenly **react** in a counterclockwise direction.
Figures 4 and 5 show examples of a Hole Hawg® properly braced for forward rotation.
A. Forward (clockwise) rotation
B. Reaction
C. Brace drill with pipe handle here
D. Brace drill with motor housing here
If the bit binds, the pipe handle or the motor housing braced against the stud will hold the drill in position.

Bracing for reverse rotation

Fig. 6

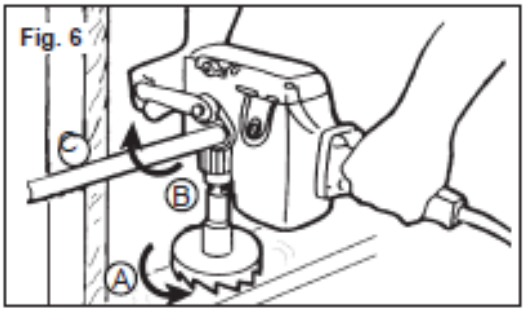

Fig. 7

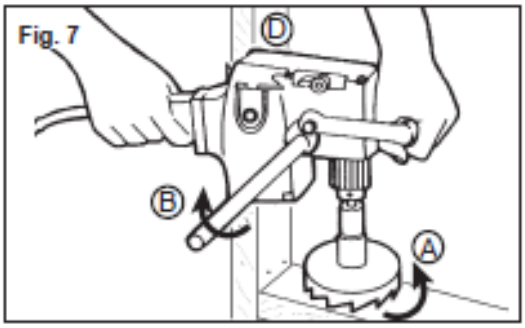

When drilling in reverse, the bit will **rotate** in a counterclockwise direction. If the bit binds in the hole, the bit will come to a sudden stop and the drill will suddenly **react** in a clockwise direction.
Figures 6 and 7 show examples of the Hole Hawg® properly braced for reverse rotation.
A. Reverse (counterclockwise) rotation
B. Reaction
C. Brace drill with pipe handle here
D. Brace drill with motor housing here
If the bit binds, the pipe handle or the motor housing braced against the stud will hold the drill in position.

Reversing

A reversing switch is located below the trigger switch for removal of bits from holes. Permit the motor to come to a complete stop before reversing. Reversing the tool with the gears in motion may cause severe damage. When removing selfeed bits from partially drilled holes, a flick of the trigger switch will free the threaded pilot screw. When the threads are loose, lift the bit from the workpiece with the motor stopped.

Shifting Speeds

Fig. 8

Cat. No. 1675-1 has a gear shift lever on the right side of the gear case.
The high setting (1200 RPM HI) is the low torque setting and is designed for driving Selfeed bits 1-3/8" in diameter and smaller.
The low setting (300 RPM LO) is the high torque setting and is designed for driving Selfeed bits 1-1/2" in diameter and larger.
Always turn off the switch and shift while the tool is coasting to a stop. Never shift the drill while it is moving at full speed, when it is under load, or when it is stopped.

⚠ *WARNING* To reduce the risk of electric shock, check work area for hidden pipes and wires before drilling or driving screws.

Drilling

Before drilling, clamp down the material securely. A poorly secured piece of material may result in personal injury or inaccurate drilling. When drilling in light gauge metal or wood, use a wooden block to back up the material to prevent damage to the workpiece.

Mark the center of the hole to be drilled with a center punch to give the bit a start and to prevent it from "walking." Lubricate the drill bit with cutting oil when drilling iron or steel. Use a coolant when drilling nonferrous metals such as copper, brass or aluminum.

To start a selfeed bit, run the threaded feed screw into the work by flicking the trigger switch, permitting the bit to coast until the teeth contact the work surface. Align the bit properly before proceeding. This will reduce cocking and jamming when starting. To reduce jamming on breakthrough, decrease the drilling pressure when the feed screw point breaks through the workpiece. Proceed with steady, even pressure.

⚠ *WARNING* To reduce the risk of injury, always wear eye protection.

Chuck Removal

To remove the chuck from the drill:

1. Unplug tool.
2. Fully open the chuck jaws
3. Remove the left-handed thread screw from inside the chuck by turning it clockwise.
4. Pull the chuck off of the spindle.
   NOTE: If the chuck does not pull off of the spindle easily, tap the side of the chuck with a hammer to loosen it. If this doesn't work, contact a *MILWAUKEE* service center.

ACCESSORIES

⚠ *WARNING* To reduce the risk of injury, always unplug the tool before attaching or removing accessories. Use only specifically recommended accessories. Others may be hazardous.

For a complete listing of accessories refer to your *MILWAUKEE* Electric Tool catalog or go on-line to www.milwaukeetool.com. To obtain a catalog, contact your local distributor or a service center.

MAINTENANCE

⚠ *WARNING* To reduce the risk of injury, always unplug your tool before performing any maintenance. Never disassemble the tool or try to do any rewiring on the tool's electrical system. Contact a *MILWAUKEE* service facility for ALL repairs.

Maintaining Tools

Keep your tool in good repair by adopting a regular maintenance program. Before use, examine the general condition of your tool. Inspect guards, switches, tool cord set and extension cord for damage. Check for loose screws, misalignment, binding of moving parts, improper mounting, broken parts and any other condition that may affect its safe operation. If abnormal noise or vibration occurs, turn the tool off immediately and have the problem corrected before further use. Do not use a damaged tool. Tag damaged tools "DO NOT USE" until repaired (see "Repairs").

Under normal conditions, relubrication is not necessary until the motor brushes need to be replaced. After six months to one year, depending on use, return your tool to the nearest *MILWAUKEE* service facility for the following:

- Lubrication
- Brush inspection and replacement
- Mechanical inspection and cleaning (gears, spindles, bearings, housing, etc.)
- Electrical inspection (switch, cord, armature, etc.)
- Testing to assure proper mechanical and electrical operation

⚠ *WARNING* To reduce the risk of injury, electric shock and damage to the tool, never immerse your tool in liquid or allow a liquid to flow inside the tool.

Cleaning

Clean dust and debris from vents. Keep the tool handles clean, dry and free of oil or grease. Use only mild soap and a damp cloth to clean your tool since certain cleaning agents and solvents are harmful to plastics and other insulated parts. Some of these include: gasoline, turpentine, lacquer thinner, paint thinner, chlorinated cleaning solvents, ammonia and household detergents containing ammonia. Never use flammable or combustible solvents around tools.

Repairs

If your tool is damaged, return the entire tool to the nearest service center.

LIMITED WARRANTY - USA AND CANADA

Every *MILWAUKEE* power tool (including cordless product – tool, battery pack(s) - see separate & distinct CORDLESS BATTERY PACK LIMITED WARRANTY statements & battery charger and Work Lights*) is warranted to the original purchaser only to be free from defects in material and workmanship. Subject to certain exceptions, *MILWAUKEE* will repair or replace any part on an electric power tool which, after examination, is determined by *MILWAUKEE* to be defective in material or workmanship for a period of five (5) years* after the date of purchase unless otherwise noted. Return of the power tool to a *MILWAUKEE* factory Service Center location or *MILWAUKEE* Authorized Service Station, freight prepaid and insured, is required. A copy of the proof of purchase should be included with the return product. This warranty does not apply to damage that *MILWAUKEE* determines to be from repairs made or attempted by anyone other than *MILWAUKEE* authorized personnel, misuse, alterations, abuse, normal wear and tear, lack of maintenance, or accidents.

*The warranty period for, Job Site Radios, M12™ Power Port, M18™ Power Source, and Trade Titan™ Industrial Work Carts is one (1) year from the date of purchase. The warranty period for a LED Work Light and LED Upgrade Bulb is a limited LIFETIME warranty to the original purchaser only, if during normal use the LED bulb fails the Work Light or Upgrade Bulb will be replaced free of charge.

*This warranty does not cover Air Nailers & Stapler, Airless Paint Sprayer, Cordless Battery Packs, Gasoline Driven Portable Power Generators, Hand Tools, Hoist – Electric, Lever & Hand Chain, M12™ Heated Jackets, Reconditioned product and Test & Measurement products. There are separate and distinct warranties available for these products.

Warranty Registration is not necessary to obtain the applicable warranty on a *MILWAUKEE* power tool product. The manufacturing date of the product will be used to determine the warranty period if no proof of purchase is provided at the time warranty service is requested.

ACCEPTANCE OF THE EXCLUSIVE REPAIR AND REPLACEMENT REMEDIES DESCRIBED HEREIN IS A CONDITION OF THE CONTRACT FOR THE PURCHASE OF EVERY *MILWAUKEE* PRODUCT. IF YOU DO NOT AGREE TO THIS CONDITION, YOU SHOULD NOT PURCHASE THE PRODUCT. IN NO EVENT SHALL *MILWAUKEE* BE LIABLE FOR ANY INCIDENTAL, SPECIAL, CONSEQUENTIAL OR PUNITIVE DAMAGES, OR FOR ANY COSTS, ATTORNEY FEES, EXPENSES, LOSSES OR DELAYS ALLEGED TO BE AS A CONSEQUENCE OF ANY DAMAGE TO, FAILURE OF, OR DEFECT IN ANY PRODUCT INCLUDING, BUT NOT LIMITED TO, ANY CLAIMS FOR LOSS OF PROFITS. SOME STATES DO NOT ALLOW THE EXCLUSION OR LIMITATION OF INCIDENTAL OR CONSEQUENTIAL DAMAGES, SO THE ABOVE LIMITATION OR EXCLUSION MAY NOT APPLY TO YOU. THIS WARRANTY IS EXCLUSIVE AND IN LIEU OF ALL OTHER EXPRESS WARRANTIES, WRITTEN OR ORAL. TO THE EXTENT PERMITTED BY LAW, *MILWAUKEE* DISCLAIMS ANY IMPLIED WARRANTIES, INCLUDING WITHOUT LIMITATION ANY IMPLIED WARRANTY OF MERCHANTABILITY OR FITNESS FOR A PARTICULAR USE OR PURPOSE; TO THE EXTENT SUCH DISCLAIMER IS NOT PERMITTED BY LAW, SUCH IMPLIED WARRANTIES ARE LIMITED TO THE DURATION OF THE APPLICABLE EXPRESS WARRANTY AS DESCRIBED ABOVE. SOME STATES DO NOT ALLOW LIMITATIONS ON HOW LONG AN IMPLIED WARRANTY LASTS, SO THE ABOVE LIMITATION MAY NOT APPLY TO YOU. THIS WARRANTY GIVES YOU SPECIFIC LEGAL RIGHTS, AND YOU MAY ALSO HAVE OTHER RIGHTS WHICH VARY FROM STATE TO STATE.

This warranty applies to product sold in the U.S.A. and Canada only.

Please consult the 'Service Center Search' in the Parts & Service section of *MILWAUKEE*'s website www.milwaukeetool.com or call **1.800.SAWDUST (1.800.729.3878)** to locate your nearest service facility for warranty and non-warranty service on a Milwaukee electric power tool.

LIMITED WARRANTY - MEXICO, CENTRAL AMERICA AND CARIBBEAN

TECHTRONIC INDUSTRIES' warranty is for 5 year since the original purchase date.

This warranty card covers any defect in material and workmanship on this Power Tool.

To make this warranty valid, present this warranty card, sealed/stamped by the distributor or store where you purchased the product, to the Authorized Service Center (ASC). Or, if this card has not been sealed/stamped, present the original proof of purchase to the ASC.

Call toll-free 1 800 832 1949 to find the nearest ASC, for service, parts, accessories or components.

Procedure to make this warranty valid

Take the product to the ASC, along with the warranty card sealed/stamped by the distributor or store where you purchased the product, and there any faulty piece or component will be replaced without cost for you. We will cover all freight costs relative with this warranty process.

Exceptions

This warranty is not valid in the following situations:

a) When the product is used in a different manners from the end-user guide or instruction manual.

b) When the conditions of use are not normal.

c) When the product was modified or repaired by people not authorized by TECHTRONIC INDUSTRIES.

Note: If cord set is damaged, it should be replaced by an Authorized Service Center to avoid electric risks.

Model: _____

Date of Purchase: _____

Distributor or Store Stamp:

SERVICE AND ATTENTION CENTER
Av Presidente Mazarik 29 Piso 7, 11570 Chapultepec Morales
Miguel Hidalgo, Distrito Federal, Mexico
Ph. 52 55 4160-3547

IMPORTED AND COMMERCIALIZED BY:
TECHTRONIC INDUSTRIES MEXICO, .S.A. DE C.V.
Av Presidente Mazarik 29 Piso 7, 11570 Chapultepec Morales
Miguel Hidalgo, Distrito Federal, Mexico

The Lewis Forged Hook bolts were ordered from Lewis Nut & Bolt Company:

https://www.lewisbolt.com/standard-hook-bolt

Length: 16 inches

Thread Length: 5 inches

Lewis Part: HK2H2

Diameter	Length	Head Length	Head Height	Head Width	Number of Fins	Fin Dimensions	Overall Shank Width	Thread Per Inch	Thread Length Nominal
3/4"	As Ordered	2"	1-1/4"	3/4"	4	3/16" x 3"	1-1/8"	10	As Ordered

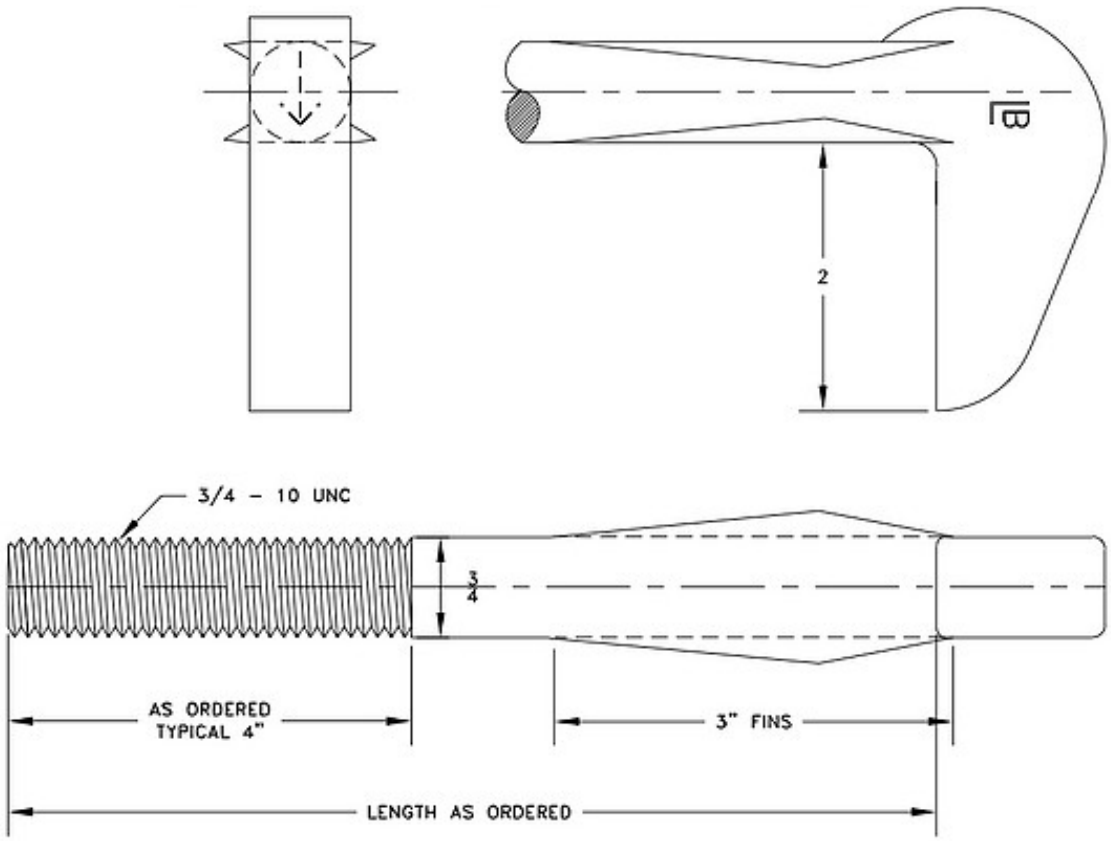

Hook Bolt ¾" diameter, 2" hook
used to fastne timbers to bridge structure
Exceeds ASTM A307
Typical tensile strength 90,000 – 100,000 psi

Mill certification for Square body hook bolts:

INSPECTION REPORT

Customer: VIRGINIA TECH

P.O. No 6PC

Date: 3/26/2018

Description: HOOK BOLTS

UNITED STEEL AND FASTENERS, INC.

1500 Industrial Drive, Itasca, IL 60143

Test Piece No.	Specification / Size	Tension Test: Yield Strength	Tension Test: Tensile Strength	Tension Test: Elongation	Tension Test: Reduction	Hardness	Heat No.	Chemical Composition (%): C	Si	Mn	P	S	Cr	Mo			PART NUMBER
	3/4 X 16						M50621603	0.16	0.23	0.37	0.026	0.008					.75C16.00HB SQTHD5

Reference:

OFFICIAL SEAL
JENNIFER R OLSON
NOTARY PUBLIC, STATE OF ILLINOIS
My Commission Expires Nov 18, 2019

This is to certify that the above results are true and correct in every detail.

Q.A.

11/12/03 QMF 29B

Square hook bolts were specified as ASTM A36 material.

3/4-10 X 16” Hook Bolt Square Body w/5” Thread

QUICKSET SYSTEM INSTALLATION

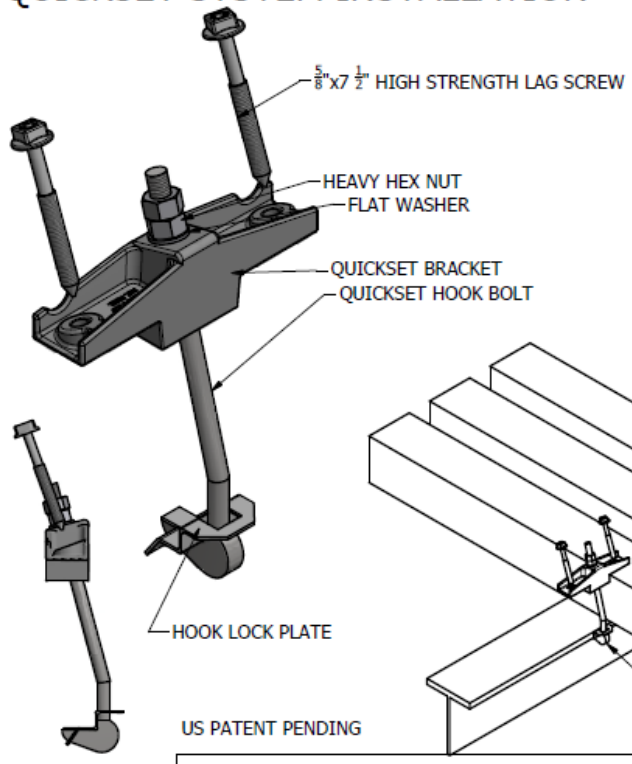

1. SLIDE HOOK BOLT THROUGH HOOK LOCK PLATE UNTIL SEATED ON HOOK AS SHOWN
2. ASSEMBLE THE BOLT ONTO THE BRACKET WITH A FLAT WASHER AND NUT.
3. THREAD THE NUT ONTO THE BOLT, BUT DO NOT TIGHTEN IT
4. REACH THE BOLT BETWEEN TIMBERS AND HOOK ONTO BEAM FLANGE BELOW
5. PLACE BRACKET SO THAT IT SITS FLAT ON TIMBER AND BOLT IS FULLY ENGAGED ON FLANGE
6. RUN NUT DOWN ON BOLT UNTIL ASSEMBLY IS SNUG
7. DRIVE LAG SCREWS IN HOLES IN BRACKET
   3/8" PRE-DRILL IS RECOMENDED
8. TIGHTEN NUT SNUGGLY (20-50 FT-LBS)
9. ADD SECOND NUT (RECOMMENDED)
   FIRST NUT SHOULD NOT BE A LOCK NUT
   SECOND NUT MAY BE A LOCK NUT

US PATENT PENDING

NOV 16, 2015

LEWIS
BOLT & NUT COMPANY
30105 SIXTH AVE
LA JUNTA, CO 81050
719-384-5400

LEWIS
BOLT & NUT COMPANY
30105 Sixth Avenue • P.O. Box 830 • La Junta, CO 81050 USA
1-719-384-5400 (Phone) • 1-719-384-0130 (Fax)

Certificate of Compliance

The parts listed below meet the customer requirements. The raw material heat numbers used for each part are listed and materials certs are attached unless otherwise noted.

Date: September 13, 2017

Customer Order #	Lewis P/N	QTY	Lot #	Heat #
PO TESTING	Mill 125668			
	HK2H2075-1600P	25	166230	58027145
	HK2BK075-1900P	25	166229	100885084
	BQBLN075-1400P	25	83150	
			Nortrak cert Attached	
	RHSQH063-0750P	50	164499	NF16103203
	I-HKLP2075P	50	81709	0382004879
	NFHC2075P	125	85214	N/A
	NFHAL075P	125	85271	N/A
	I-ETSP-075P	50	82184	351505541

Tim Austin
Lab Manager

"We help keep the world on track"

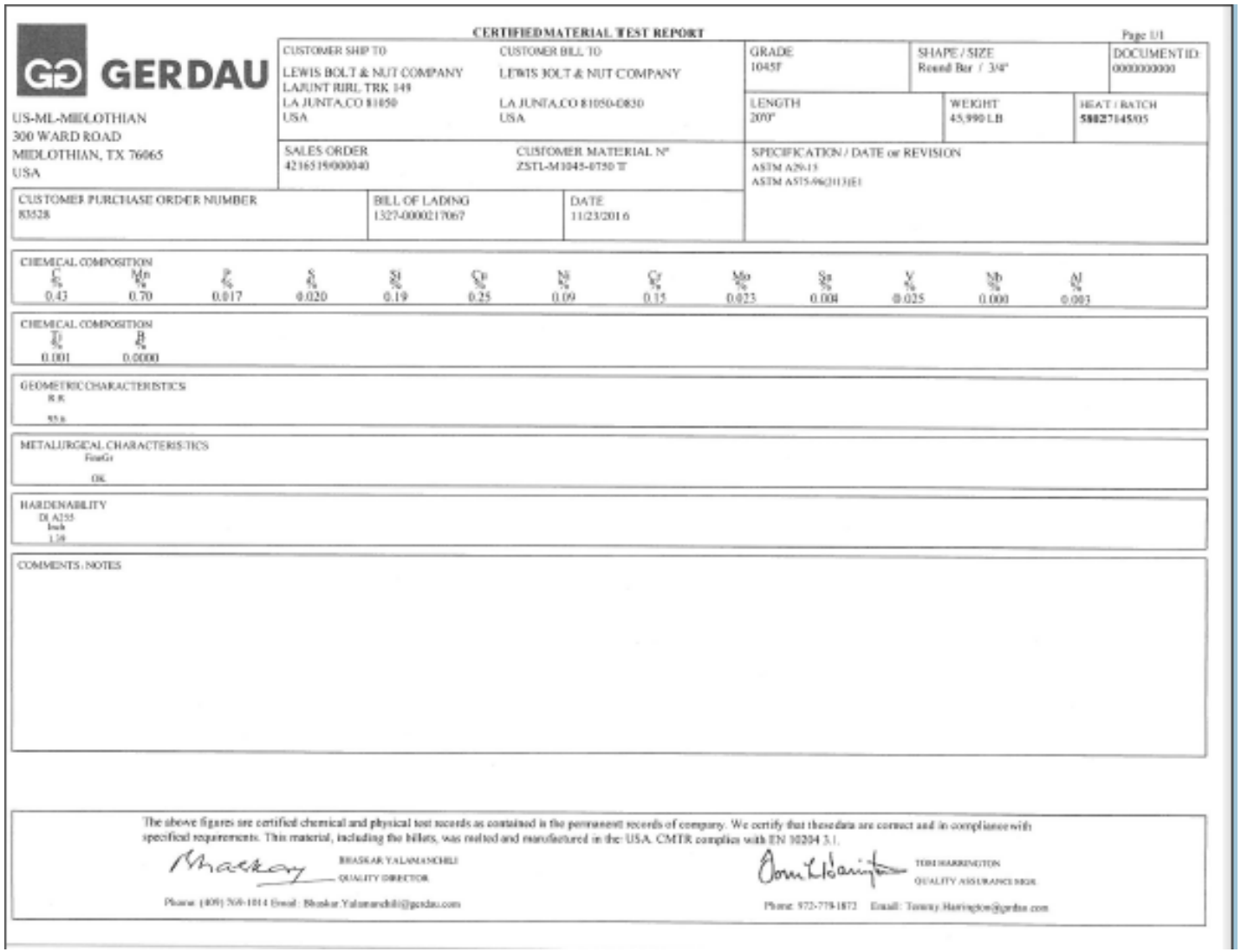

GERDAU

US-ML-MIDLOTHIAN
300 WARD ROAD
MIDLOTHIAN, TX 76065
USA

CERTIFIED MATERIAL TEST REPORT

Page 1/1

CUSTOMER SHIP TO	CUSTOMER BILL TO	GRADE	SHAPE / SIZE	DOCUMENT ID
LEWIS BOLT & NUT COMPANY LAJUNT RIRL TRK 149 LA JUNTA,CO 81050 USA	LEWIS BOLT & NUT COMPANY LA JUNTA,CO 81050-0830 USA	1045F	Round Bar / 3/4"	0000000000

LENGTH	WEIGHT	HEAT / BATCH
209"	45,990 LB	**5802714505**

SALES ORDER	CUSTOMER MATERIAL N°	SPECIFICATION / DATE or REVISION
4216519000040	ZSTL-M1045-0750 T	ASTM A29-13 ASTM A575-96(2013)E1

CUSTOMER PURCHASE ORDER NUMBER	BILL OF LADING	DATE
83528	1327-0000217067	11/23/2016

CHEMICAL COMPOSITION

C %	Mn %	P %	S %	Si %	Cu %	Ni %	Cr %	Mo %	Sn %	V %	Nb %	Al %
0.43	0.70	0.017	0.020	0.19	0.25	0.09	0.15	0.023	0.008	0.025	0.000	0.003

CHEMICAL COMPOSITION

Ti %	B %
0.001	0.0000

GEOMETRIC CHARACTERISTICS
RR
95.6

METALURGICAL CHARACTERISTICS
FineGr
OK

HARDENABILITY
DI A255
Inch
1.39

COMMENTS / NOTES

The above figures are certified chemical and physical test records as contained in the permanent records of company. We certify that these data are correct and in compliance with specified requirements. This material, including the billets, was melted and manufactured in the USA. CMTR complies with EN 10204 3.1.

BHASKAR YALAMANCHILI
QUALITY DIRECTOR
Phone: (409) 769-1014 Email: Bhaskar.Yalamanchili@gerdau.com

TOM HARRINGTON
QUALITY ASSURANCE MGR
Phone: 972-779-1872 Email: Tommy.Harrington@gerdau.com

NUCOR
Nucor Steel Nebraska

Mill Certification

03/06/2017

MTR#: 9847
Lot #:10088508420
2911 E NUCOR ROAD
PO BOX 309
NORFOLK, NE 68701 US
402-644-0200
Fax: 402-644-0329

Sold To: LEWIS BOLT & NUT COMPANY
PO BOX 830
30105 6TH AVE
LA JUNTA, CO 81050 US

Ship To: LEWIS BOLT & NUT CO
30105 6TH AVE
LA JUNTA, CO 81050 US

Customer P.O	84677	Sales Order #	10001478 - 1.1
Product Group	Hot Roll - Engineered Bar	Product #	3008740
Grade	1045CV1	Lot #	10088508420
Size	0.75"	Heat #	100885084
BOL #	BOL-108361	Load #	9847
Description	HR-EB RD 0.75" 1045CV1 20' 0" 3001-6000 lbs	Customer Part #	ZSTL-M1045-0750
Production Date	02/11/2017	Qty Shipped LBS	39802
Product Country Of Origin	United States	Qty Shipped EA	1325
Original Item Description		Original Item Number	

I hereby certify that the material described herein has been manufactured in accordance with the specifications and standards listed above and that it satisfies those requirements.

Melt Country of Origin : United States — Melting Date: 01/07/2017

C (%)	Mn (%)	P (%)	S (%)	Si (%)	Ni (%)	Cr (%)	Mo (%)	Cu (%)	Ti (%)	V (%)	B (%)
0.44	0.84	0.020	0.024	0.20	0.09	0.18	0.02	0.31	0.000	0.020	0.000

Nb (%)	Zr (%)	Sn (%)	Al (%)	Pb (%)	Ca (%)
0.002	0.000	0.012	0.00	0.000	0.000

Austenitic fine grain by chemical analysis per the latest revision of ASTM A29
Reduction Ratio 99.72 : 1

Other Test Results
Macroetch E381 Surface : 1 — Macroetch E381 Mid Radius : 1 — Macroetch E381 Center : 1
DI Calculated (IN) : 1.40

Comments:
All manufacturing processes of the steel materials in this product, including melting, have been performed in the United States.
All products produced are weld free.
Mercury, in any form, has not been used in the production or testing of this material.
Test conform to ASTM A29-15, ASTM E415 and ASTM E1019-resulphurized grades or applicable customer requirements.
All material melted at Nucor Steel Nebraska is produced in an Electric Arc Furnace.
Strand Cast
ISO-17025 LAB accreditation cert available upon request.
Exporting Country-USA
Sales@nucorne.com

Jim Hill, Division Metallurgist

voestalpine Nortrak Inc.

660 E. Kenwood Ave.
Decatur, IL 62526
T. 217-876-9160
F. 217-876-6258
www.voestalpine.com/nortrak

September 29, 2016

Physical Certification

Per ASTM A536-84 (Reapproved 2004)

voestalpine Nortrak Inc. hereby certifies that the shipment indicated by the attached receiving ticket meets or exceeds the necessary requirements. A proper sampling process has been applied and testing has been performed to assure compliance. The attached analysis report provides evidence that the material meets or exceeds the standard.

Certified by:

Jeffrey T. Pyatt
QA Manager

voestalpine

Date Shipped	09/15/2016
Customer	LEWIS BOLT & NUT COMPANY
Quantity	3,896
Part #	U99-01800
Description	QUICKSET BRACKET
Destination	LEWIS BOLT & NUT COMPANY
Date Code	238, 243
PO #	3273491

APPENDIX B : GRAPHS AND SUPPLEMENTAL RESULTS

Supplemental graphs that were not included in Chapter 4 of this report are shown in this section. This section also contains additional pictures of failed specimens that were tested as a part of this research project.

Vertical load – 5 kip

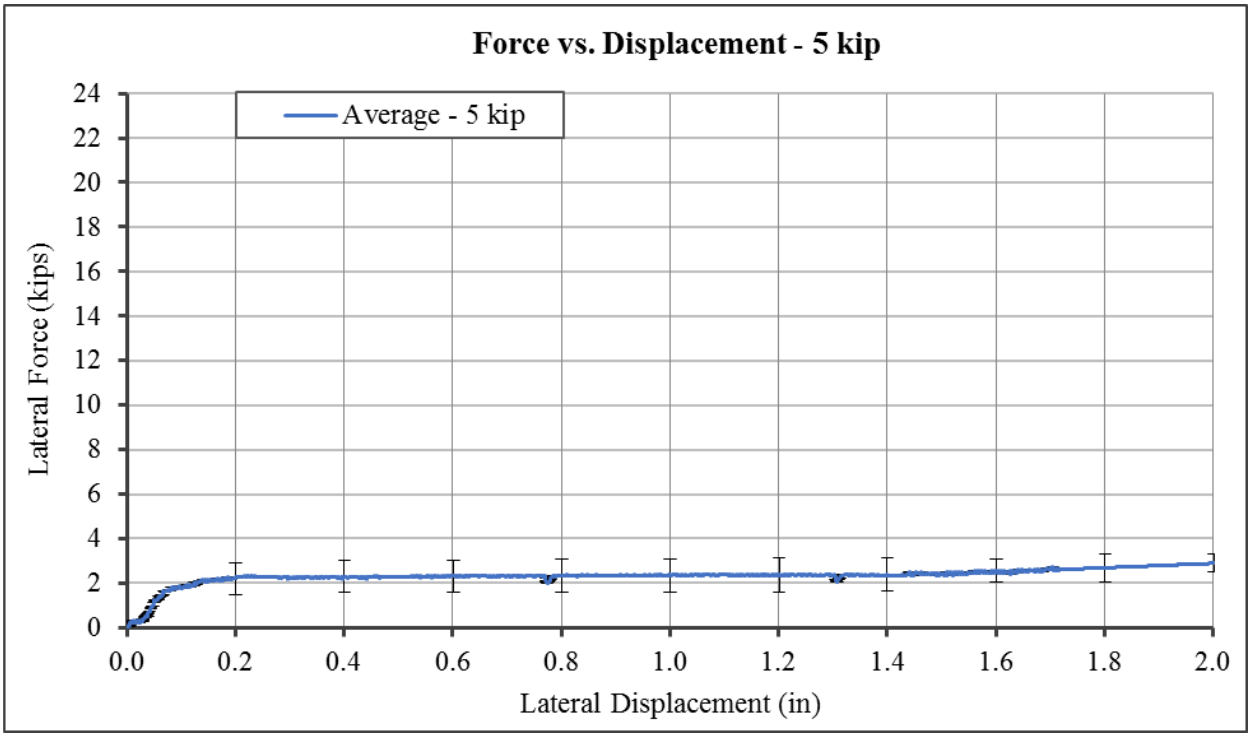

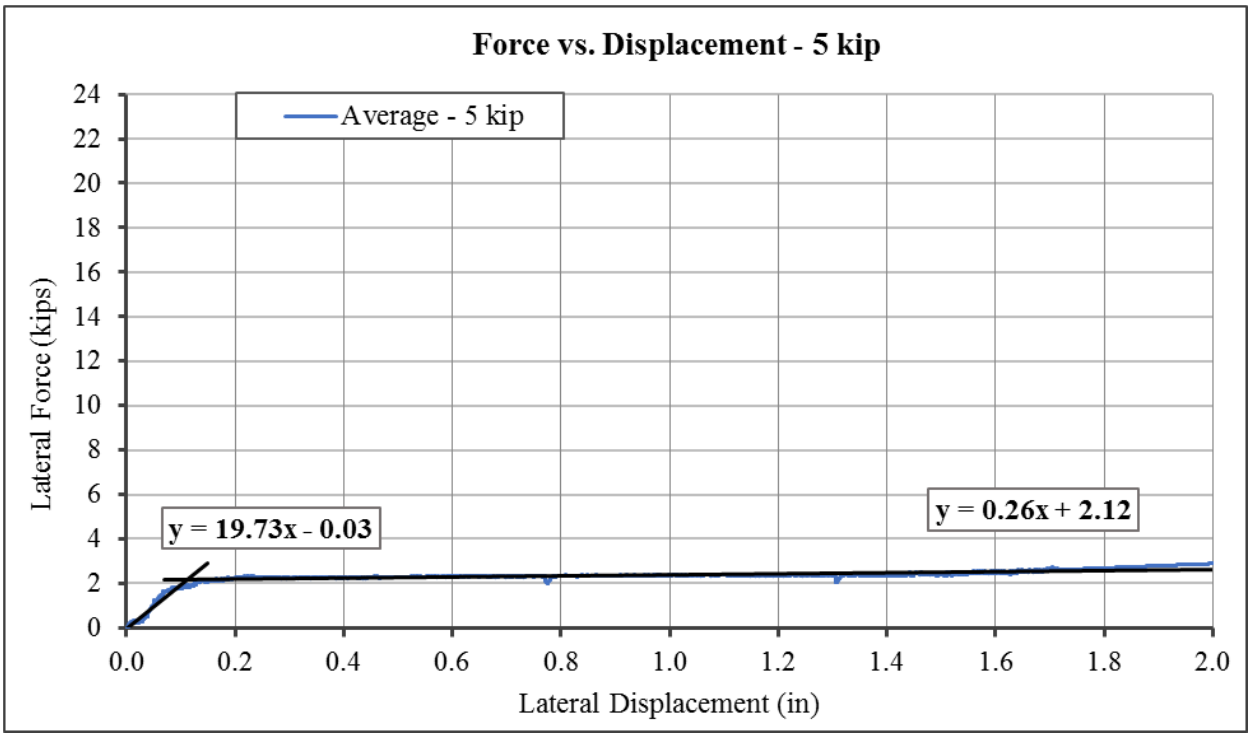

Vertical load – 15 kip

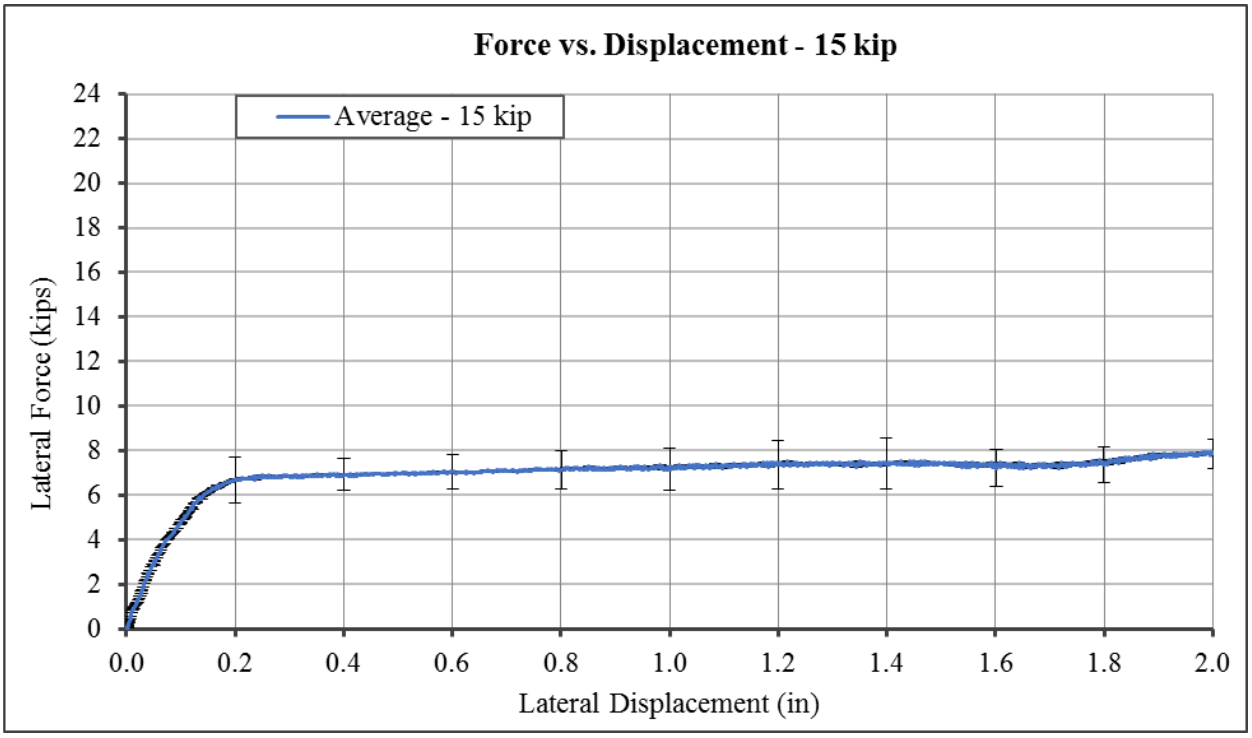

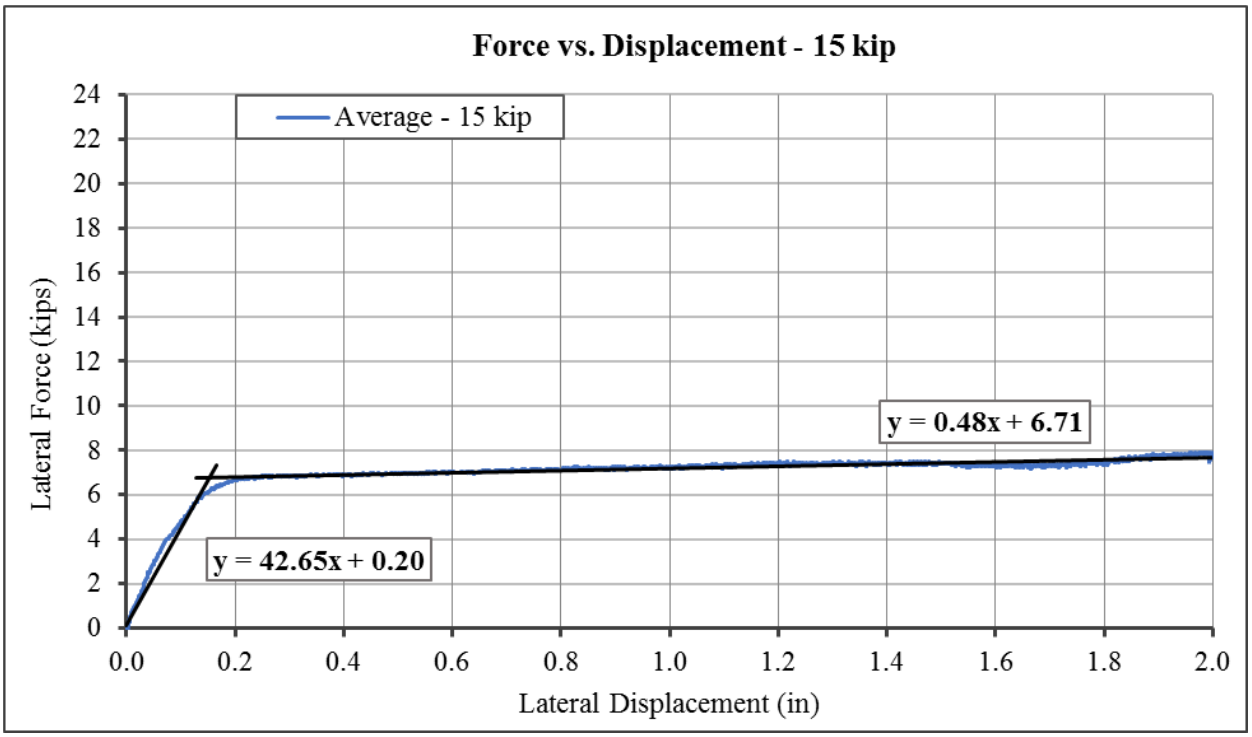

Vertical load – 25 kip

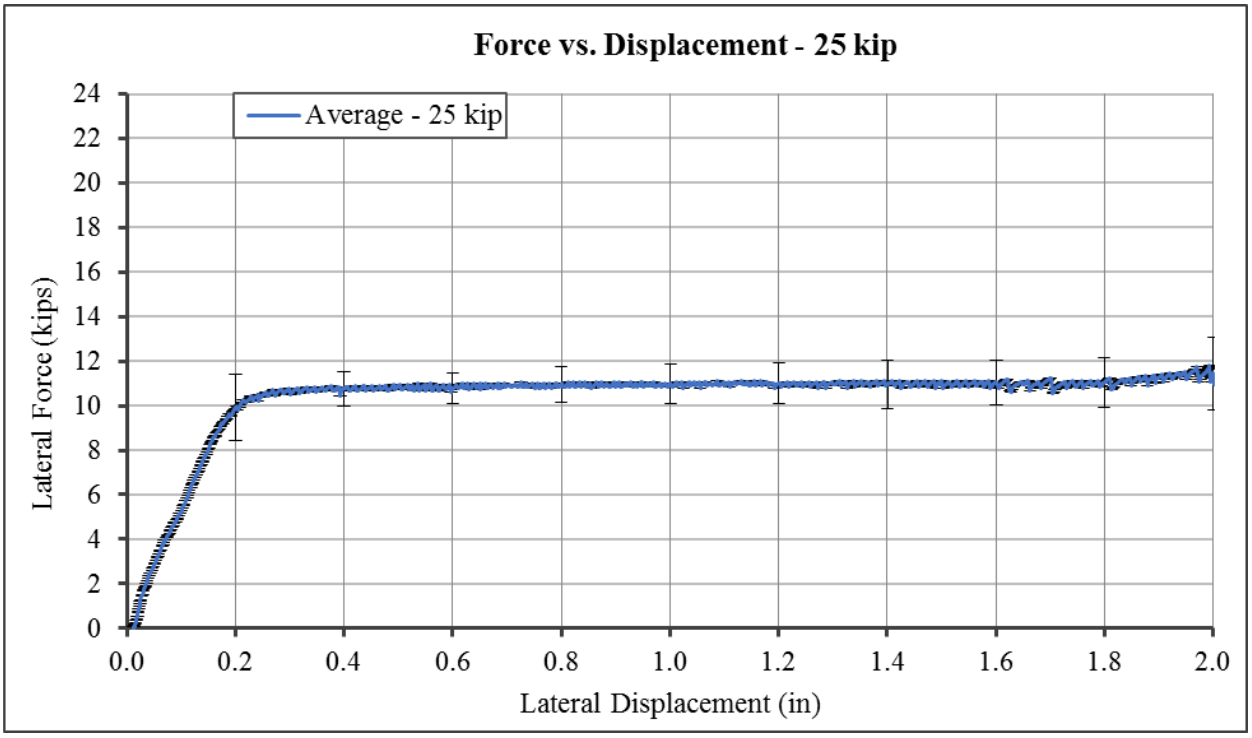

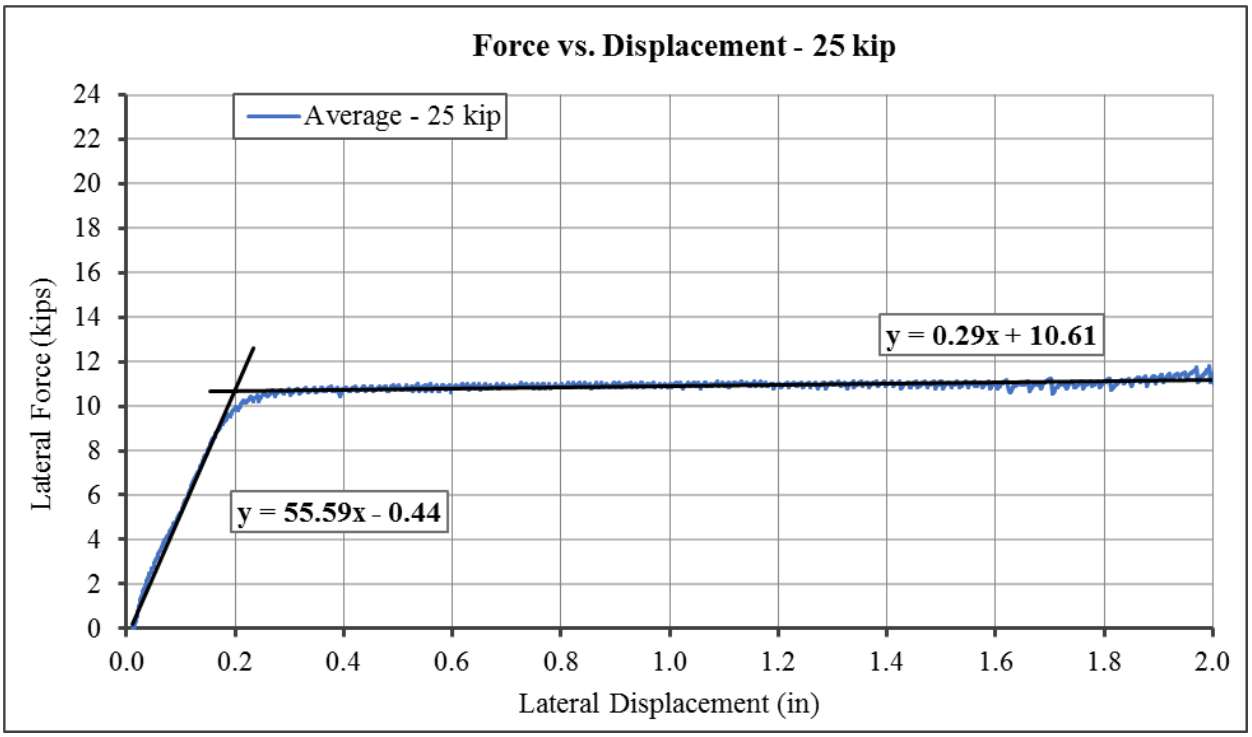

Vertical load – 35 kip

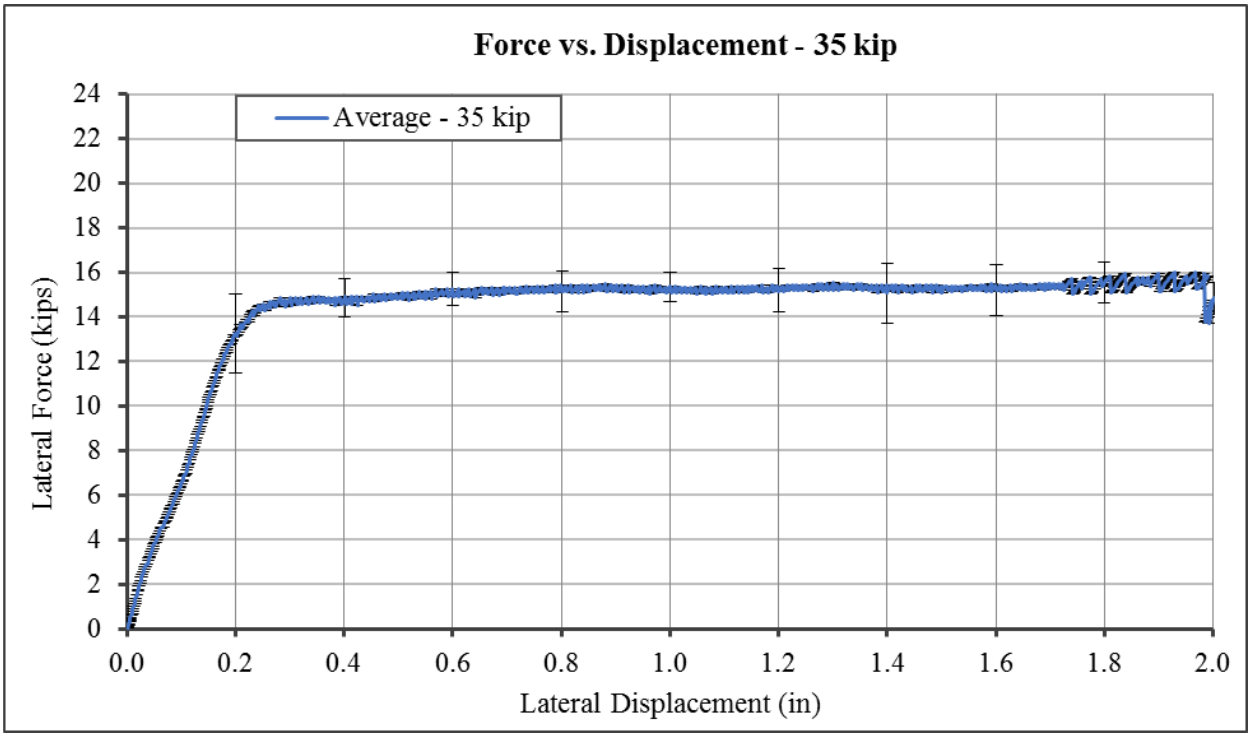

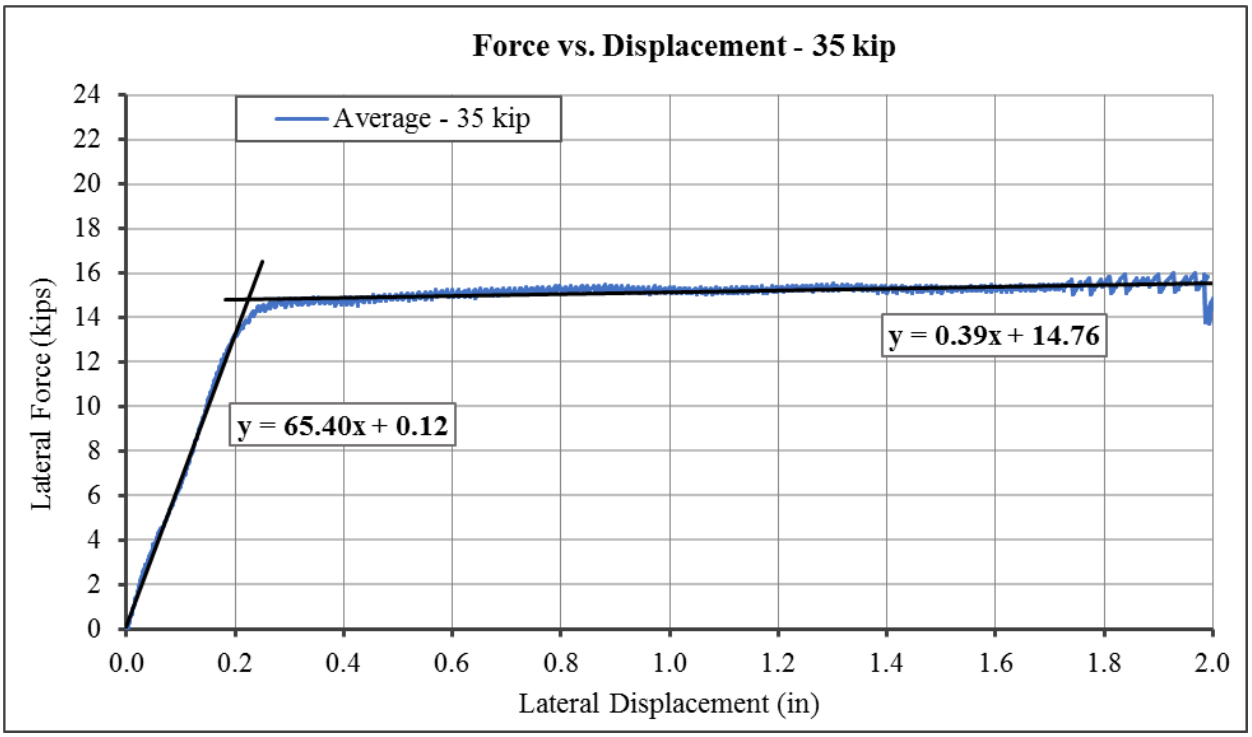

Vertical load – 45 kip

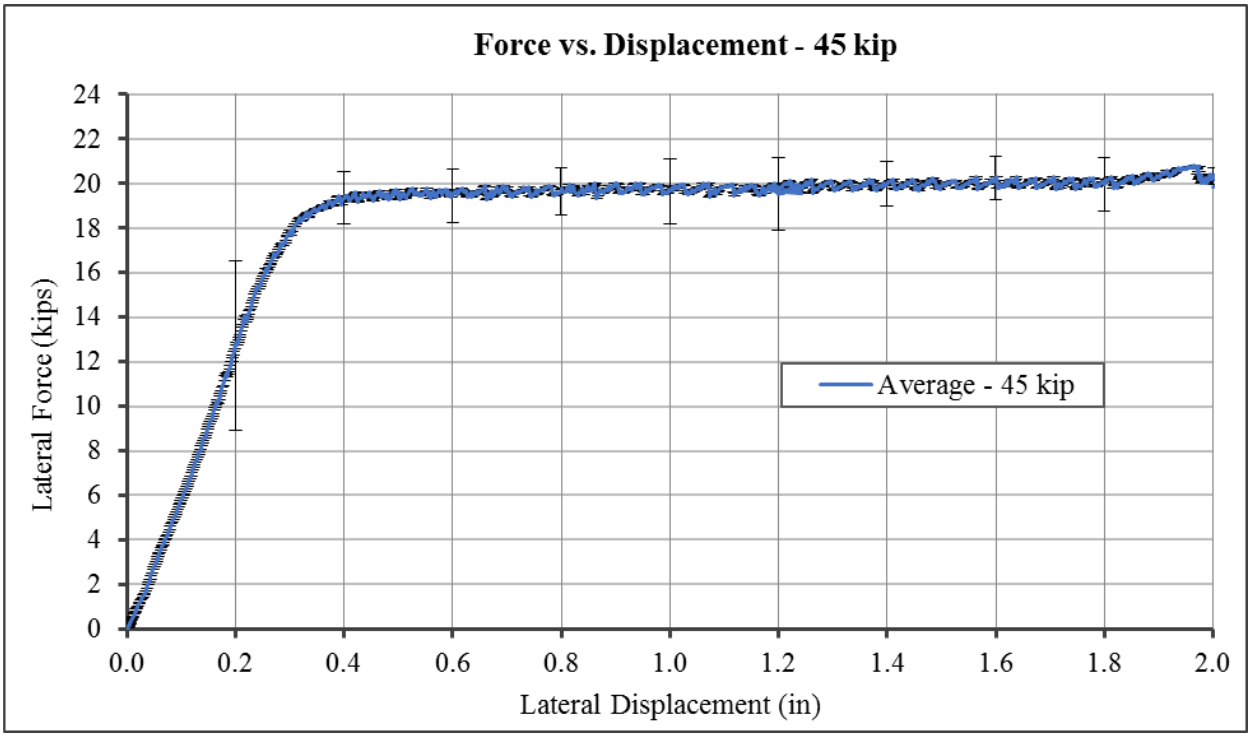

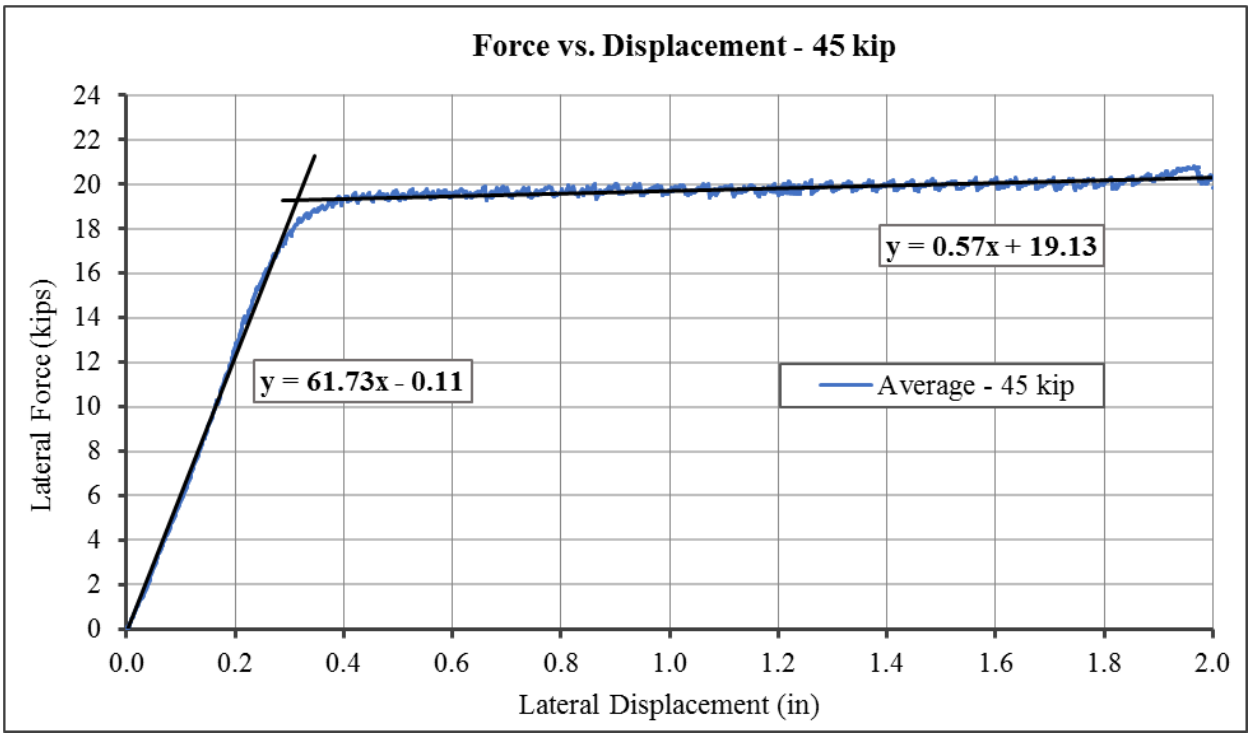

Dapped Specimen: D1

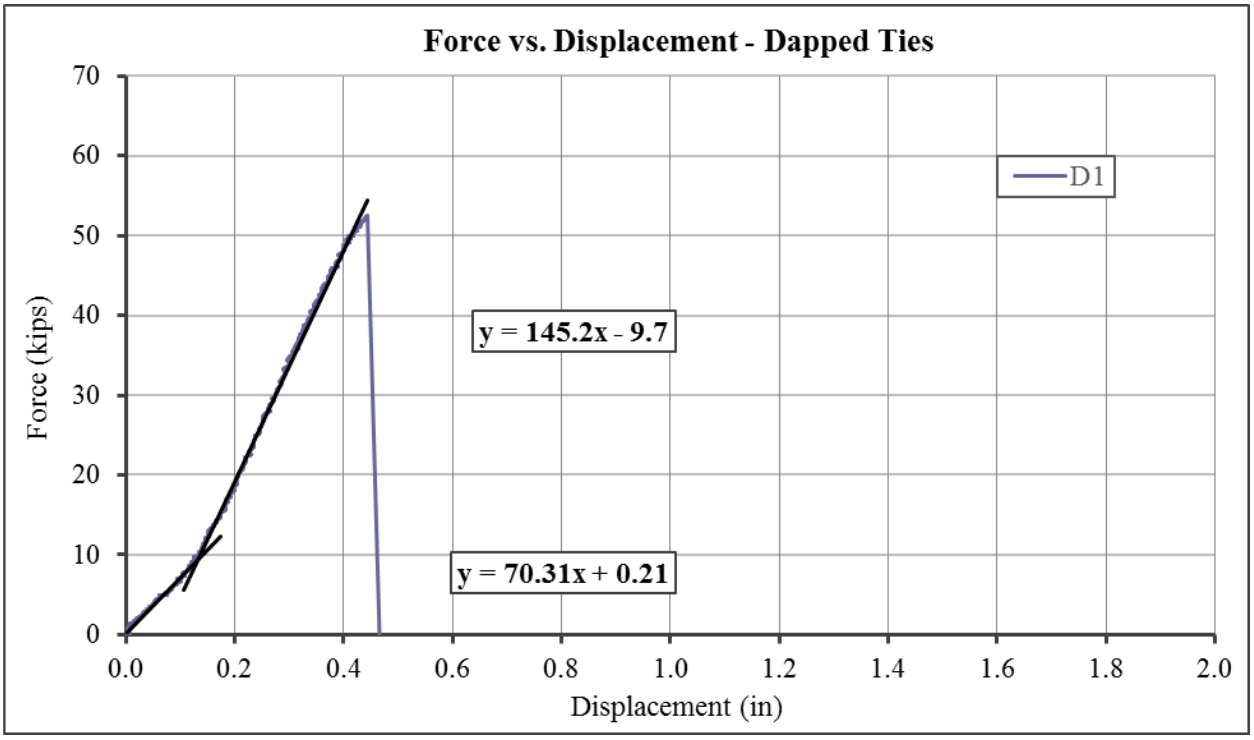

Dapped Specimen: D2

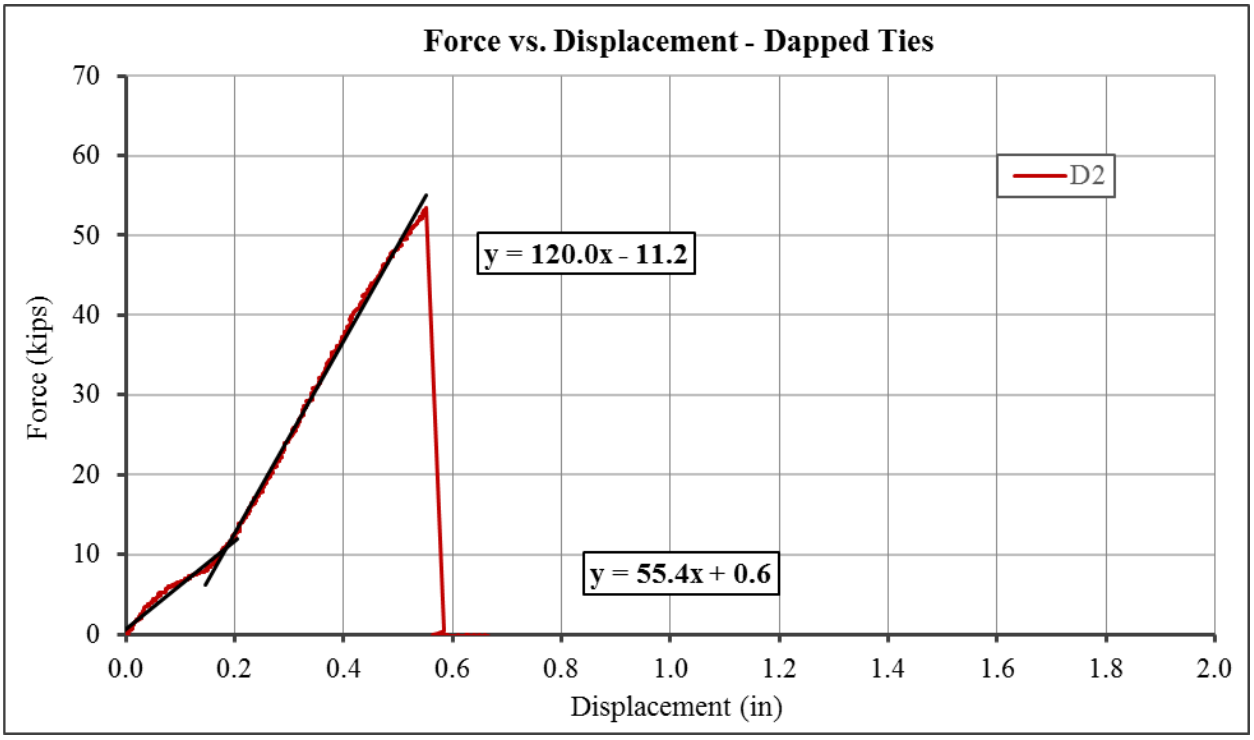

Dapped Specimen: D3

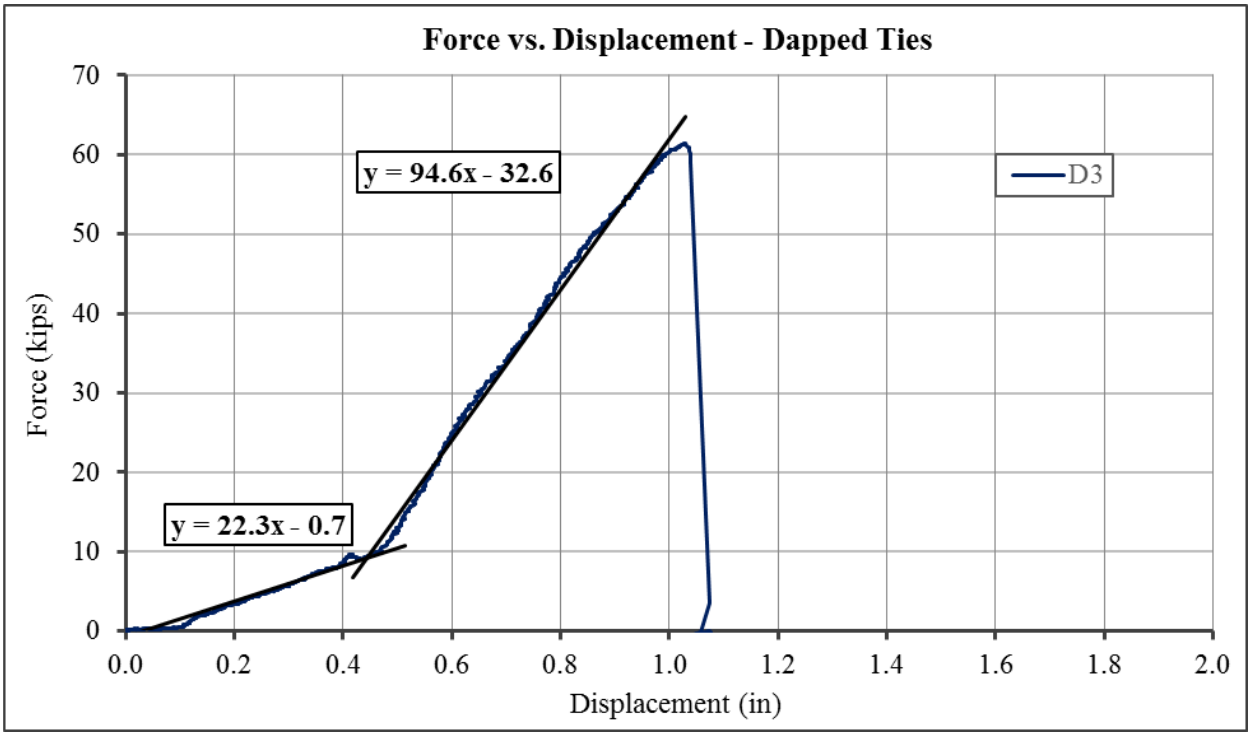

Dapped Specimen: D4

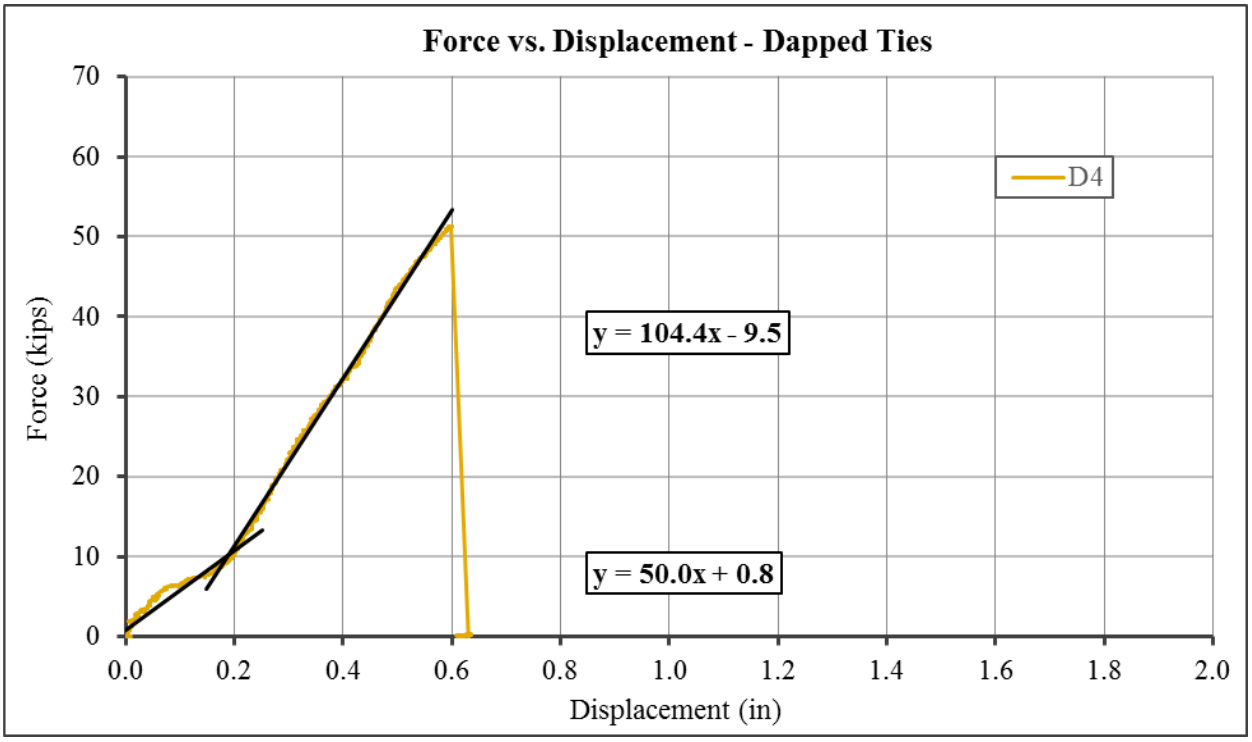

Dapped Specimen: D5

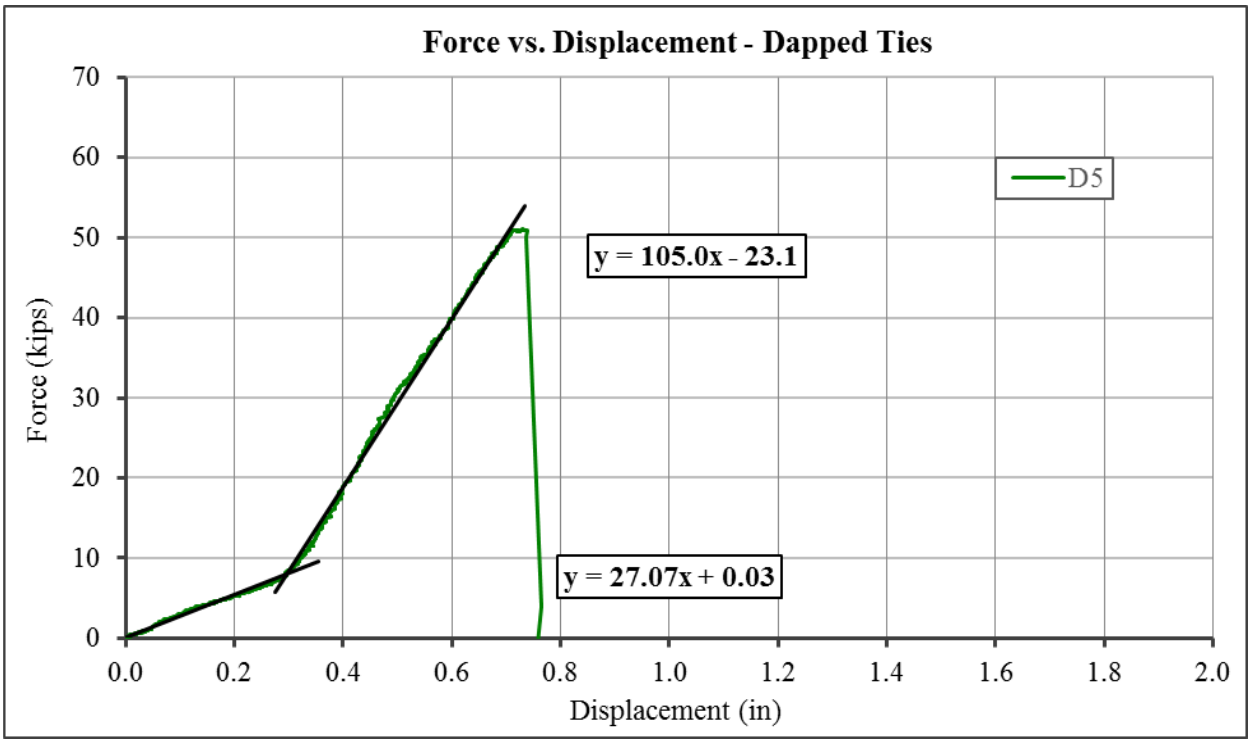

Deformed Square Body Hook Bolts

Square body hook bolt	
Hook Bolt	Angle (deg)
4A	18
1A	23
5A	16
1B	23
7A	27
Average	**21**

Deformed Round Body Hook Bolts

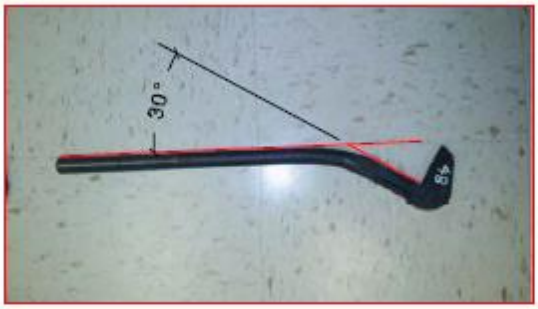

Lewis Forged Hook Bolt	
Hook Bolt	Angle (deg)
2A	24
4B	30
3B	36
2B	27
3A	28
Average	29

APPENDIX C : DRAWINGS

Details of the drawings for the structural test set are shown in this section.

Elevation View:

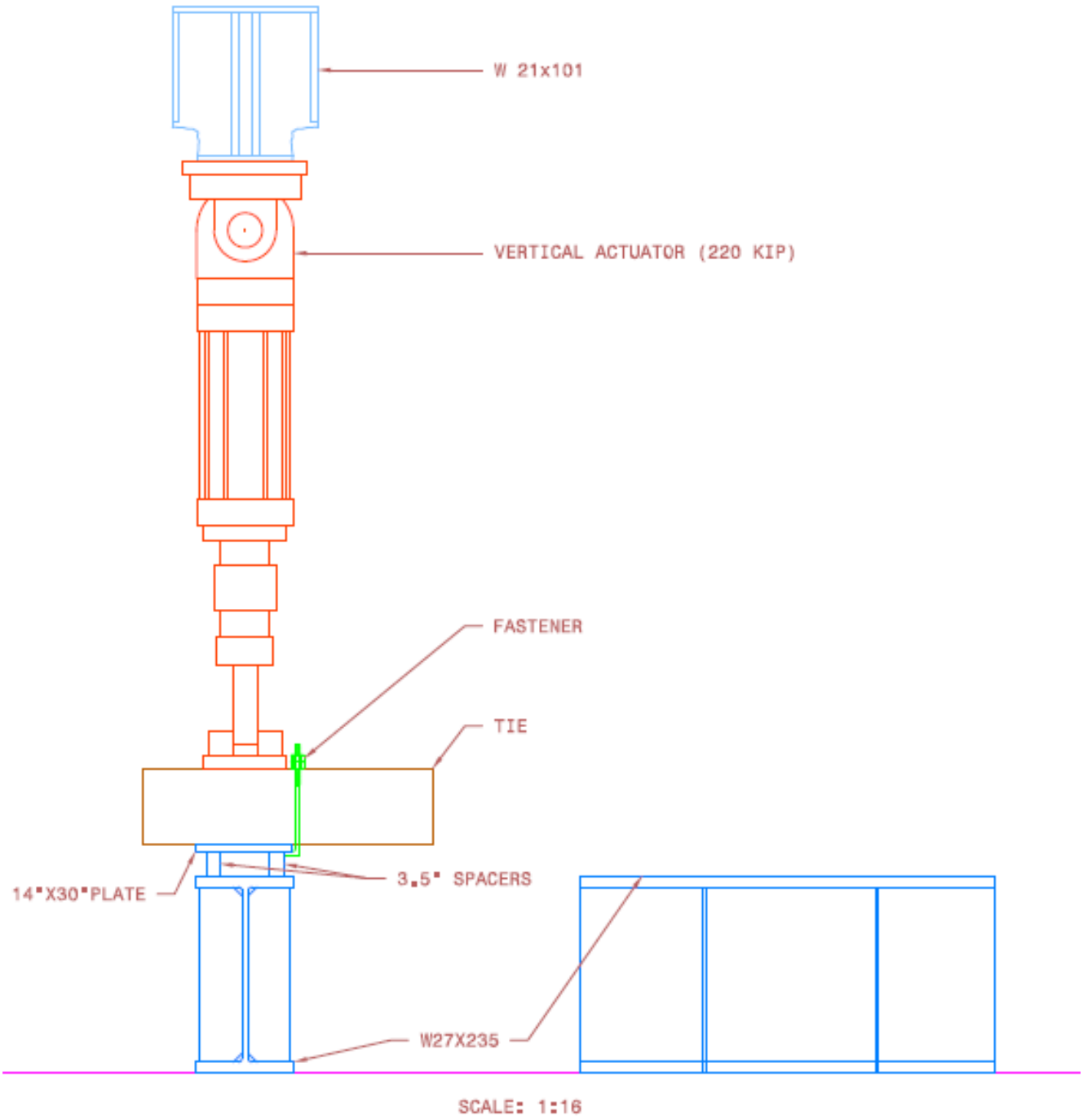

Plan View:

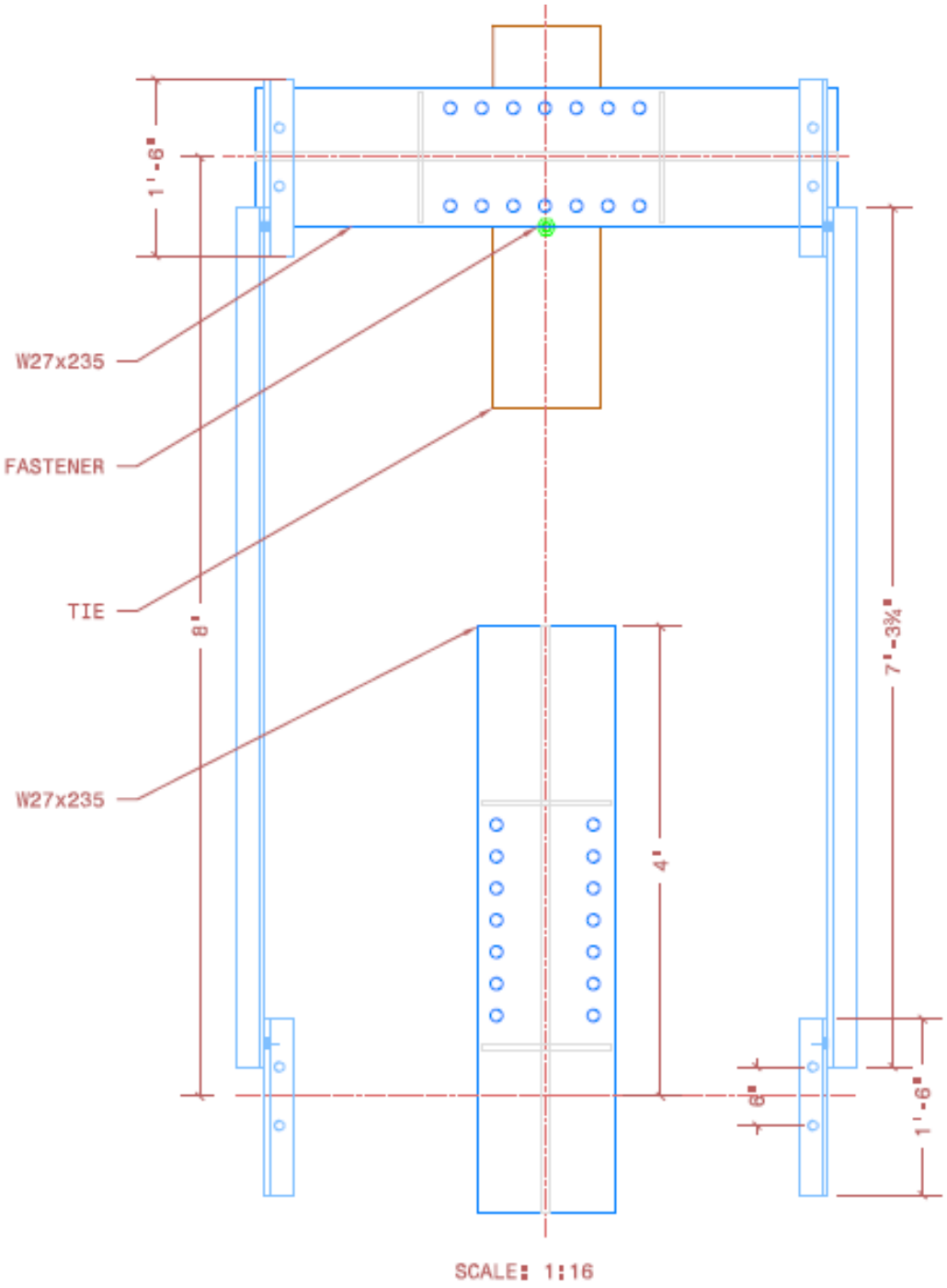

Elevation Side View:

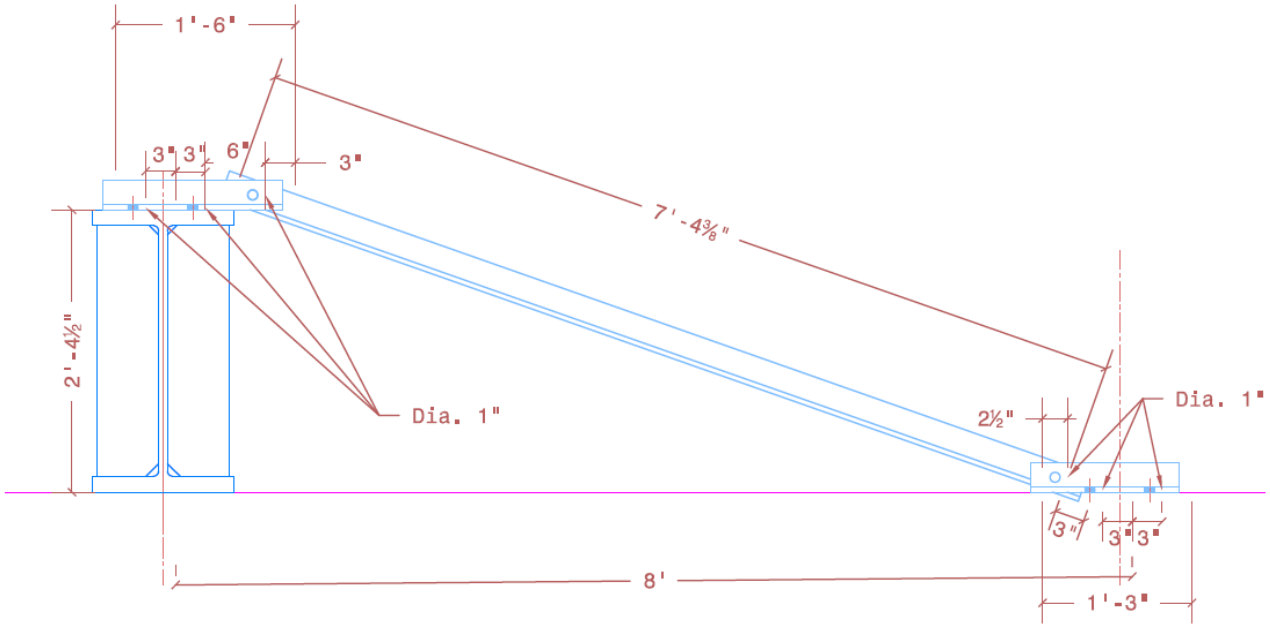

ALL ANGLES ARE 3 X 3 x $\frac{1}{2}$"

SCALE: $\frac{3}{4}$"= 1'-0

Plate Dimensions:

LATERAL ACTUATOR - GIRDER PLATE

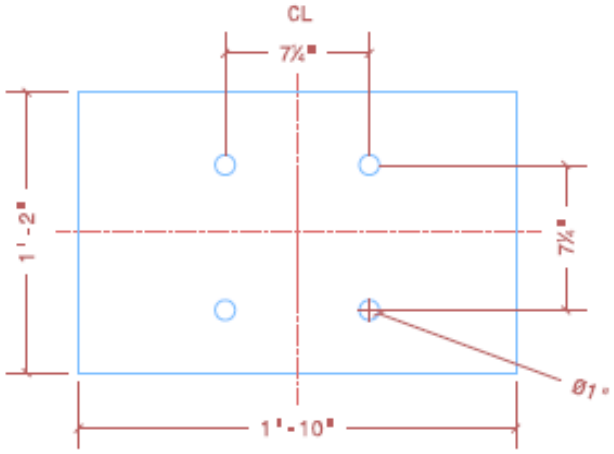

LATERAL ACTUATOR - TIE PLATE

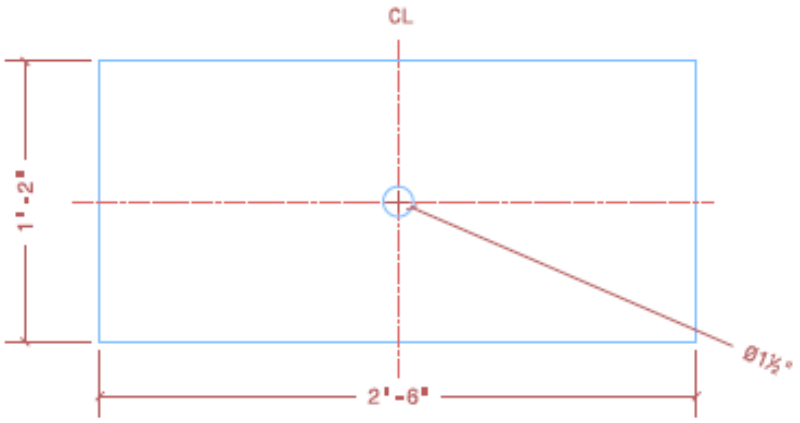

SCALE: 1:8